AD-A187 377 PROCESS DESIGN MODEL FOR A SINGLE-ZONE TUNNEL DRYER(U) 1/2
AIR FORCE INST OF TECH WRIGHT-PATTERSON AFB OH
B A FLAKE DEC 87 AFIT/CI/NR-87-79T

UNCLASSIFIED F/G 13/1 NL

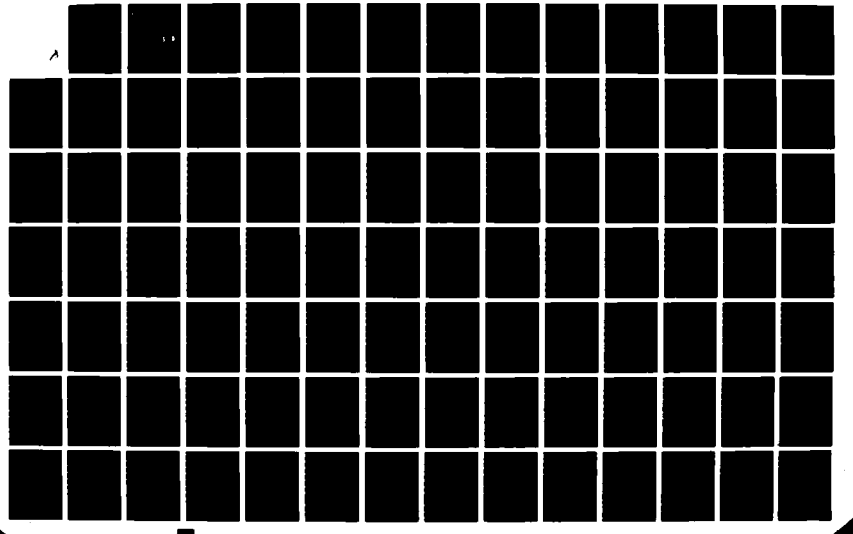

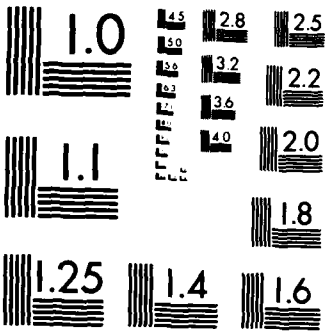

UNCLASSIFIED
SECURITY CLASSIFICATION OF THIS PAGE (When Data Entered)

REPORT DOCUMENTATION PAGE		READ INSTRUCTIONS BEFORE COMPLETING FORM
1. REPORT NUMBER AFIT/CI/NR 87- 79T	2. GOVT ACCESSION NO.	3. RECIPIENT'S CATALOG NUMBER
4. TITLE (and Subtitle) Process Design Model For A Single-Zone Tunnel Dryer		5. TYPE OF REPORT & PERIOD COVERED THESIS/DISSERTATION 6. PERFORMING ORG. REPORT NUMBER
7. AUTHOR(s) Barrett Adams Flake		8. CONTRACT OR GRANT NUMBER(s)
9. PERFORMING ORGANIZATION NAME AND ADDRESS AFIT STUDENT AT: The University of Texas		10. PROGRAM ELEMENT, PROJECT, TASK AREA & WORK UNIT NUMBERS
11. CONTROLLING OFFICE NAME AND ADDRESS AFIT/NR WPAFB OH 45433-6583		12. REPORT DATE 1987 13. NUMBER OF PAGES 157
14. MONITORING AGENCY NAME & ADDRESS(if different from Controlling Office)		15. SECURITY CLASS. (of this report) UNCLASSIFIED 15a. DECLASSIFICATION/DOWNGRADING SCHEDULE

16. DISTRIBUTION STATEMENT (of this Report)

APPROVED FOR PUBLIC RELEASE; DISTRIBUTION UNLIMITED

17. DISTRIBUTION STATEMENT (of the abstract entered in Block 20, if different from Report)

18. SUPPLEMENTARY NOTES
APPROVED FOR PUBLIC RELEASE: IAW AFR 190-1

LYNN E. WOLAVER 28 OCT 87
Dean for Research and
Professional Development
AFIT/NR

19. KEY WORDS (Continue on reverse side if necessary and identify by block number)

20. ABSTRACT (Continue on reverse side if necessary and identify by block number)
ATTACHED

DD FORM 1 JAN 73 1473 EDITION OF 1 NOV 65 IS OBSOLETE

SECURITY CLASSIFICATION OF THIS PAGE (When Data Entered)

PROCESS DESIGN MODEL FOR A SINGLE-ZONE TUNNEL DRYER

by

BARRETT ADAMS FLAKE, B.S.

THESIS

Presented to the Faculty of the Graduate School of

The University of Texas at Austin

in Partial Fulfillment

of the Requirements

for the Degree of

MASTER OF SCIENCE IN ENGINEERING

THE UNIVERSITY OF TEXAS AT AUSTIN

December 1987

ABSTRACT

Many products must be dried in their manufacture. The process of evaporating moisture from these products is energy intensive. As a consequence of limited energy resources, there has been advancement in both drying technology and drying theory. However, drying has evolved from an ancient art and implementation of new technology has been slow.

Dielectric heating at radio frequencies (RF) or microwave frequencies is a relatively recent technological advancement in the drying industry, and theoretical and experimental studies of dielectrically-assisted drying are the subject of ongoing investigation. Transfer of this new knowledge to dryer designers through appropriate design tools will accelerate the incorporation of dielectric heating into commercial drying processes.

Directed toward a larger goal of predictive design models of dielectrically-assisted dryers, the objective of this work is to develop a fundamental model of the drying processes in a continuous convective tunnel dryer. A model of the drying process consists of two subsidiary models. One represents the transport of the product through the dryer, an equipment model, and the other describes the drying kinetics of the product. For conventional convective drying, the product model may be represented by a characteristic drying curve which allows prediction of drying rates under various external convective conditions.

Although a subject of concurrent investigation, to date, a characteristic drying curve to describe the drying kinetics of materials dried with dielectric heat has not been developed. The model given in this work simulates the drying processes in conventional convective drying and has been developed such that dielectrically-assisted drying may be incorporated in future versions with appropriate drying kinetics models. Model predictions for conventional convective drying have been verified with published calculations and experimental data.

TABLE OF CONTENTS

LIST OF FIGURES

NOMENCLATURE

A	Exposed Surface Area (m^2)
A_x	Cross Sectional Flow Area of Product (m^2)
b	Product Depth (m)
Bi_m	Mass Transfer Biot Number
C_p	Specific Heat (kJ/kg K)
C_{pa}	Specific Heat of Dry Air (kJ/kg K)
C_{pf}	Specific Heat of Saturated Liquid Water (kJ/kg K)
C_{ps}	Specific Heat of Dry Product (solid) (kJ/kg K)
C_{pv}	Specific Heat of Water Vapor (kJ/kg K)
C_{py}	Specifc Heat of Humid Air (kJ/kg K)
D	Molecular Weight Ratio of Water to Air
$\mathcal{D}$	Diffusion Coefficient (m^2/s)
F	Mass Transfer Coefficient, molar basis ($mole/m^2s$)
G	Air Flow Rate, dry air mass basis ($kg_{dry\ air}/s$)
h	Convective Heat Transfer Coefficient ($kW/m^2\ K$)
h^*	Convective Heat Transfer Coefficient, corrected for high mass flux ($kW/m^2\ K$)
h_a	Total Air Enthalpy, air and vapor ($kJ/kg_{dry\ air}$)
h_{da}	Dry Air Enthalpy (kJ/kg)
h_f	Saturated Liquid Water Enthalpy (kJ/kg)

h_{fg}	Latent Enthalpy of Vaporization (kJ/kg)
h_v	Vapor Enthalpy (kJ/kg)
K_o	Mass Transfer Coefficient (kg/m^2s)
L	Product Mass Flow Rate, dry product mass basis ($kg_{dry\ product}/s$)
Le	Lewis Number
Lu	Luikov Number
M_g	Molecular Weight of Air (kg/kmole)
M_w	Molecular Weight of Water (kg/kmole)
$\underline{N}$	Drying Intensity
NTU	Number of Transfer Units, dryers
Nu	Nusselt Number
N_v	Drying Rate Flux (kg/m^2s)
N_{vo}	Drying Rate Flux from Fully Wetted Surface (kg/m^2s)
p_a	Air Pressure (Pa)
P_d	Specific Dielectric Power Deposition in Dry Poduct (kW/m^3)
P_o	Specific Dielectric Power Deposition in Water (kW/m^3)
Pr	Prandtl Number
P_w	Specific Dielectric Power Deposition in Wet Product (kW/m^3)
p_w	Partial Vapor Pressure of Water (Pa)
p_{ws}	Water Vapor Saturation Pressure (Pa)
Q_{as}	Heat Source in Air Stream (kW)
$Q_{vol\ dry}$	Heat Source in Dry Product (kW)

$Q_{vol\ wet}$	Heat Source in Wet Product (kW)
Re	Reynolds Number
rh	Relative Humidity
Sc	Schmidt Number
Sh	Sherwood Number
T_a	Air Temperature (°C)
T_{as}	Adiabatic Saturation Temperature (°C)
T_{dp}	Dew Point Temperature (°C)
T_e	Evaporative Plane Temperature (°C)
T_s	Product Surface Temperature (°C)
T_{wb}	Wet Bulb Temperature (°C)
V_s	Product Velocity (m/s)
X	Product Moisture Content, dry product mass basis ($kg_{water}/kg_{dry\ product}$)
X^*	Equilibrium Moisture Content (kg/kg)
X_{cr}	Critical Moisture Content (kg/kg)
Y_a	Air Humidity, dry air mass basis ($kg_{water}/kg_{dry\ air}$)
Y_s	Humidity at Product Surface (kg/kg)
Y_{sat}	Saturation Humidity (kg/kg)
Y_w	Saturation Humidity at Wet Bulb Temperature (kg/kg)
z	Distance from Product Inlet (m)

Greek and Other Symbols

β	Coefficient in Heat and Mass Transfer Analogy Expression
ρ_a	Air Density (kg/m^3)
ρ_s	Product Density, dry solids (kg/m^3)
ξ	Depth of Evaporative Plane (m)
κ_d	Dry Product Thermal Conductivity (kW/m K)
κ_a	Air Thermal Conductivity (kW/m K)
μ	Dynamic Viscosity (kg/m s)
ν	Kinematic Viscosity (m^2/s)
ϕ	Humidity Potential Coefficient
f	Relative Drying Rate
Φ	*Characteristic Moisture Content*
τ	Time (s)
η	Relative Depth in Product

CHAPTER 1

INTRODUCTION

Many products such as foods, paper, lumber, pharmaceuticals and chemicals must be dried in their manufacture. Beyond mechanical dewatering, such as squeezing or centrifuging, these products are dried by the addition of heat such that moisture is vaporized and expelled into the atmosphere.

Drying is an energy intensive process. A 1975 study sponsored by the Environmental Protection Agency stated that 5.9 percent of the yearly energy use of the six most energy-intensive United States industries was consumed in drying operations (29). According to a 1978 study, annual energy use of industrial drying operations in the United Kingdom amounted to 4130 megawatts[sic], approximately 12 percent of the nation's industrial energy use (27). As a consequence of the recognition of limited energy resources, there has been advancement in both drying technology and drying theory. However, since drying has gradually evolved from an ancient art, implementation of new technology has been slow. Also, complex drying theory is still inadequate for use in the design of most dryers (28).

Dielectric heating at radio frequencies (RF) or microwave frequencies is a relatively recent technological advancement in the drying industry. Although the addition of dielectric heating has great potential for increased production and

improved product quality and plant efficiency, it represents a relatively large capital investment and, in turn, requires judicious design and application. Its implementation has been slowed by an insufficient base of knowledge and experience on the part of dryer designers.

Theoretical and experimental studies of dielectrically-assisted drying are the subject of ongoing investigation. Transfer of this new knowledge to dryer designers through appropriate design tools will greatly accelerate the incorporation of dielectric heating into commercial drying processes.

1.1 TYPES OF DRYERS AND DRYING ENHANCEMENT

Industrial dryers may be classified by the way heat is delivered to the material (11). Many dryers are of convective design where heated gas, usually air, contacts and heats the material while simultaneously entraining removed moisture. In tray dryers, material is spread on trays over which heated air is circulated. The material may dry in a batch process, or for greater throughput, material may be fed continuously on a band or belt. Granular materials may be dried by passing air through the product in a through-circulation dryer. Here, material is continuously fed on a perforated belt such that air may be blown through the product. If the air flow is increased sufficiently to suspend the granular material, the dryer is termed a fluidized bed dryer.

Thin materials, such as paper webs, are commonly dried in conductive dryers. The material is rolled or drawn over heated cylinders to vaporize the

moisture. Papermaking machines use a series of steam heated cylinders to produce paper sheet from wet pulp.

Although infrared radiative heating is present to some extent in convective and conductive dryers, it is the primary mode of heat transfer in some dryers. Infrared heating from sources such as high temperature quartz lamps is used to dry thin films or coatings such as enameled paint or surface moisture in textile processing and metal fabrication.

The rate at which a material dries depends upon the rate of heat transfer. High heat transfer rates are achieved by increasing the temperature potential between the heat source and the product. There are, of course, practical limits to the temperatures used in drying due to material quality and composition constraints. Also, higher drying temperatures produce higher potential for energy losses in the drying process.

High frequency electromagnetic radiation, specifically radio frequency (RF) and microwaves, may be used to generate heat within the product to enhance drying rates. Since water is dielectrically lossy, moist materials are heated when placed in microwave or RF fields. The volumetric quality of dielectric heating can provide for high heating rates without diminishing material quality or plant efficiency. Consequently, greatly increased drying rates have been achieved in dryers augmented with dielectric heating.

1.2 REVIEW OF DRYER DESIGN LITERATURE

The literature on drying mechanisms and general theory of dielectric heating of materials dates back 60 to 70 years. The purpose of this section is to cite references specifically concerned with the design methodology of drying systems. Specific literature on detailed drying behavior will be cited in later sections of this report as appropriate.

The model developed here is based largely on the work of Keey (3,11,15,16,20,26). A text by Keey (3) on industrial drying operations presents analyses of the process conditions in continuous convective dryers. In the analysis, the drying rate is determined from a function of moisture content and external air conditions as given by the product's "characteristic drying curve". The characteristic drying curve is developed and analyzed in earlier works by Keey, et al (11,15,16). Use of the characteristic drying curve with analytical methods in the process design of continuous drying equipment is discussed in a subsequent paper (20); and in a related paper (26), the characteristic drying curve is used to investigate drying rate profiles in continuous convective dryers of various configurations.

Reay (2) discusses the use of theory in the design of dryers, pointing out the advantages and limitations of the particle (product) transport and drying kinetics theories. An overall model of a drying system is defined as a drying kinetics model, such as the characteristic drying curve, and a particle transport (equipment) model. The system model can be used to perform parametric studies

of dryer performance in the preliminary design stage, as Reay suggests through the dryer design scheme shown in Figure 1-1, and can provide critical inputs to economic assessments. Reay notes the inadequacies of current theory in the design of dryers as supported by an inquiry among dryer manufacturers conducted by van Brakel (1).

Other texts on drying and mass transfer operations also give analyses of the drying process. Treybal (7) and Lydersen (30) derive expressions for heat and mass balances at the material surface where the drying rate is obtained from an assumed or experimental drying rate curve (drying rate versus moisture content). Similarly, Nonhebel and Moss (10) devote a chapter to simplified drying theory in which the drying rate is computed from an experimental drying rate curve.

1.3 OBJECTIVES OF THE PRESENT WORK

A long range objective of the dielectric-enhancement drying program at the University of Texas, Austin is to develop complete predictive capability for application of dielectric heating in industrial drying processes. One element is the development of appropriate process models and the work presented in this report represents a first step. The primary focus here is the development of a model for conventional convective drying through use of the characteristic drying curve which, in its present form, will not satisfactorily predict the effects of dielectric heating. The model is structured, however, to incorporate the dielectric phenomenon in later versions.

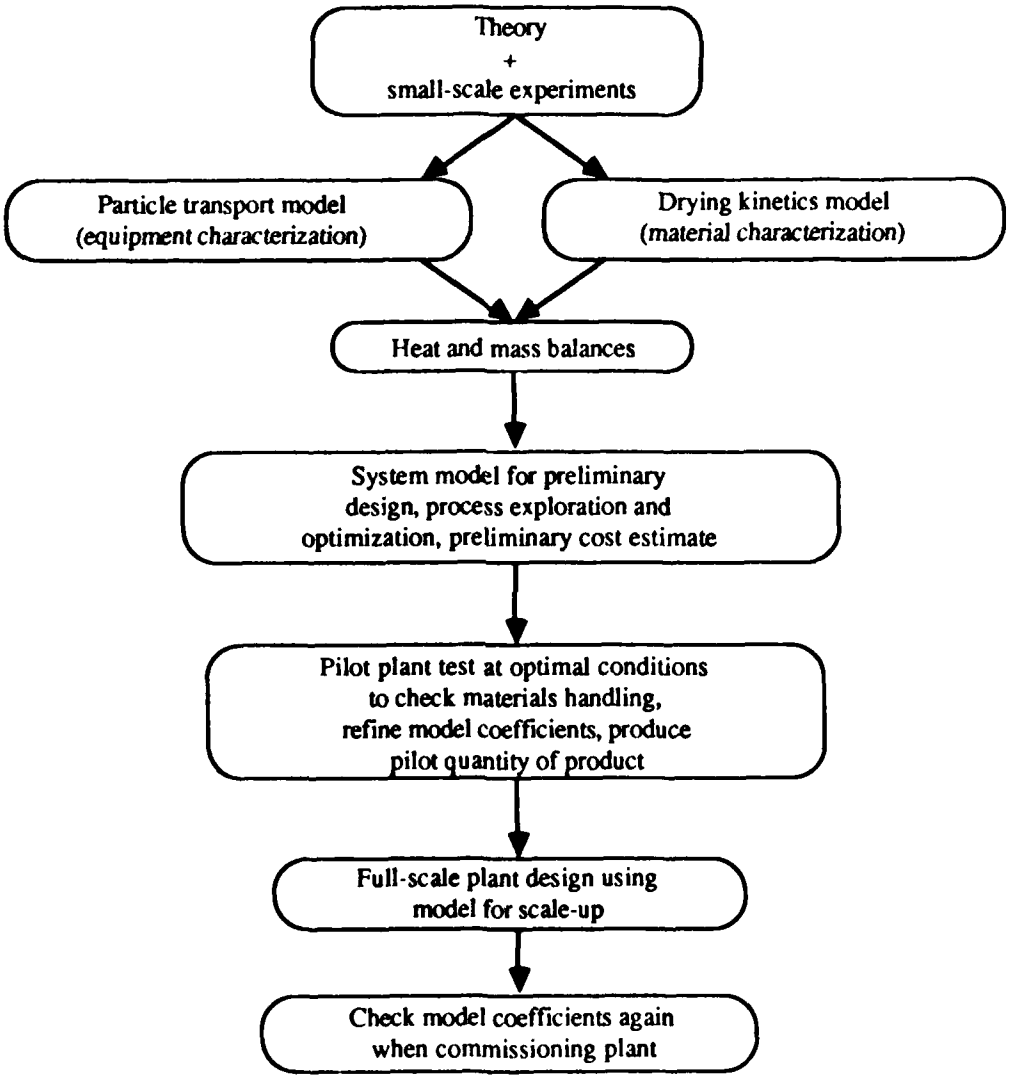

Figure 1-1. The "scientific" approach to dryer design. From Reay (2)

Successful application of dielectrically-augmented drying encompasses a number of tasks. In addition to theoretical and experimental investigations of kinetics of dielectrically-assisted drying, the means of transforming this information into a useful design must be established. Although the general approach to modeling the drying process as shown in Figure 1-1 is valid, the current given methods have several shortcomings. Computation of drying time is generally shown as an analytical integration of a drying rate curve. Or, the integration is accomplished by stepwise calculations of drying rate, referring to psychrometric charts at each step to predict the changing air conditions. Obviously, use of a computer for numerical integration of the drying curve, with a numerical model of air-water thermodynamic properties is a more efficient method. Development of a model of the drying process which includes both conventional and dielectric heating is a prerequisite to the construction of a design model.

In this study, the continuous convective tunnel dryer has been selected as the basis for the design model. This type of dryer is widely used in industry and has been most extensively analyzed in the drying literature. Bench-scale drying rigs with a convective cross flow of air over the material are less complicated than, for example, rigs designed for through circulation or fluidized bed geometries; therefore basic drying kinetics data are more available in the existing literature for convective tunnel drying.

Such drying kinetics data are critcal in the development of a dryer process model. At present little data exists in the literature for dielectrically-

enhanced drying. Therefore, dielectric heating is considered in this work only in general terms. However, the model, which principally describes conventional convective dryers, is structured to include future development of dielectric heating.

The objectives of the present work are to:

- develop a fundamental model of the drying process in a continuous convective tunnel dryer,
- identify an appropriate product kinetics model for integration into the dryer model,
- write a computer code to interface the tunnel dryer model with the product kinetics model which allows for the future addition of dielectric heating,
- validate predictions of the overall system model by comparing with published calculations and experimental data for conventional convective dryers,
- recommend revisions and/or additions to the model, particularly concerning the incorporation of dielectric heating, and identify areas needing further investigation.

The achievement of these objectives is a necessary first step in the transfer of new basic knowledge of dielectrically-enhanced drying processes into useful design tools.

CHAPTER 2

DRYER DESIGN THEORY

2.1 CONCEPTUAL DESCRIPTION OF DRYER DESIGN PROCEDURE

Historically, industrial dryers have been designed from experience and laboratory or pilot scale experiments without regard to drying theory. In response to a question concerning the relevance of drying theory to dryer design, a dryer manufacturer replied: "It is possible to dry a product from experience without having any theoretical basic knowledge. But one cannot, without experience, design a dryer on the basis of the available theoretical knowledge" (1). Only in recent years has the body of basic knowledge grown to be used in theoretical models as a predictive tool for the dryer designer.

2.1.1 Dryer Design from Theoretical Modeling

In considering the path leading to a complete design of a dryer, the designer will decide upon the extent of use of laboratory or pilot scale experiments versus the use of theoretical models for predicting the operation of the constructed dryer. Each type of model, experimental or theoretical, has its own individual merits. If the designer were to run numerous large scale experiments, the experimental model may conform very closely with the final design. But large scale experiments are expensive, representing a large fraction of the overall cost of

design. If the designer were to extensively use a computational model built from theory, the time and expense in performing the dryer simulations would be small in comparison with experimental work. However, there are real limitations on how well models can simulate actual drying processes. Useful computational models of the drying process are not wholly derived from theory. Relevant parameters used in the model, such as the material physical properties and diffusion parameters associated with the heat and mass transfer, are commonly obtained from inexpensive small scale experiments if not already available in the literature. Also, experimental drying rate data can yield empirical functions for use in a design model.

For any particular application there is some optimum balance of both theoretical and experimental modeling in the design. The balance will depend on the amount of experience with similar equipment and materials, the costs of performing the experiments, and the availability of theoretical models that sufficiently describe the drying process. At this time, there is relatively little experience in the design of dryers that incorporate dielectric heating. This lack of experience, and the expense of building large scale experimental dielectric drying apparatus, makes theoretical models of the dielectrically-enhanced drying process especially useful. Some relevant parameters used in the theoretical model can be obtained from data gained in the experimental work, resulting in more realistic simulations. Also, the theoretical model may be used to predict the effect of proposed changes in the operation of the completed full-scale dryer before committing to large capital investments (2).

2.1.2 Desired Capabilities of a Design Model

After selecting the type of dryer, the designer must chose a set of design and operating parameters that meets the specifications established by the user. The primary parameters include throughput or product flow rate, temperature constraints established by the type and desired finished quality of the product, desired final moisture content of the dried product and the entering moisture content of wet product. The primary results of the design are the major dimensions of the dryer, the cross sectional area to accommodate the required product and air flow rates and the required length of the dryer. The air flow conditions of temperature, velocity and mass flow rate throughout the dryer along with energy requirements are also determined.

In designing a conventional dryer for the given specifications, there are many design parameters that can be varied. The temperature, humidity, velocity and mass flow rate of the air stream removing the moisture from the dryer, as well as the convective flow geometry can be varied within the established design constraints. Also the amount and means of heat transfer can be varied within the specified temperature constraints of the product. In most dryers, convection from hot air is the primary mode of heat transfer to the product. The rate of convective heating is proportional to the convective heat transfer coefficient and the temperature potential between the surface and the bulk air stream. The primary control over convective heating is by varying the velocity of the air stream, which affects the convective heat transfer coefficient, and changing the bulk air temperature, affecting the temperature potential. The designer can vary the bulk air stream temperature

through the dryer by changing the air mass flow rate or by heating the air stream through heat exchangers such as steam coils. The designer may consider using isothermal air conditions where heat is added throughout the length of the dryer to maintain a constant air temperature. Methods commonly used to augment convective heating is radiation from hot surfaces or elements visible to the product and conduction by direct contact with the product, for example wet paper webs dried by hot rollers (3).

Of current interest are dryers incorporating microwave or radio frequency dielectric heating. When coupled with conventional drying, the dielectric heating rate becomes an additional parameter which may be controlled by the designer. Although dielectric energy is radiative, its volumetric absorption quality, in contrast to the surface absorption of infrared, makes the heating of materials fundamentally different . The amount of dielectric heating can be varied by altering the amount of time the product is in the electric field, which corresponds to the length of the region of dielectric application, and by changing the intensity of the electric field. Further discussion considering dielectric heating in dryer design is presented in Chapter 5.

2.2 MODELING DRYING PROCESSES

An overall drying process model must include a model of the drying product that will allow the prediction of drying rates within the dryer. This product model may be constructed from empirical data or from drying theory. If constructing an empirical model from experimental data, knowledge of drying

theory is required in the data analysis to produce empirical relationships that describe the drying behavior over a wide range of drying conditions. Drying theory can be separated into the study of thermal and moisture mass transport within a material and the study of the thermal and mass transport between the material and the air stream.

2.2.1 Air Properties and the Air/Water Interface

Moisture removed from a product by drying results in the humidification of air. As the product progresses through the dryer, the confined air stream becomes progressively humidified. Just as the temperature of the air stream limits the convective heat transfer to the product, the humidity level of the air stream at a particular position in the dryer controls the local convective drying rate, since this drying rate is proportional to the humidity potential between the moist product and the air stream. In order to compute changes in air conditions due to simultaneous humidification and heat loss due to convection, a model of the thermodynamic properties of moist air is required.

Dry air is composed of a mixture of gases, the primary constituents being nitrogen, oxygen, argon and carbon dioxide. The primary constituent of interest in the case of drying is water vapor, which will hereafter be referred to simply as "vapor". It is convenient to describe the humidity, as well as other thermodynamic properties, on a dry air mass basis, the ratio of the mass of vapor to the mass of dry air (kilograms H_2O per kilogram dry air). Here it is important to note the distinction between absolute humidity as defined above, and relative

humidity. Relative humidity is a percentage measure of the air humidity to the humidity of saturated air at the given temperature. An alternate definition of relative humidity is given as the ratio of the partial pressure of water vapor to the saturated vapor pressure. (3)

In order to evaluate an energy balance between the moist product and the air stream, the enthalpy of moist air must be characterized. Assuming an ideal solution, the enthalpy of moist air can be defined as the sum of the partial enthalpies of the components.(4) This definition does not account for the relatively small heat of mixing and other residual enthalpies, which amount to only 0.63 kJ/kg for air saturated with water vapor at 60° C (3). Accordingly, for the air/water vapor mixture the expression for enthalpy is

$$h_a = h_{da} + Y_a h_v \qquad (2\text{-}1)$$

where h_a is the enthalpy of the humid air, h_{da} is the enthalpy of dry air, h_v is the enthalpy of the moisture vapor and Y_a is the humidity.

During drying, water vapor is transferred from the exposed surface of the material into the air stream and heat may be, in general, transferred to the surface from the air stream (Figure 2-1). During conventional drying vapor diffusion between the surface and the bulk air stream determines the drying rate. According to Fick's law, the diffusive flux is proportional to the vapor concentration gradient. Although vapor concentration may be expressed in terms of

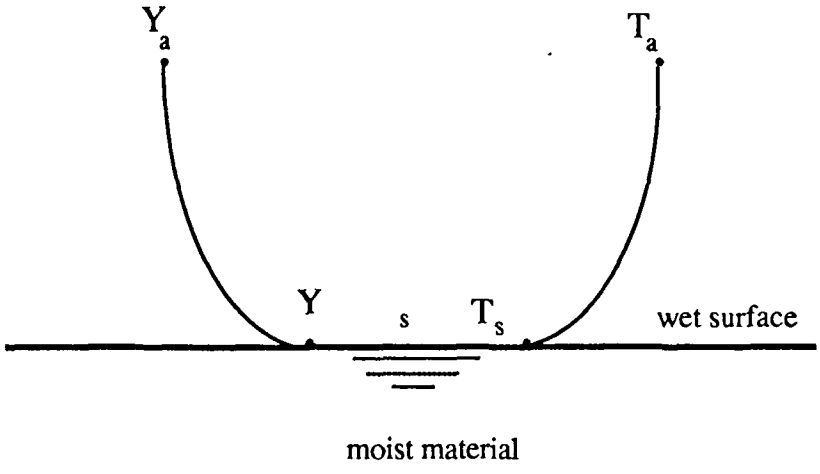

Figure 2-1. Humidity and temperature profiles near a wet surface.

vapor pressure, it is more convenient for the purposes of dryer analysis to express the concentration in terms of the humidity Y.

From Fick's law and some constant property assumptions, an expression for the rate of vapor transfer from a moist material surface diffusing into the air stream may be derived from film theory.(3) The vapor flux is given by

$$N_w = F\, M_w \ln\left[\frac{D + Y_s}{D + Y_a}\right] \qquad (2\text{-}2)$$

where the logarithmic term is the potential between the humidity at the surface Y_s and the humidity of the bulk air stream Y_a. F is a mass transfer coefficient and M_w and D are the molar mass of water and the molar mass ratio of the water to air, respectively. Note that the term for the humidity potential is not a simple linear difference between the bulk air humidity and the surface humidity, but is logarithmic.

The moisture vapor flux N_w is proportional to a logarithmic potential rather than a linear potential because the moisture mass velocity through the surface distorts the velocity and concentration profiles.(21) In the limit, at very low mass transfer rates, this effect may be neglected and the logarithmic potential approaches a linear one, hence

$$N_v = F\, M_g\, (Y_s - Y_a) \qquad (2\text{-}3)$$

where M_g is the molar mass of air. A similar expression for the heat transfer between surface and bulk conditions, the familiar Newton's law of cooling, can be written:

$$q = h\,(T_a - T_s) \tag{2-4}$$

The similarity between heat and mass transfer from a surface is discussed further in the subsection on heat and mass transfer analogies.

In practice, F and M_g shown in Eq. 2-3 are combined into a single mass transfer coefficient K_o. The single coefficient may also be used with Eq. 2-2 where FM_w is equivalent to K_oD.

$$N_v = K_o\, D \ln\left[\frac{D + Y_s}{D + Y_a}\right] \tag{2-5}$$

By expanding the logarithmic humidity potential term in Eq. 2-2, and using the single mass transfer coefficient K_o, an expression for drying flux based upon a simple linear potential may be written,

$$N_v = K_o\, \phi\, (Y_s - Y_a) \tag{2-6}$$

where the deviation of the simplified linear potential from the derived logarithmic potential attributed to significant mass transfer rates is accounted for by the coefficient, ϕ. The deviation ϕ may be given by the product of two separate coefficients

$$\phi = \phi_1\, \phi_2 \tag{2-7}$$

which result from the expansion of the logarithmic term (3). The humidity potential coefficients ϕ_1 and ϕ_2 are functions of humidity level (Y_s), and humidity potential (Y_s-Y_a) respectively. Figure 2-2 indicates the limiting magnitudes of the humidity potential coefficients as a function of the moist surface humidity. For the plot of ϕ_2^o, the bulk air stream humidity is at the limiting condition of the maximum potential, $Y_a = 0.0$, corresponding to perfectly dry air. A thorough analysis of the humidity potential coefficients and the linearized expression for flux may be found in the paper by Keey, et al.,(5) and in the text by Keey (3).

For a fully wetted surface, the water vapor immediately adjacent to the liquid surface exerts full vapor pressure such that the surface humidity is equivalent to the saturated humidity at the surface temperature. For constant pressure, the saturation humidity is a function of temperature only, therefore the drying flux from a fully wetted surface may be evaluated knowing the mass transfer coefficient, the bulk air stream humidity and the moist surface temperature. A simple surface energy balance yields

$$q = h^*(T_a - T_s) - N_v h_{fg} \qquad (2\text{-}8)$$

where q, the net heat flux transferred into the material is equivalent to the difference between the heat convected to the surface and the heat associated with the water evaporating and leaving the surface (the product of the moisture flux N_v and the latent heat of vaporization h_{fg}). Here the heat transfer coefficient, shown as h^*, differs from the conventionally derived convective heat transfer coefficient in that h^* accounts for the influence of mass transfer at the surface. In most ordinary

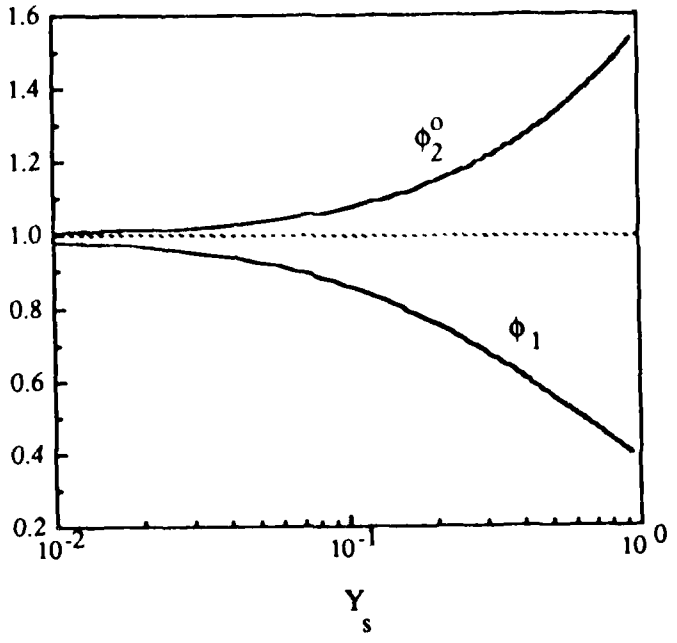

Figure 2-2. Humidity potential coefficients for water vapor diffusing through air. Adapted from Keey (3)

cases of moisture evaporating into an air stream, the influence of mass transfer on the convective heat transfer coefficient is negligible. The derivation of an expression accounting for the influence of the surface moisture mass transfer on the convective heat transfer coefficient, the Ackermann correction, is shown in Keey (3); in the balance of this discussion, the correction will be assumed to be negligible.

Upon combining Eqs. 2-6 and 2-8, and assuming $h^* = h$, the resulting surface energy balance

$$q = h(T_a - T_s) - K_o \phi (Y_s - Y_a) h_{fg} \tag{2-9}$$

shows that the rates of the simultaneous heat and mass transfer at the surface depend upon the transport coefficients h and K_o. In separate boundary layer analyses of these two coefficients, the governing equations describing the transport of either heat or mass at a surface are very similar. Thus, there is an analogy between heat and mass transfer. When the equations supporting the analysis are normalized, the dimensionless form of the transport coefficients (the Nusselt number and the Sherwood number) show the same dependence upon the Reynolds number, $Re_x = ux/\nu$,and similar dependence upon the respective dimensionless property parameters for heat and mass transfer, the Prandl number and the Schmidt number.

$$Pr = \frac{C_p \mu}{\kappa} \tag{2-10}$$

$$Sc = \frac{\mu}{\rho D} \tag{2-11}$$

$$Nu_L = \frac{hL}{\kappa} = f(Re,Pr) \tag{2-12}$$

$$Sh_L = \frac{K_o L}{D} = f(Re,Sc) \tag{2-13}$$

Empirical correlations for convective heat or mass transfer coefficients are presented in terms of these dimensionless parameters. Correlations for mass transfer coefficients are less abundant in the literature than for convective heat transfer coefficients, and thus mass transfer correlations are often obtained from heat transfer correlations through the use of heat and mass transfer analogies. The Sherwood number may be obtained from a correlation of the Nusselt number by simply replacing the the Prandl number with the Schmidt number.

At this point, it should be stressed that the analogy between heat and mass transfer contains the very important assumption of a relatively low mass transfer rate at the surface. Although the governing boundary layer equations for heat and mass transfer are similar, the boundary condition of a significant mass velocity at the surface distorts the velocity, concentration, and temperature profiles. The concentration profile is affected to a greater extent than the temperature profile and the rate coefficients do not hold the same proportionality given by the heat and mass transfer analogy. Thus, the heat and mass transfer analogy relates the transport coefficients, h and K_o, under conditions of low mass transfer at the surface. A complete and detailed coverage of the analogies of heat and mass

transfer is found in the text on the analysis of heat and mass transfer by Eckert and Drake (6).

The heat and mass transfer analogy, assuming turbulent flow over the surface, yields the Chilton-Colburn expression (3)

$$\frac{K_o}{h} = \frac{\beta\, Le^{2/3}}{C_p} \tag{2-14}$$

where Le is the Lewis number, the ratio of Prandl to Schmidt number (31)

$$Le = \frac{Pr}{Sc} = \frac{C_p\, \rho\, D}{\kappa} \tag{2-15}$$

This dimensionless parameter, particularly in the European literature, is also known as the Luikov number, Lu.

The dimensionless coefficient β accounts for differences in the way the mean velocity is computed in heat and mass transfer. An expression for determining β is given by Keey (3) and shown in Appendix B; for an air water system the value of β is near 1.0. The specific heat, C_P, is evaluated at the mean conditions of the humid air between the surface and the bulk air stream. The magnitude of the Lewis number for an air water system is near 1 such that a rough estimate of the mass transfer coefficient may be found by dividing the convective heat transfer coefficient by the mean specific heat of the humid air stream.

Another approach to describing the relationship between the heat and mass transfer coefficients is derived from the surface energy balance, Eqn. 2-9, for an equilibrium, steady state condition where the net heat flux is zero. That is, the

heat convected to the surface from the air stream is exactly balanced by the heat content of the evaporative flux.

$$h(T_a - T_s) = K_o \phi (Y_s - Y_a) h_{fg} \qquad (2\text{-}16)$$

Consider steady flow of air at bulk air conditions of T_a and Y_a, over a fully wetted surface. Given the heat and mass transfer coefficients, h and K_o, and considering that the terms ϕ and h_{fg} may be determined from the moisture and temperature values, the remaining unknown variables are the surface temperature T_s and the surface humidity Y_s. Recalling that at constant pressure the surface humidity is a function only of the surface temperature, the remaining variable that may by solved for, T_s, is known as the wet bulb temperature, T_w. The wet bulb temperature is defined as the equilibrium temperature reached by a small amount of liquid evaporating into a very large mass of unsaturated humid air (7). The large mass of air and the small mass of liquid mandates that the air conditions of temperature and humidity are constant. To determine air humidity, a sling psychrometer may be used where the steady state temperature of a wetted bulb moved rapidly through the air corresponds to the wet bulb temperature. The wet bulb temperature along with the ordinary air temperature (dry bulb temperature) is taken to determine the air humidity or relative humidity through the use of either a graphical model of the air water system (a psychrometric chart) or iterative solution of analytical equations.

Rewriting Eq. 2-16,

$$\frac{Y_s - Y_a}{T_a - T_s} = \frac{h}{K_o \phi h_{fg}} \qquad (2\text{-}17)$$

the dependence of the equilibrium conditions on the ratio of the heat and mass transfer coefficients is shown. Recall that both the coefficients are equivalently dependent upon the Reynolds number such that their ratio cancels this dependence. Between very low Reynolds numbers, where the relative magnitude of the mass velocity invalidates the heat and mass transfer analogy, and very high Reynolds numbers, where viscous dissipation may void the analogy, the wet bulb temperature is independent of flow velocity or geometry, and governed by the diffusive and thermodynamic properties of the humid air only.

A related psychrometric property is the adiabatic saturation temperature. Consider the process shown in Figure 2-3 in which humid air enters an adiabatic control volume at a given temperature, humidity, and dry air mass flow rate, contacts the liquid in the volume, gaining moisture and changing temperature, and leaves the volume at different conditions. If the volume is very long such that the air leaves at a saturated condition, and moisture is supplied at the leaving saturated temperature of the humid air at a rate such that the amount of liquid moisture in the volume is constant, the corresponding energy balance yields(7)

$$\frac{Y_{as}-Y_{a1}}{T_{a1}-T_{as}} = \frac{C_{pv}}{h_{fg}} \qquad (2\text{-}18)$$

The adiabatic saturation temperature for air at a given temperature and humidity is dependent upon the thermodynamic parameters of humid specific heat and latent heat of vaporization.

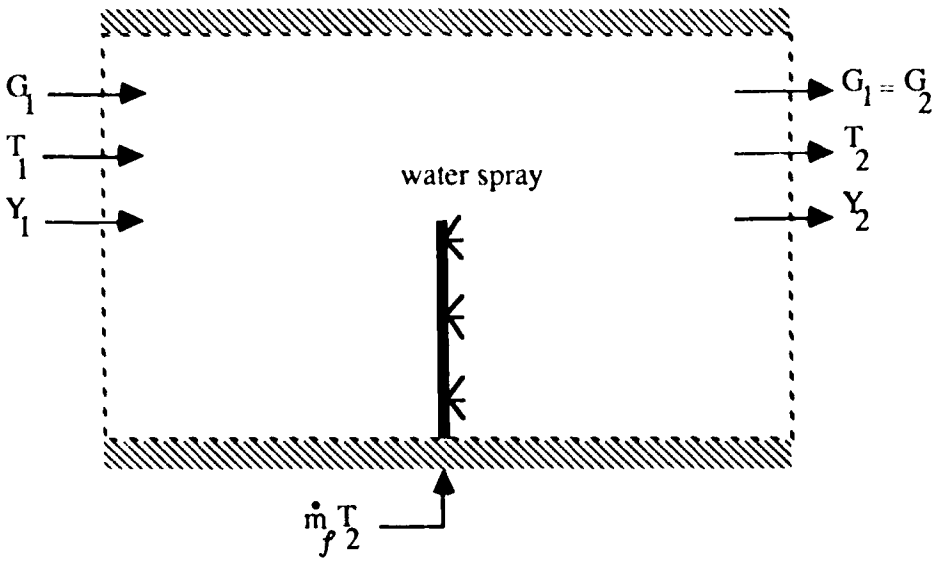

Figure 2-3. Control volume for adiabatic saturation process

Assuming ϕ=1 the combination of Eqs. 2-14 and 2-17 gives a similar expression for the wet bulb process

$$\frac{Y_s - Y_a}{T_a - T_s} = \frac{C_p}{\beta \, Le^{2/3} \, h_{fg}} \qquad (2\text{-}19)$$

Note that for the air water system β is very close to one and the Lewis number for humid air at less than extreme conditions is also very close to one. It then follows that, except for extreme conditions, Eqs. 2-18 and 2-19 are approximately equivalent and the wet bulb temperature is approximately the same as the adiabatic saturation temperature. Some thermodynamic models of the air water system used for analysis of air conditioning equipment, such as psychrometric charts, use the adiabatic saturation temperature as a parameter but will refer to this temperature as the thermodynamic wet bulb temperature. It is reasoned that the term "wet bulb temperature" is used because the actual wet bulb temperature is easily measured in the field by instruments like the sling psychrometer. In the ASHRAE Fundamentals Handbook, the analysis of an expression called the thermodynamic wet bulb temperature is based upon the energy balance of adiabatic saturation (8). This approximate equivalence of wet bulb temperature and adiabatic saturation temperature is shown to hold for the air water system and may not apply to other vapor-gas systems. The deviation of wet bulb temperature from adiabatic saturation temperature increases as the wet bulb temperature decreases. An analysis of this deviation as applied to drying may be found in the paper by Ashworth and Keey (2).

2.2.2 Moisture Transport in Porous Solids

Drying of a moist product is a complicated process, involving coupled heat and mass transfer, the mass transfer being the movement of the moisture through and out of the product and the heat transfer being the energy or heat transferred into the product required to evaporate the moisture. The complications arise from the consideration of the numerous relevant parameters needed to give even a very rough prediction of the dynamic moisture and temperature profiles and moisture and heat fluxes of drying product. In a text on practical industrial drying by Nonhebel and Moss, a list of some 34 factors affecting drying of solids is presented (10). Some of the primary factors include transport coefficients such as the thermal conductivities of the wet solid, the nearly dry solid and the moisture, and the moisture diffusivity of the solid. For any given product of interest, these properties are most likely variable and anisotropic.

The relative dryness of a material is quantified by its moisture content. In the course of drying, some materials shrink or otherwise alter the available displacement of moisture in the material. It is therefore most convenient to define moisture content, as well as moist product enthalpy, on a bone dry mass of solids basis. In this manner moisture content is given as the ratio of the mass of moisture to the mass of bone dry solid (e.g., kilogram H_2O per kilogram of dry solid).

The term "bone dry" is best understood after considering the hygroscopicity or nonhygroscopicity of a moist material. Moisture contained in the material may be either free or bound; the vapor pressure exerted by bound moisture

is less than that of free moisture. Materials with bound moisture (e.g., potatoes, fruits, clay, bar soap and silica gel) are said to be hygroscopic, while those materials which contain only free moisture (e.g., sand) are said to be nonhygroscopic. A hygroscopic material has a given equilibrium moisture content, X^*, when in equilibrium with air at a given relative humidity. Although simply stated here, hygroscopicity can be a matter of degree. Materials with chemically bound moisture, such as water of crystallization or cellular moisture, are highly hygroscopic. Some materials have lightly bound moisture, bound by weak links with confining walls of capillaries with micropores smaller than one micron, and may be said to be slightly hygroscopic. A thorough discussion of hygroscopicity is found in Reference 11. Bone dry mass refers to the mass of a material, hygroscopic or nonhygroscopic, that contains no moisture, either free or bound.

As a product dries, internal moisture is driven to the surface where it is removed into the air stream. The mechanisms of moisture movement within a material relevant to drying, in addition to simple gravity driven flow, are in general classified in four basic categories (7,11):

> Capillary flow. In a porous or granular material, such as sand, unbound liquid moisture is transported through the interstices or capillaries of the solid, driven primarily by surface tension forces. This movement also describes the moisture flow apparent in wetting a wick. One description of the potential for this flow is the gradient of the fractional volume of moisture. Porous materials in which capillary flow predominates during drying are commonly referred to as capillary porous, and are generally nonhygroscopic or slightly hygroscopic.

Vapor diffusion. Vapor from subsurface evaporation will diffuse through a solid in the presence of a vapor pressure gradient. Applying heat to one surface while drying from the other creates a temperature gradient with a corresponding vapor pressure gradient.

Liquid diffusion. Moisture concentration gradients between the high concentration region of the moist interior and the low concentration region near the surface may drive diffusion of liquid moisture. This description of moisture movement is limited to drying solid solutions, such as soaps, glues or gelatins, and to certain cases of drying bound moisture as in clay, flour, paper and wood. Liquid diffusion differs from capillary flow in that a solid-liquid interface is not necessarily present.

Pressure driven flow. If a material changes its solid structure during drying as evidenced by shrinkage, moisture may be forced through the material and driven to the surface. Internal pressure gradients may also be produced by internal heating of the product, as in dielectrically assisted drying.

Condensation and evaporation. This process occurs in porous materials when liquid present in the waist or constrictions of pores, evaporates into a more voluminous region of the pore and then condenses at another waist or constriction, bridging it with liquid.

Different mechanisms of drying may be evident for particular stages of drying as shown in Figure 2-4. A detailed explanation of the mechanisms of drying may be found in texts by Luikov, Keey, and Treybal (12,11,7).

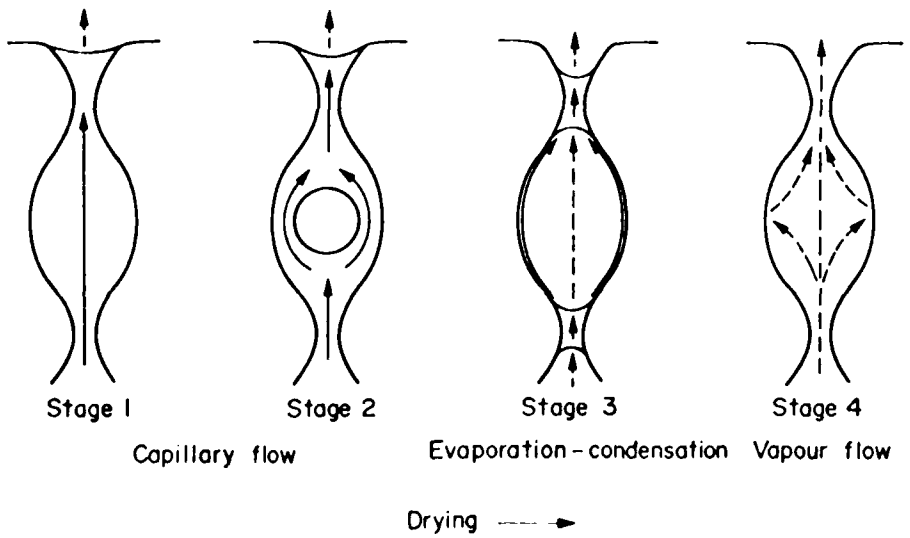

Figure 2-4. Moisture at various stages in the drying of a porous material
From Keey (3)

2.2.3 Modeling of Drying

The prediction of drying rates solely from theoretical modeling seldom results in accurate predictions except for simple materials in which the mechanisms for heat and moisture transfer are well understood. The more common approach to describing drying behavior for use in dryer design is to empirically study the drying rate based upon the effect of external conditions (13). Experimental drying rate data for a sample of material is taken under constant external conditions of air humidity, temperature, and velocity. The fundamental measurement is mass of the sample as a function of time, as shown in Figure 2-5a. Here, the dry material mass is subtracted from the overall mass measurement to show the moisture mass as a function of time. Care is taken to ensure no particles of material are entrained into the air flow such that the only change in mass measured is that of the moisture.

To describe the drying rate of the material using this experimental data, the slope of the mass-time curve is calculated and plotted against moisture content, as shown in Figure 2-5b. Following this curve, the drying proceeds from right (high moisture content) to left (low moisture content). In practice various mathematical functions are fit to different regions of the mass-time curve and the time derivatives of these functions computed. Either method yields a moisture mass flow which, when divided by the exposed surface area from which the drying took place, gives the drying rate flux N_v. This plot of drying rate flux vs. moisture content is referred to as the drying rate curve and is applied extensively in the design and evaluation of conventional drying equipment.

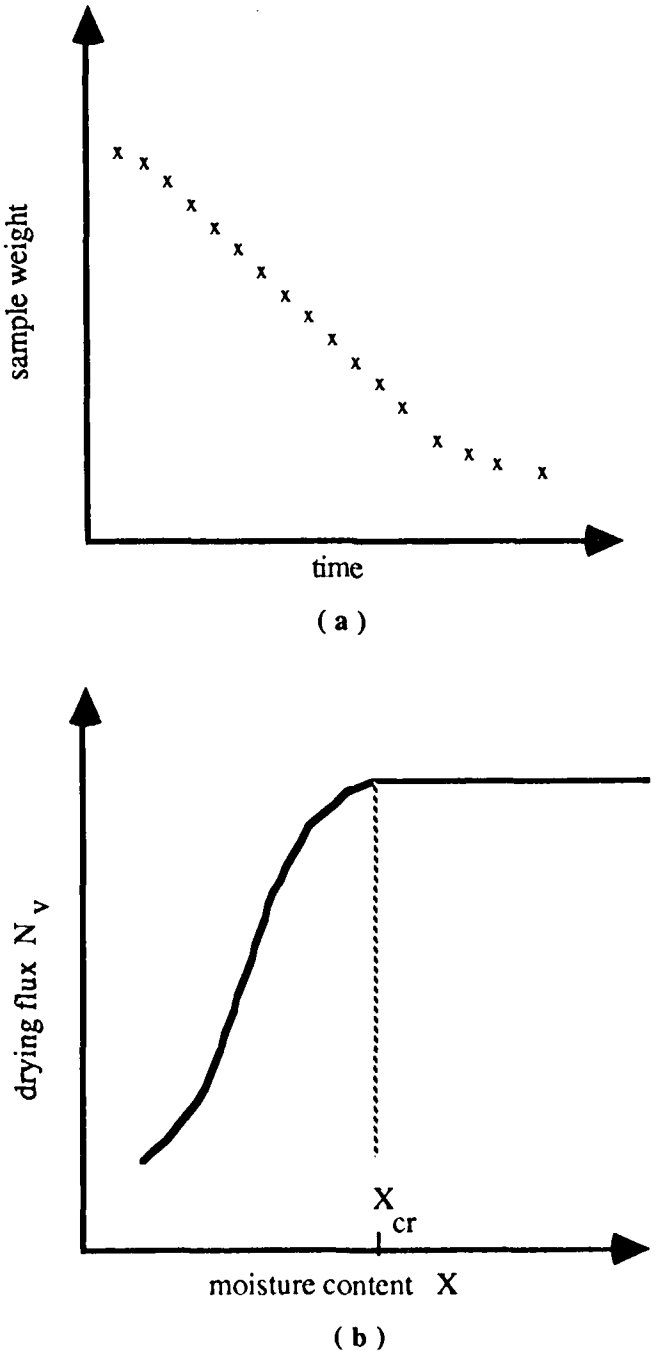

Figure 2-5. a) Typical experimental drying test data
b) Drying rate curve

If the drying experiment begins with a saturated material such that the surface is fully wetted, the wet surface will quickly approach the wet bulb temperature, and the surface humidity will be nearly equivalent to the saturated humidity at the wet bulb temperature, Y_w. Thus a constant drying rate will occur and the external air conditions, air temperature, humidity and velocity, will entirely determine the drying rate. According to Eq. 2-6 the constant drying rate N_{vo} will be

$$N_{vo} = K_o \phi (Y_w - Y_a) \tag{2-20a}$$

Or in terms of the logarithmic potential, the flux is given by

$$N_{vo} = K_o D \ln\left[\frac{D + Y_w}{D + Y_a}\right] \tag{2-20b}$$

During this period, the rate of liquid moisture driven to the surface by the internal mechanisms of moisture movement must be sufficient to keep the surface fully wetted. Although simply described here, the period of constant drying rate is still not fully understood, and may not appear for the drying of highly hygroscopic materials (14). When moisture no longer moves to the surface at the same rate as the free evaporation, the drying rate falls and is controlled by the internal mechanisms of moisture transport. Materials with different internal moisture transport mechanisms will exhibit different shapes of drying rate curves during the falling rate period. Materials classified as capillary porous generally have a linear falling rate period while hygroscopic porous or colloidal materials will exhibit more

complex, nonlinear falling rates. A thorough discussion is presented by van Brakel (14) on the period of constant drying rate and subsequent diminished drying rate.

The moisture content at which the drying rate changes from a constant rate to a falling rate, as shown in Figure 2-5b, is called the critical moisture content X_{cr}. Below the critical moisture content, drying is hindered by limitations on internal moisture movement. Where there is no sharp change in the drying rate curve, the critical moisture content may be estimated graphically. The critical moisture content is not constant for a given material but depends upon the initial drying rate, the material thickness, and the material temperature (11). Critical moisture contents for certain materials are listed in the Chemical Engineer's Handbook(13), but should be taken only as typical values.

Although data may be taken for a given material over a range of constant external conditions, the general form of the drying rate curve may be similar in each case. The shape of the similar curves is a characteristic of the given material; thus it should be possible to create a "characteristic drying curve" by normalization of the drying rate and moisture content (3). Although the characteristic drying curve arises from the similarity of experimental data, theoretical development shows that there is no true single characteristic drying curve for a material. The theoretical curve is shown to be a function of the material form, thickness, initial drying rate, and the wet bulb temperature of the air stream. However, for a continuous dryer in which the material form and thickness as well as inlet drying conditions are not changed, the influence of the wet bulb temperature is second order and a single characteristic curve may be assumed (18).

An obvious basis for normalizing the drying rate under purely convective heating conditions is the constant drying rate N_{vo}, which represents the drying rate from a fully wetted surface. The relative drying rate f, is defined as

$$f = \frac{N_v}{N_{vo}} \tag{2-21}$$

and accordingly, the relative moisture content is normalized on the basis of the critical moisture content. For a nonhygroscopic material the characteristic moisture content Φ is

$$\Phi = \frac{X}{X_{cr}} \tag{2-22}$$

where X and X_{cr} are averaged moisture contents for the material as the moisture content will have a gradient through the depth of the material. For hygroscopic materials, the normalized moisture content represents the amount of free, unbound moisture.

$$\Phi = \frac{X-X^*}{X_{cr}-X^*} \tag{2-23}$$

where X^* is the equilibrium moisture content for hygroscopic material at a given value of the air humidity.

A typical characteristic drying curve is shown in Figure 2-6. where

$$f = f(\Phi) \tag{2-24}$$

At characteristic moisture contents above $\Phi = 1$, the drying is unhindered and the relative drying rate is therefore equal to one. For moisture contents below critical

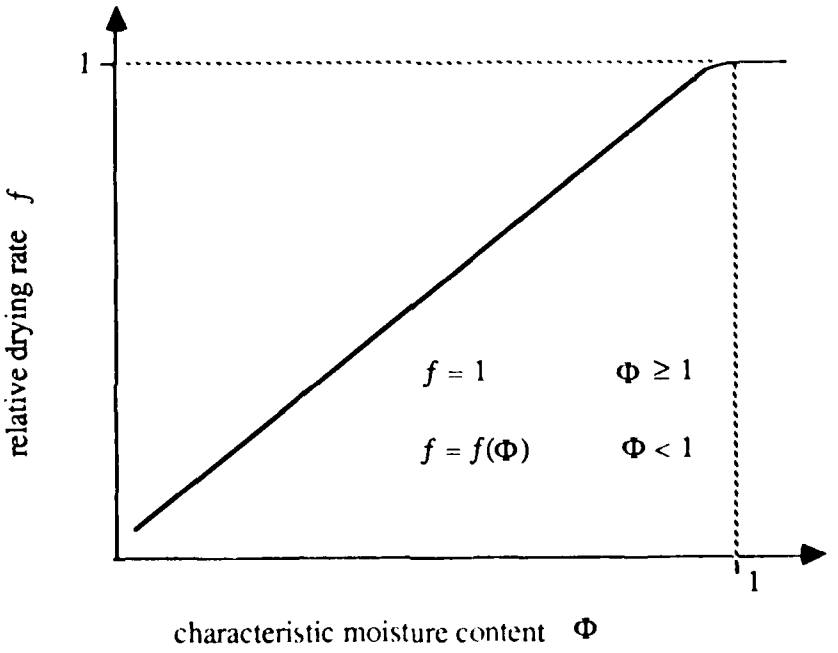

Figure 2-6. Characteristic drying curve

the drying rate may be predicted from the characteristic drying curve by combining the definition of the relative drying rate with Eq. 2-20a or 2-20b for the drying rate from a fully wetted surface at humidity Y_w,

$$N_v = f K_o \phi (Y_w - Y_a) \tag{2-25a}$$

$$N_v = f K_o D \ln\left[\frac{D + Y_w}{D + Y_a}\right] \tag{2-25b}$$

All of the parameters used to evaluate the drying rate from Eqs. 2-25a and 2-25b, except the relative drying rate f, are computed solely from the external air conditions: Y_w, the saturated wet bulb humidity, Y_a, the bulk air humidity, ϕ, the humidity potential coefficient which is a function of Y_w and Y_a, and K_o the mass transfer coefficient. It is the function for the relative drying rate in terms of a characteristic moisture content, $f = f(\Phi)$, that fully accounts for the hindered drying rate due to the internal mechanisms of moisture movement.

Although assumed to be derived from experimental data, the characteristic drying curve may in principle be derived analytically or numerically from theory describing the falling drying rate. Using simplified drying models, Keey and Suzuki derive analytical expressions for characteristic drying curves typical of porous non-hygroscopic materials (15,16).

The concept of the characteristic drying curve is a powerful tool for the dryer designer in that the drying rate for a given material under the varying range of air conditions encountered in a dryer may be computed from Eqs. 2-25a or 2-25b if

the characteristic drying curve is available from limited laboratory or theoretical studies. It is important to note, however, that the drying rate curve as discussed above will in general not be applicable to drying with dielectric or radiative heat sources (e.g. infrared). Successful incorporation of these phenomena will require a redefinition of the procedure by which drying rate data are normalized. This is discussed at greater length in Chapter 5.

In addition to use of the experimentally determined characteristic drying curve, two simplified models of the diminished drying rate have been used in the analysis of drying for porous materials (3). Predicted characteristic drying curves often differ from the experimentally determined drying curves and hence, in general, should not be used in dryer design. Simple drying models, however, provide insight into the physical processes responsible for qualitative drying behavior.

Following the constant rate period where the surface is fully wetted, the wetted surface model describes the subsequent decrease in the drying rate as a consequence of the surface becoming only partially wetted. As drying proceeds the wet surface becomes discontinuous with dry regions appearing (17). Reduction in the surface area from which the moisture evaporates accounts for the diminishing drying rate. For the simply described wetted surface model, the relative drying rate f has been derived as

$$f \quad \Phi^{2/3} \tag{2.26}$$

Use of the wetted surface model as an analytical tool is limited. It is not physically realistic except in the case of very thin materials such as paper webs (3).

The other simplified model, which has been more widely discussed in the literature is the receding plane model. This model assumes that as drying progresses into the falling rate period, a plane of moisture from which evaporation takes place recedes into the material parallel to the surface. Drying is hindered due to the thermal and vapor diffusive resistance of the dry region. Experimental studies have supported this theory for describing the drying of porous non-hygroscopic materials (18).

Considering constant and isotropic diffusivities of vapor and heat, the humidity and temperature gradients in the dry region should be as shown in Figure 2-7. Although drying is a transient phenomenon, quasi-steady analysis with linear profiles is valid if the time scale for the rate of recession is large compared to the time required for a steady state response of the temperature and humidity gradients to the moving boundary. Arzan and Morgan (18) investigated this assumption through use of a numerical model of the drying process considering a transient receding plane and found that during all but the terminal period of drying, the quasi-steady treatment was valid. The authors were inconclusive concerning the validity during the final stages of drying to a bone dry material.

The receding evaporative plane model has been used to predict characteristic drying curves for porous non-hygroscopic materials.(15,16) The function for the relative drying rate is developed in terms of the depth of the

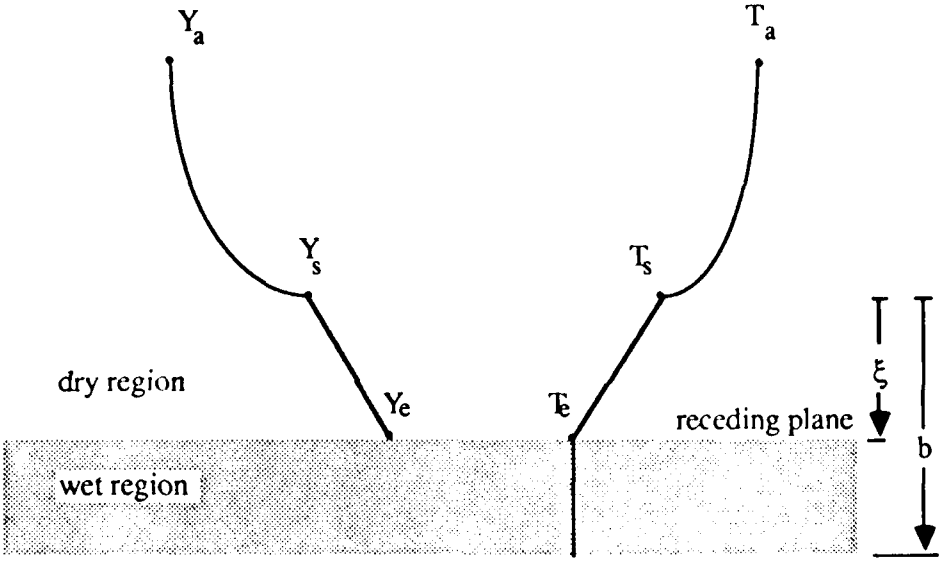

Figure 2-7. Humdity and temperature profiles associated with the receding plane model of moisture movement

evaporative plane ξ relative to the total thickness b, and the mass transfer Biot number, $Bi_m = K_o b/\underline{D}_a$, where $\underline{D}_a$ is the vapor diffusivity in the dry region. The depth of the plane depends on the distribution of the moisture below. If drying is rapid, a sharply defined front may sweep through the material as shown in Figure 2-8b. For mild drying conditions, the moisture gradient below the front will be less severe as show in Figure 2-8a. Rather than using the diffusion model for moisture transport, another approach for predicting drying characteristics is to use the relationship between the capillary suction pressure and the moisture content. This approach, along with the evaporative plane model, is used for predicting drying rate curves and critical moisture contents of coarse granular materials (19).

The moisture content profile is a function of the diffusion of moisture in the wet region, and of the boundary conditions. Assuming Fickian movement of moisture beneath the front, and a constant moisture diffusivity, a parabolic profile as shown in Figure 2-8a may be derived (16). The evaporative plane is the boundary at which the moisture evaporates and diffuses out through the surface. The evaporative flux is proportional to the moisture concentration gradient at this boundary. For a constant material dry density ρ_s, the boundary condition is

$$N_v = \rho_s \underline{D}_a \left.\frac{\partial X}{\partial y}\right|_{y=\xi} \qquad (2\text{-}27)$$

Of course, for an impermeable boundary at the bottom of the material, y = b, the boundary condition is that of zero moisture flux.

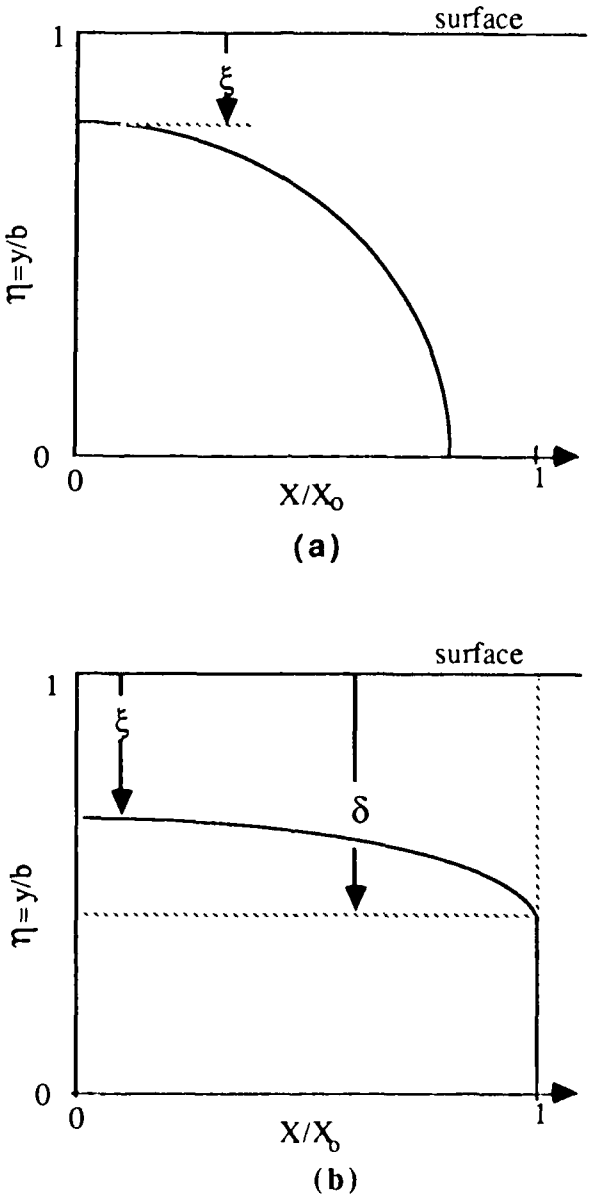

Figure 2-8. Moisture content profiles associated with the receding evaporative plane in a) gentle drying, and b) intensive drying

At the onset of hindered drying, when the material is at an average critical moisture content X_{cr}, the front is at the surface ($\xi = 0$) and the parabolic profile extends through the material. Using this profile and the given boundary conditions, the local critical moisture content at the base of the material, X_{1cr}, is given as

$$X_{1cr} = \frac{N_{vo} b}{2\rho_s D_a} \tag{2-28}$$

And for this profile, the average critical moisture content is simply

$$X_{cr} = \frac{2}{3} X_{1cr} \tag{2-29}$$

For a given porous nonhygroscopic material, the receding plane model along with the foregoing assumptions, yields a function for the critical moisture content in terms of the initial drying rate and the material thickness. The same analysis is used to derive an expression for the critical moisture content in the case of high intensity drying where the moisture content profile is as shown in Figure 2-8b. For the high intensity case, the region of diminished moisture content does not extend through the material as the region below δ remains at the initial moisture content X_o. In this case the critical moisture content is given by (3)

$$X_{cr} = \left[1 - \frac{2}{3} \frac{N_v b}{\rho_s X_o D_a}\right] X_o \tag{2-30}$$

The dimensionless parameter used in Eqs. 2-28 and 2-30, $\frac{N_v b}{\rho_s X_o D_a}$, is called the intensity of drying, N. For larger values of N the drying is severe and the moisture content profile has a narrow zone of steep gradient as shown in Figure 2-8b. For

smaller values of N there is a wide zone indicative of gentle drying conditions as shown in Figure 2-8a. It is shown that for a drying intensity of N greater than 2, the parabolic profile does not extend through the entire depth of the material (Figure 2-8b) and the drying is classified as high intensity. For N less than 2 the drying is classified as low intensity (3).

Figure 2-9 shows the relationship between critical moisture content and the drying intensity given by Eqs. 2-28 and 2-29. This theoretical critical point curve is for a nonhygroscopic slab-form material with constant diffusivity. For real materials the moisture diffusivity D_a is not constant but dependent upon the moisture content. Some consideration of variable diffusivity with the evaporative plane model is given in the referenced literature (15,16,3).

2.2.4 Applied Drying Theory

In applying drying theory to a usable model for design, the modeling problem can be separated into two distinct areas: 1) model of the drying kinetics, referred to as the "product model", and 2) model describing the material's interaction with the air stream, the "equipment model" (2).

For the model developed in this report, the characteristic drying curve, along with equilibrium and critical moisture content data, provides the product model. The characteristic drying curve will predict the local drying rate as a function of the local mean moisture content and the local external air conditions, determined from experimental drying rate data or from theory.

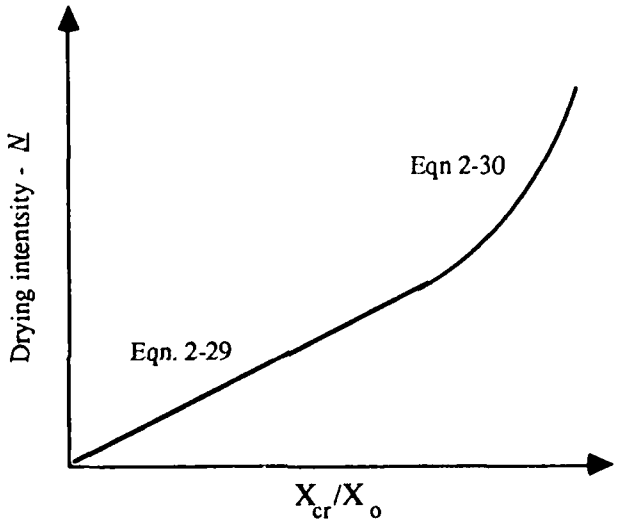

Figure 2-9. Theoretical critical point curve for nonhygroscopic porous materials with constant diffusivities. Adapted from Keey (3)

The equipment model developed here is for a continuous single-zone convective tunnel dryer as shown in Figure 2-10. In the tunnel dryer the air flow may either be concurrent, i.e., in the same direction as the material flow, or countercurrent, i.e., opposite the material flow. The moisture leaving the material is entrained into the air stream, whose dry mass flow rate is G, with progressive humidification from entrance to outlet. The convective heat transfer coefficient, h, and mass transfer coefficient K_o, are specified from correlations of Nusselt numbers corresponding to the flow geometry and air velocity. Wet product enters at a given moisture content X_i and product flow rate L, and is delivered at the exit at a desired moisture content X_e.

The equipment model also specifies the means for providing heat transfer to the product. The process through the length of the tunnel dryer may, for example, be adiabatic or isothermal, in which heat is added continuously to the air stream to maintain a constant temperature. Of particular interest in this work is the use of dielectric heating to heat the material. The equipment model can be used to define desirable location and intensity of dielectric heating to reduce drying equipment costs.

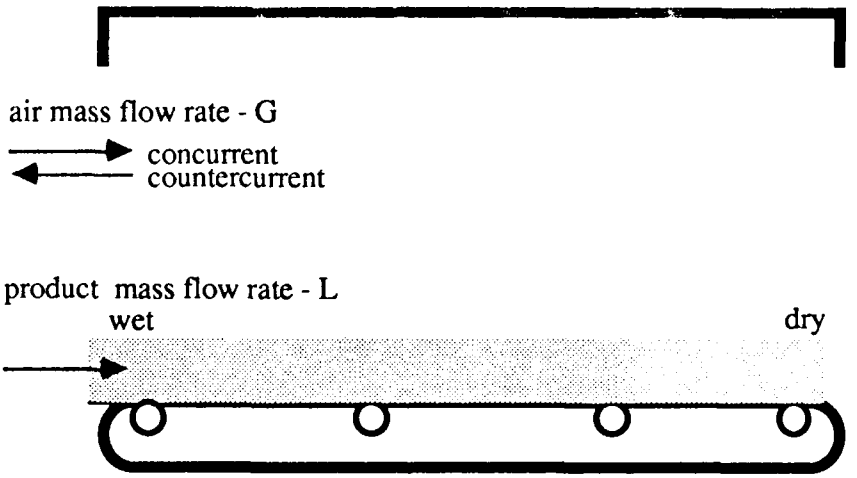

Figure 2-10. Continuous convective tunnel dryer

CHAPTER 3

ANALYTICAL FORMULATION

3.1 INTRODUCTION

To predict the process conditions in a continuous convective tunnel dryer, a differential control volume analysis is used (Figure 3-1) where Δz defines the length of the control volume. Assuming steady state conditions, energy and mass balances are derived for the control volume and the resulting equations solved numerically. The drying rate flux is found from the characteristic drying curve for the product, which specifies the drying rate flux as a function of the moisture content and local external conditions. Although the characteristic drying curve allows prediction of drying rates without specifically defining the means of moisture transport within the material, some model of the thermal transport in the material is needed to evaluate the heat flux. Using a quasi-steady analysis, the receding evaporative plane model discussed in Chapter 2 defines boundary conditions for heat conduction within the material. The differential analysis will provide the drying flux, temperature, and humidity profiles through the length of the dryer, and hence the dryer length required for a given set of initial operating conditions and product moisture specifications.

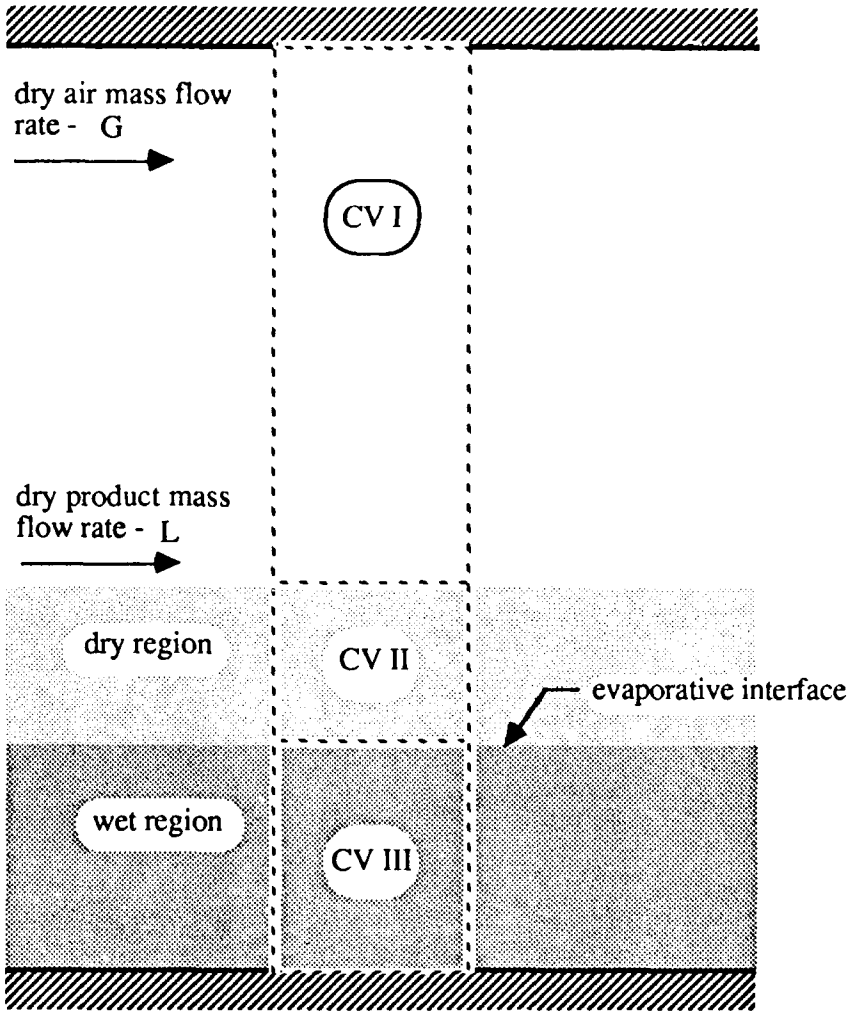

Figure 3-1. Control volumes in tunnel dryer

3.2 DEFINITION OF CONTROL VOLUMES

Assuming the receding evaporative plane model of moisture movement, three adjacent control volumes as shown in Figure 3-1 are specified for analysis. A lumped parameter analysis will be made for the y-direction thermal and mass transport between the regions. Control volume I (CV I) corresponds to the region of moist air bounded between the surface of the material and the insulated top of the tunnel dryer. CV II is the dry region of the material bounded above by the surface and below by the receding evaporative front. CV III encompasses the wet region of the material below the evaporative plane. During the initial stages of drying, the surface may be fully wetted in which case CV II, the dry region, will not exist.

3.3 HEAT AND MASS BALANCES

For the general case of hindered drying an evaporative plane will exist (Figure 3-1) and energy balances for the three control volumes yield Eqs. 3-1 through 3-3. The complete derivation of all energy and mass balance equations is detailed in Appendix A. Due to the low thermal conductivities of commonly dried materials and the small temperature gradient in the z-direction, axial conduction is neglected in the analysis. Also, the enthalpy of wetting of the material, and the amount of air entering the material are considered to be negligible.

The assumption of a linear temperature profile in the dry region, as discussed in Chapter 2, corresponds to a quasi-steady analysis. Although this analysis of the convective dryer considers the evaporative plane to be transient with

respect to position in the z-direction rather than with time, the assumption remains valid.

For the control volume encompassing the humid air, shown in Figure 3-2, an energy balance yields

$$N_v h_v + Q_{as} = G \frac{\partial h_a}{\partial z} + h(T_a - T_s) \tag{3-1}$$

The enthalpy change of the humid air is equivalent to the difference between the vapor enthalpy entering from the material, $N_v h_v$, and the heat convected to the surface plus any source of air heating in the volume, Q_{as}.

An energy balance about the dry region, CV II yields

$$h(T_a - T_s) + P_d \xi = \frac{\xi}{b} L C_{ps} \frac{\partial \bar{T}_{II}}{\partial z} + \kappa_d \frac{(T_s - T_e)}{\xi} \tag{3-2}$$

In Eq. 3-2, the left-hand side terms are the convective heating and dielectric heating of the region where P_d is the volumetric power density for the dry material. These terms correspond to Q_{conv} and $Q_{vol\text{-}dry}$ as shown in Figure 3-2. This entering energy is balanced by the heat conducted to the wet region and the sensible heat changes in the region shown as Q_{cond} and $Q_{sens\text{-}dry}$ in Figure 3-2. Here κ_d and C_{ps} are the thermal conductivity and the specific heat of dry material respectively and $\bar{T}_{II}$ is the mean temperature in the region. The enthalpy change due to the net convective transport of vapor through the dry region is neglected. For Eqs. 3-1 and 3-2, it is therefore assumed that the enthalpy of the vapor, h_v, corresponds to the interface temperature, and does not change as the vapor diffuses through the dry

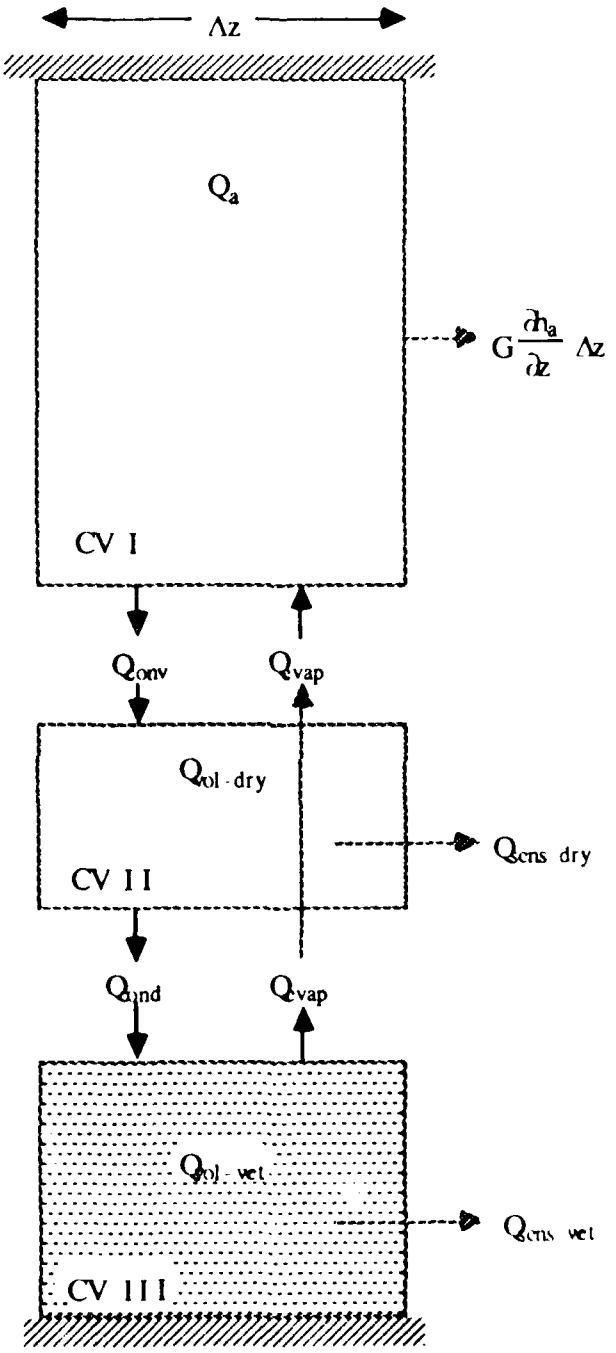

Figure 3-2. Energy balance terms

region. The actual enthalpy of the vapor leaving the surface will be between two extremes. In one case, as has been assumed, the leaving vapor temperature remains at T_e; in the other, the leaving vapor temperature is equal to the surface temperature, T_s, i.e., the "dry" material and diffusing vapor are in thermal equilibrium. If the vapor and material do not interact thermally, the vapor temperature will remain constant through the dry region. Although the actual leaving vapor temperature will be somewhere between T_e and T_s, the difference in vapor enthalpy evaluated at the two extreme temperatures is small in comparision with the enthalpy of vaporization.

An energy balance about CV III yields

$$\kappa_d \frac{(T_s-T_e)}{\xi} + P_w (b-\xi) = N_v h_{fg} + L\left[XC_{pf}+\frac{b-\xi}{b} C_{ps}\right]\frac{\partial T_e}{\partial z} \qquad (3\text{-}3)$$

For the wet region, the heat conducted from the dry region, plus any volumetric heating such as dielectric, $Q_{vol\text{-}wet}$, where P_w is the volumetric power deposition in the wet material, results in the evaporation of moisture, $N_v h_{fg}$ (Q_{evap} in Figure 3-2) and the specific heating of the moisture and solid in the region with specific heats C_{pf} and C_{ps} respectively.

For the quasi-steady assumption, the vapor flux does not change through the dry region. The moisture mass balances for the air and wet material control volumes yield

$$N_v = G \frac{\partial Y_a}{\partial z} \qquad (3\text{-}4)$$

$$N_v = -L \frac{\partial X}{\partial z} \qquad (3\text{-}5)$$

According to Eq. 3-4 the vapor flux from the surface N_v humidifies the air across the control volume. Eq. 3-5 shows that the vapor flux is equal to the change in the moisture content X across the control volume. Although air enters the porous material as moisture leaves, its influence upon the heat and mass balance is negligible (3).

Eqs. 3-1 through 3-5 provide the basis for a model of the heat and mass transfer process within the differential control volume. It is evident from the number of unknown variables, however, that these five equations are not sufficient for a solution. Considering z the independent variable, the air temperature T_a, air humidity Y_a, surface temperature T_s, evaporative interface temperature T_e, moisture content X, and drying flux N_v are the primary dependent variables. In addition to a relationship between N_v and the other variables, expressions for variable properties and for the rate coefficients h and K_o are required for solution.

In some cases, the drying time is minimized by keeping the air temperature as high as practically possible within constraints of material quality. Heat is added to the air stream, by steam coils for example, to maintain a constant air temperature. In this case, instead of the air temperature being variable, the amount of heat added to the air stream Q_{as} is taken as a dependent variable to maintain the constant temperature.

Many of the properties of air and water used in the analysis, such as specific heats and thermal conductivities, are temperature dependent and may vary significantly over the range of temperatures encountered in drying. The

expressions for variable properties used in the analysis are listed in Appendix B. The product properties are assumed to be constant.

3.4 AIR ENTHALPY EXPRESSION

The humid air enthalpy, h_a, in Eq. 3-1, is a function of the air temperature and the air humidity for a given pressure as shown in Eq. 2-1. The enthalpies of the air and vapor may be determined from the specific heats. By definition

$$C_p = \left.\frac{\partial h}{\partial T}\right|_p \tag{3-6}$$

and the enthalpy h at temperature T_1 may be found by integrating C_p from a reference temperature T_{ref} to T_1. For temperatures normally encountered in drying, it is sufficiently accurate to determine the enthalpy of air or vapor in a given phase by evaluating the temperature dependent specific heats at the arithmetic mean between T_1 and T_{ref} such that (3)

$$h = \overline{C_p}\,(T_1 - T_{ref}) \tag{3-7}$$

For the remainder of the analysis T_{ref} will be taken as 0° C, and the specific heat, C_p, will be evaluated at mean temperature. Also, water as a saturated liquid at 0° C is the reference enthalpy for water in either liquid or vapor phase. To evaluate the enthalpy of vapor in humid air from this reference, consider the process as moisture in air is cooled from a vapor at T_1 to the liquid state at 0° C. First, the air is cooled to the dew point temperature, T_{dp}. Next, all vapor is condensed at T_{dp} and then the

liquid cooled to the reference temperature, 0° C. The enthalpy change for the cooling process corresponding to this path is given by

$$h_v = C_{pf}T_{dp} + h_{fg} + C_{pv}(T_1-T_{dp}) \tag{3-8}$$

where C_{pf} and C_{pv} are the specific heats of liquid and vapor respectively and h_{fg} is the heat of vaporization at T_{dp}. Therefore, the enthalpy of humid air at a temperature of T_1 and humidity Y_1 is given by the summation of h_v and h_{da}

$$h_a = C_{pa}T_1 + Y_1(C_{pf}T_{dp} + h_{fg} + C_{pv}(T_1-T_{dp})) \tag{3-9}$$

where C_{pa} is the specific heat of dry air.

The dew point temperature T_{dp} has been introduced for use in determining the air enthalpy. For air conditions at a given temperature T_a, and humidity Y_a, the temperature at which air is saturated at the given humidity is defined as the dew point temperature. At a given air pressure

$$Y_{sat}(T_{dp}) = Y_a \tag{3-10}$$

The saturated humidity of air, Y_{sat}, at a given temperature and pressure is found by evaluating the saturation pressure of water vapor p_{ws}, at the given temperature. This is shown in Appendix B.

3.5 DRYING RATE EQUATION

If the material is saturated with moisture such that $X > X_{cr}$, the surface will be fully wetted and the drying rate is given by Eq. 2-4

$$N_v = K_o D \ln\left[\frac{D + Y_s}{D + Y_a}\right] \tag{3-11}$$

where the surface humidity Y_s is determined from the surface temperature T_s.
If the drying is hindered ($X < X_{cr}$), the drying flux N_v is evaluated from Eq. 2-25b.

$$N_v = f K_o D \ln\left[\frac{D + Y_w}{D + Y_a}\right] \tag{3-12}$$

This equation introduces another primary unknown, the relative drying rate f. The relative drying rate is a function of the characteristic moisture content Φ where Φ is evaluated from the moisture content X and the critical moisture content X_{cr}. If the material is hygroscopic, the characteristic moisture content is also a function of the equilibrium moisture content X^* as given in Eq. 2-23.

Also, Y_w, the saturated humidity at the wet bulb temperature, must be evaluated. The saturated wet bulb humidity and corresponding wet bulb temperature are functions of the air temperature and humidity as given by Eq. 2-16 , which, with the logarithmic potential, is

$$h(T_a - T_w) = K_o D \ln\left[\frac{D + Y_w}{D + Y_a}\right] h_{fg} \tag{3-13}$$

The saturated wet bulb humidity and wet bulb temperature are found by simultaneous solution of Eq. 3-13 and equations that give the relationship between air temperature and saturated humidity. Eq. 3-14 shows the relationship between the partial pressure of water vapor in air, p_w, and air humidity,

$$Y_a = D \frac{p_w}{(p_a - p_w)} \tag{3-14}$$

where D is the ratio of the molecular weight of air to water, and p_a is the total pressure of the air/vapor mixture. The relationship between saturated partial vapor pressure of air as a function of air temperature is given in Appendix B For convenience in analysis and computation, the relationship between saturated humidity and air temperature is stated as a known function,

$$Y_{sat} = Y_{sat}(T_a) \tag{3-15}$$

3.5.1 Product Model

The characteristic drying curve presents a function for the relative drying rate f in terms of normalized moisture content Φ

$$f = f(\Phi) \tag{3-16}$$

Although not necessarily constrained to this simple form, Keey(3) provides examples where $f = \Phi^n$. For example, a drying process involving peeled timber veneers is approximated with $n=\frac{3}{4}$.

The effects of dielectric heating on drying curves is the focus of current study. To achieve an understanding of dielectrically enhanced drying, it is necessary to determine which parameters should be used to normalize the drying rate and moisture content to give a characteristic drying curve valid over a range of external and dielectric heating conditions. The constant drying rate for conventional drying is determined from a surface energy balance where the fully wetted surface temperature has reached the wet bulb as shown in Eq. 2-20. With dielectric

heating, the moist material is sensibly heated and a constant drying rate may occur after the material reaches its boiling point. Steady-state conditions (constant drying rate) may exist at temperatures below the boiling point if heat is removed from the material by convection into the air stream. For high intensity dielectric heating, capable of inducing boiling, and with relatively small convective heating or cooling, it may be assumed that the constant drying rate is simply proportional to the amount of dielectric energy supplied to the material. Experimental data have suggested that the constant rate period may prevail to very low moisture contents yielding a correspondingly small critical moisture content (24). Hence, the normalization parameters for X_{cr} and N_{vo}, for cases of dielectrically augmented heating are functions of the dielectric power as well as external air conditions, but the relationships have not yet been determined from either analytical or experimental work. Further studies of the normalization question are crucial in order to expand the concept of characteristic drying curves for analysis over a range of both external and internal heating conditions.

The instantaneous position of the evaporative plane below the material surface is a function of both the moisture content and moisture distribution in the material. From an analysis of the characteristic drying curve, assuming constant moisture diffusivity in a porous nonhygroscopic material, the follow relation between the characteristic moisture content Φ and the depth of recession ξ, is derived (15).

$$\Phi = f\left[1 - \frac{\xi}{b}\right]^2 \qquad (3\text{-}17)$$

Note that for the case of $f = \Phi$, ξ is zero and no front is present. This linear falling rate curve is said to be characteristic of slow drying of thick material very slowly and is supported by experimental data (15).

3.5.2 Transport Coefficients

The convective heat transfer coefficient, h, may be computed from empirical relations. Most published correlations are for cases of simple geometries and well defined flows, while relations for practical drying conditions are relatively scarce. In the absence of heat transfer data for the specific material and dryer application, approximate relations may be adequate for preliminary design and comparison of dryer configurations (3). The Nusselt number is usually given as a function of the Reynolds and Prandl numbers as shown in Eq. 3-18.

$$Nu = C_1 \, Re^m \, Pr^n \tag{3-18}$$

where the coefficients C_1,m, and n are dependent upon the particular flow velocity, geometry and thermal boundary conditions (22). For air within the temperature range of interest here, the Prandl number may be considered constant and the relation may be expressed as

$$Nu = C_2 Re^m \tag{3-19}$$

For internal or external turbulent flow, and a moderate Prandl number, correlations typically give $m = \frac{4}{5}$ and n between $\frac{1}{3}$ and $\frac{1}{2}$ depending upon the thermal boundary conditions. External flow correlations may be applied in the tunnel dryer using a

length averaged Nusselt number, Nu_L. For material laid on trays, Treybal (7) recommends

$$Nu_L = 0.055\ Re_L^{0.8} \tag{3-20}$$

The mass transfer coefficient, K_o, may be calculated through the heat and mass transfer analogy discussed in Chapter 2. Given the Lewis number and mean specific heat for the air, Eq. 2-14 is rearranged to give

$$K_o = h\frac{\beta\ Le^{2/3}}{C_p} \tag{3-21}$$

where C_p, the specific heat of the total gas flow, and the properties used in computing the Lewis number are evaluated at the film temperature, $(T_a + T_s)/2$, and film humidity, $(Y_a + Y_s)/2$ (20).

3.5.3 Number of transfer units, NTU

Dryer performance may be evaluated considering the "number of transfer units" associated with a dryer. Similar in concept to the NTU associated with heat exchangers, rather than describing the heat transfer capacity, the number of transfer units for a dryer describes the evaporative (mass transfer) capacity. The number of transfer units for drying is given as (3)

$$NTU = \int_{inlet}^{outlet} \frac{dY_a}{Y_s - Y_a} \tag{3-22a}$$

where Y_a and Y_s are the bulk air and surface humidities. For computation, Eq. 3-22a is approximated by

$$NTU = \sum_{1}^{N+1} \frac{\Delta Y_a}{Y_s - Y_a} \tag{3-22b}$$

3.6 COMPUTATIONAL PROCEDURE

The differential energy and mass balance equations are discretized and solved numerically along with the characteristic drying curve equation, rate coefficient equations, and variable property equations. The first order nonlinear differential equations are discretized with simple difference elements. For example,

$$\frac{\partial T}{\partial z} = \frac{\Delta T}{\Delta z} \tag{3-23}$$

$$\frac{\partial X}{\partial z} = \frac{\Delta X}{\Delta z} \tag{3-24}$$

where a difference element is given as

$$\Delta T = T_i - T_{i-1} \tag{3-25}$$

Here, i is the current step and i-1 is the previous step. Beginning with the given inlet conditions, the set of nonlinear equations are solved at each (ith) step.

Rather than dividing the length of the dryer into i Δz increments, it is more convenient to take the moisture content, X, as the independent variable and step through the length of the dryer in ΔX increments from the entering wet material moisture content to the desired exit moisture (23). At each ΔX step, the

corresponding length, Δz, is solved for along with the other dependent variables. This is computationally convenient because the primary variable of interest, N_v, is given as a function of X.

The preceding analysis results in fourteen equations and fourteen dependent variables for the general case of hindered drying ($f = f(\Phi)$). Tables 3-1 and 3-2 summarize the dependent variables and equations with short descriptions. The basic computational procedure for solution of the governing equations is to decrement the moisture content, X, by a given ΔX, from the inlet moisture content to the exit moisture content, and solve the set of non-linear equations for the dependent variables at each step. A flow chart of the computational procedure is shown in Figure 3-3.

Following from the start, the program reads the input data from a file and then calculates a constant step size (ΔX) based upon the difference between the inlet and outlet moisture contents and the number of steps. The Fortran variables that represent the dependent variables of the analysis must be set at some initial value before calling the nonlinear equation solver subroutine. The set of nonlinear equations is especially sensitive to changes in the wet bulb temperature when the air and wet bulb humidities are very close. A good initial guess for the wet bulb temperature is necessary for convergence for the system. Therefore, the initial guesses for both the wet bulb and dew point temperatures are made by solving the wet bulb and dew point equations, Eqs. 3-10 and 3-13, through an initial call to the nonlinear equation solver subroutine. The initial guesses of air temperature and product temperature are simply their given input values. However, the initial

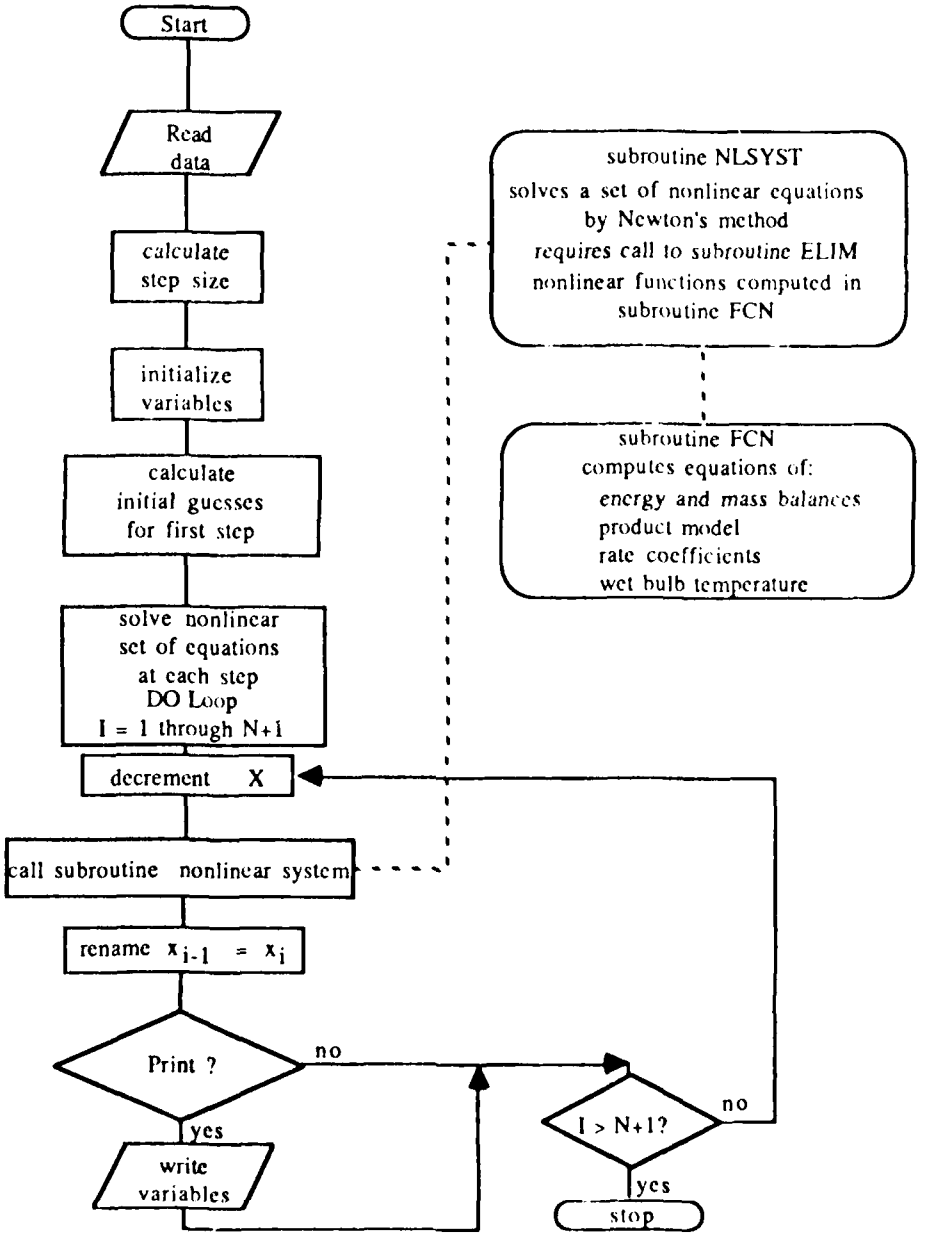

Figure 3-3. Computational flow chart

guesses of drying flux, and Δz must be first calculated. After the initialization of the Fortran variables, a DO loop is entered which decrements the moisture content and calls the nonlinear system of equations solver at each step from initial to exit moisture content. After each call, the solved discretized variables are reset to be the i-1 value at the next call. Also, if the step is at a print interval the variables are written to file.

The system of nonlinear equations is solved by a subroutine called NLSYST, taken from a numerical analysis text (24). Newton's method is employed where the partial derivatives of functions representing the equations are estimated by perturbing the variables with a small change and dividing this into the result of the function change. The matrix corresponding to Taylor series expansions of the functions with the approximated values of the partial derivatives is then solved by an accompanying matrix solving subroutine, ELIM, which yields improved values for the dependent variables. The procedure continues until a convergence criterion is satisfied. NLSYST is limited in that for convergence, the initial guesses must be relatively close. Also, the magnitude of the perturbation must be small enough to give a good estimate of the partial derivatives without excessive round-off error (24). As given in the reference, the perturbation, DELTA, is a constant input argument of the subroutine NLSYST. Since the set of nonlinear equations solves for variables with large differences in magnitude (N_v is of order 10^{-3} and h_a of order 10^2), the subroutine is modified such that the perturbations are computed as a given percentage of the variable's current value. Although the computational model is presented with the subroutine NLSYST, other subroutines may be used.

TABLE 3-1

Summary Descriptions of Dependent Variables

Variable	Description
N_v	drying rate flux
T_a	air temperature
Y_a	air humidity
T_w	wet bulb temperature
Y_w	saturated wet bulb humidity
T_{dp}	dew point temperature
h_a	humid air enthalpy
T_s	surface temperature
T_e	evaporative plane and wet region temperature
f	relative drying rate
ξ	depth of receding evaporative plane
h	convective heat transfer coefficient
K_o	mass transfer coefficient
Δz	the control volume length

TABLE 3-2

Summary Descriptions of Equations

Equation	Description
3-1	energy balance, air region, CV I
3-2	energy balance, dry region, CV II
3-3	energy balance, wet region, CV III
3-4	moisture mass balance, air region, CV I
3-5	moisture mass balance, wet region, CV III
3-9	humid air enthalpy expression
3-10	dew point temperature definition
3-12	drying rate equation
3-13	surface energy balance defining wet bulb conditions
3-15	relationship between saturated humidity and temperature
3-16	characteristic drying curve function
3-17	evaporative plane position ξ
3-19	convective heat transfer coefficient correlation
3-21	heat and mass transfer analogy relating transport coefficients h and K_0

CHAPTER 4

VALIDATION STUDIES

4.1 INTRODUCTION

Studies were carried out to determine the degree of agreement between the dryer model and experimentally and analytically derived drying data. The three case studies described in this chapter consider comparisons to both analytical and experimental results for drying in a convective tunnel dryer without dielectric heating. To predict drying times in the case of dielectric heating, an appropriate product model of drying in a dielectric field is necessary, and as mentioned in Chapter 3, development of such product models is a topic of current investigations beyond the scope of this report. The product model, whether for convective drying or dielectrically-enhanced drying, describes how the drying rate is hindered by moisture transport through the material. Even without a reliable product model for dielectrically-heated material, the dryer model may still be used with dielectric heating for cases in which the material does not hinder the drying, i.e., when the material moisture content is above saturation, with a corresponding fully wetted surface.

4.2 MODEL VERIFICATION STUDIES

4.2.1 Adiabatic Saturation and Isothermal Chamber Simulation

In the initial stages of the model development, two limiting-case drying scenarios were simulated and the results were analyzed for rational behavior. One scenario was as an adiabatic saturation chamber as shown in Figure 2-7. If the material surface remains fully wetted throughout the adiabatic dryer, i.e. no hindered drying, and the air flow rate is such that the surface temperature approaches its saturation value, then the air temperature will approach the adiabatic saturation temperature. The model predictions are presented in Figure 4-1a. For this case the air enters at 26.67° C and 0.00981 kg/kg, corresponding to a wet bulb temperature of 18.33° C. At these conditions the adiabatic saturation temperature is within 0.15° C of the wet bulb temperature (9). As shown in Figure 4-1a, the air temperature approaches 18.3° C through a very long dryer length.

An isothermal configuration was also run to examine the approach of the product temperature to the constant air temperature. The temperature of the fully wetted surface will follow the wet bulb temperature which increases as the air is humidified. At saturation, the air temperature and wet bulb temperature are identical. The results are shown in Figure 4-1b, where the air temperature is constant at 60° C and is humidified to saturation. On the basis of these "sanity" checks, it is concluded that the heat and mass balances are properly computed and that the calculated psychrometric air properties are in good agreement with published psychrometric data.

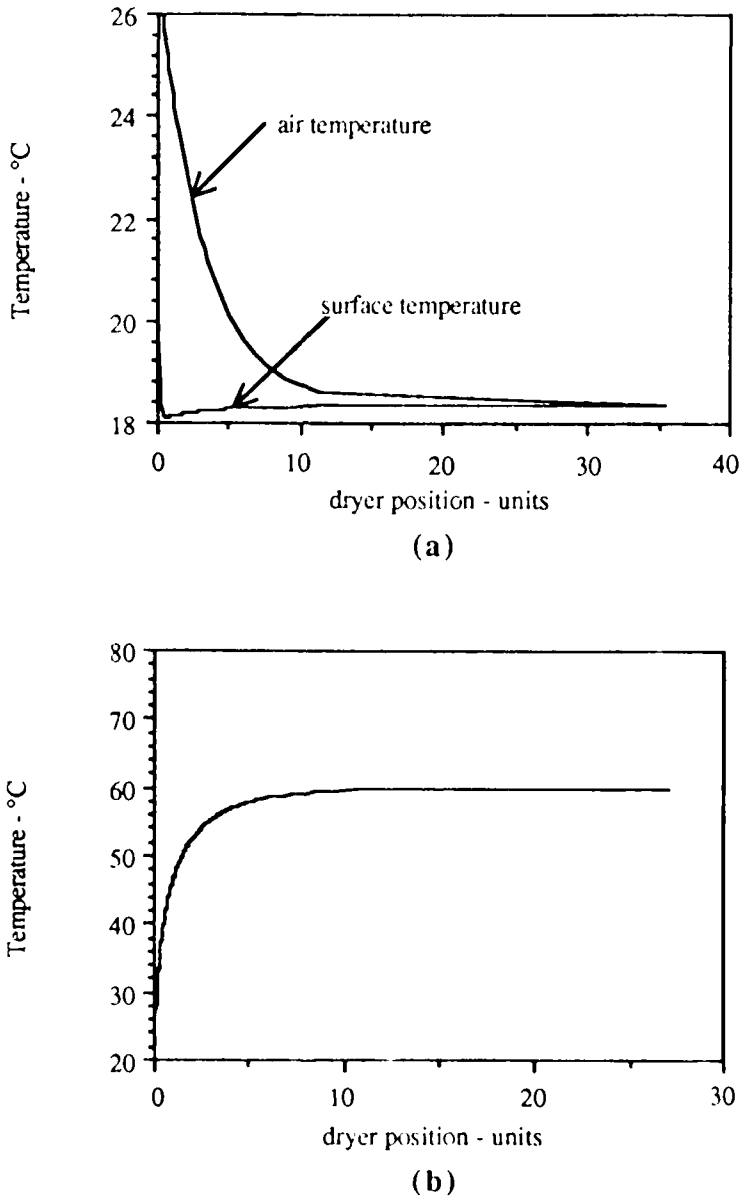

Figure 4-1. a) Air and moist surface temperatures for adiabatic configured dryer
b) Moist surface temperature for isothermal configuration at 60° C

4.2.2 Integration of Drying Curve

The next step in confirming model predictions is to compare the drying time produced by the model with drying time arrived at through analytical integration of a given single drying curve. Recalling the development of the characteristic drying curve discussed in Chapter 2, a water content versus time curve for constant air temperature and humidity conditions is transformed into a drying rate versus moisture content curve. The drying rate and moisture content are then normalized by the drying rate from a fully wetted surface and the critical moisture content, respectively, yielding the characteristic drying curve. Beginning with a given characteristic drying curve, the procedure may be reversed, yielding an expression for drying time as a function of moisture content under constant air conditions. The analytical results may then be compared with the predictions of the numerical model as a check on the accuracy of the numerical "denormalization" and integration procedures.

Consider a continuous tunnel dryer with very large air mass flow rate, G, such that the air conditions approach constant air temperature and humidity. This simulates the constant air conditions under which data for a drying curve is taken. For a constant product flow rate, L, and an established dryer length, the time required for drying is obtained. Assume a given function for the characteristic drying curve

$$f = f(\Phi) \tag{4-1}$$

where the relative drying rate, f, is given by

$$f = \frac{N_v}{N_{vo}} \tag{4-2}$$

and for a nonhygroscopic material the normalized moisture content is

$$\Phi = \frac{X}{X_{cr}} \tag{4-3}$$

Considering X_{cr} constant and, for constant air conditions, N_{vo} constant, Eq. 4-1 becomes

$$\frac{N_v}{N_{vo}} = f\left(\frac{X}{X_{cr}}\right) \tag{4-4}$$

The drying rate flux, N_v, is obtained from experimental data through the following definition

$$N_v = - \frac{\partial m_w}{\partial \tau} \frac{1}{A} \tag{4-5}$$

Integration of Eq. 4-5 between given moisture contents will yield the time of drying. The mass of water is related to the moisture content, X, by

$$m_w = A\ b\ \rho_s\ X \tag{4-6}$$

where A is the area of the sample, b is the sample depth, and ρ_s is the dry material (solids) density. Combining Eqs. 4-5 and 4-6, for constant area, depth, and dry density of the material yields

$$N_v = -\rho_s\ b \frac{\partial X}{\partial \tau} \tag{4-7}$$

Integrating from the given initial to final moisture content gives the time of drying

$$\tau = \rho_s \, b \int_{X_f}^{X_i} \frac{\partial X}{N_v} \tag{4-8}$$

The drying flux N_v is given as a function of the moisture content by Eq. 4-4. For this case, consider a given function

$$f = \Phi^{3/4} \tag{4-9}$$

and consequently

$$N_v = N_{vo} \left(\frac{X}{X_{cr}} \right)^{3/4} \tag{4-10}$$

Combining Eq. 4-10 with 4-8 and integrating

$$\tau = \frac{\rho_s \, b}{N_{vo}} \, X_{cr}^{3/4} \, 4 \, (X_f^{1/4} - X_i^{1/4}) \tag{4-11}$$

The drying rate from a fully wetted surface, N_{vo}, is found by Eq. 2-25b

$$N_v = f \, K_o \, D \ln \left[\frac{D + Y_w}{D + Y_a} \right] \tag{4-12}$$

where K_o, Y_w, and Y_a are determined from the constant air conditions.

For selected initial and final moisture contents, given the characteristic drying curve of Eq. 4-9 and constant air conditions, the time of drying computed by the model may be compared with the result of Eq. 4-11.

One of the model predictions is dryer length, computed from the summation of the Δz increments determined for each step. The time of drying may be calculated from the dryer length and material velocity.

$$\tau_{sim} = \frac{Z_L}{V_s} \tag{4-13}$$

where τ_{sim} is the time found in the computer simulation, Z_L is the computed length, and V_s is the velocity of the material (product). For a constant material density, ρ_s, and cross sectional flow area A_x, the solids mass flow rate may be given as

$$L = \rho_s A_x V_s \tag{4-14}$$

The cross sectional flow area is the product of the width of the material flow, which was assumed as one unit in the analysis, and the depth of material, b. For the simulation of constant air conditions, the product dry mass flow rate, L, is an arbitrary input.

For the comparison, consider a constant air temperature of 75° C, and an air humidity of 0.050 kg/kg. The corresponding wet bulb temperature and wet bulb saturated humidity are 43.8° C and 0.06473 kg/kg. Assuming a constant mass transfer coefficient of 0.10 kg/m^{2}s the constant drying rate of Eq. 4-12 is 0.0013487 kg/m^{2}s. The dry product density, ρ_s is assumed to be 100 kg/m^3, the product thickness, b, 0.01 m, and the critical moisture content, X_{cr}, 1.0 kg/kg. If the material is dried from an initial moisture content of 1.0 kg/kg to a final moisture content of 0.2 kg/kg, Eq. 4-11 gives τ = 982.48 s.

To maintain the constant air condition in the model simulation, a very large air mass flow rate was entered, $G = 5 \times 10^6$ kg/s. If the product dry mass flow rate, L, is chosen as 1 kg/s, the overall moisture mass balance for the dryer

$$G\,(Y_{a\,out} - Y_{a\,in}) = L\,(X_i - X_f) \qquad (4\text{-}15)$$

yields $\Delta Y_a = 1.6 \times 10^{-6}$, a negligible change in air humidity. Also with L = 1 kg/s, and the given solids density and depth, Eq. 4-13 gives a solids velocity, V_S, of 1 m/s. Therefore, the time of drying τ, in seconds, is numerically equal to the dryer length, Z_L, in meters.

The result of the model simulation with the previously given inputs of air conditions, moisture contents, and product model, and with a constant mass transfer rate K_o, gives a very small error (less than 0.02 percent) when compared to the result of Eq. 4-11. With the model configured for concurrent air flow and 100 nodes the dryer length is 982.2 m, and for 500 nodes, 982.3 m. Additionally, the same lengths result for running the model in the countercurrent mode, as expected. Figure 4-2 shows the model results of drying rate flux as a function of position in the dryer.

The agreement between numerical and analytical prediction of the drying time suggests that the drying model does not suffer from numerical inadequacies. However, this does not confirm the model performance under realistic drying conditions where air conditions change along the length of the dryer.

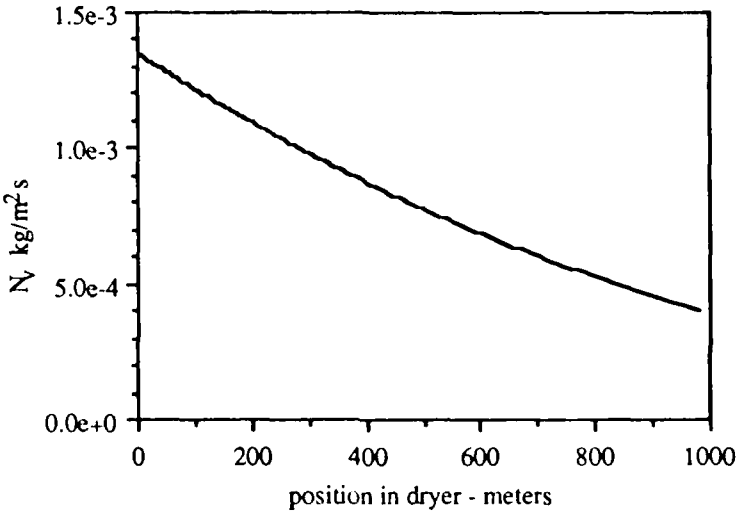

Figure 4-2. Model prediction, drying rate profile for integration of drying curve case study

4.2.3 Design Case Study

The third case study is a comparison of model predictions with a worked example from Keey (26) of drying in a conveyor (tunnel) dryer under various configurations: adiabatic countercurrent air flow, adiabatic concurrent flow, and isothermal countercurrent flow. The primary differences between the analysis in Reference 26 and that used here are the assumptions made in the reference of negligible sensible heating of the moist material and constant convective heat and mass transfer coefficients. Although the model is not limited by these simplifying assumptions, the resulting differences are negligible for this case.

The problem specifications are as follows:

MATERIAL SPECIFICATIONS:

characteristic drying curve	$f = \Phi^{3/4}$
hygroscopic material with an equilibrium moisture content given by	$X^* = 0.16rh$ (rh - relative humidity, percent)
constant critical moisture content	$X_{cr} = 1.2$ kg/kg
inlet moisture content	$X_o = 1.5$ kg/kg
outlet moisture content	$X_z = 0.15$ kg/kg
material thickness	$b = 0.010$ m
product flow rate (dry mass basis)	$L = 0.16667$ kg/s

AIR CONDITIONS:

entering air temperature	80° C
entering air humidity	0.0648 kg/kg
air flow rate (dry air basis)	22.5 kg/s

Note that in the analysis of the tunnel dryer, the computations are made from the inlet of the dryer, which is defined as the end at which the wet material enters. For the countercurrent case the air enters the dryer from the opposite end. Therefore, to begin the computational procedure, an estimate of the exiting air conditions, at the wet product inlet, must be made. The change in air humidity across the dryer can be found from Eq. 4-15, leaving only the exiting air temperature to be estimated. An iterative procedure is used in which the exiting air temperature is estimated, the resulting entering air temperature from the model output is compared with the given entering air temperature, and a new estimate is made. The estimated entering air temperature may be corrected by the difference between the output and desired exiting air temperature. Using this method for this case, convergence to within 1° C of the exiting air temperature was reached in three iterations.

In the model, additional material and air flow parameters are necessary, such as the material specific heat, thermal conductivity, and air velocity. Since the example makes reference to drying of wallboard and timber veneers, values for the material specific heat and thermal conductivity are taken from data for hardwoods (8).

material thermal conductivity, κ_d	.00016 kW/m °C
material specific heat, C_{ps}	1.256 kJ/kg °C

Also, the parameters used in the calculation of the rate coefficients must be entered in the model. The example does not specify a mass transfer coefficient, but presents the drying flux on a relative basis, in which a drying rate of 1 corresponds to drying rate of a fully wetted surface at the entering air conditions. Therefore, some nominal conditions are assigned in the model:

air velocity	4.0 m/s

and for the heat transfer correlations in which $Nu = C_2Re^m$

C_2	0.055
m	0.8
characteristic length	4.0 m

Further model specifications include the air pressure, assumed to be at one atmosphere, and amount of dielectric heating of the material, considered zero in this example. In the adiabatic case, there is no air heat source, whereas in the isothermal case the amount of air heating required to maintain constant temperature is computed at each step.

To complete the model input parameters, the number of computational steps is set at 135, giving a moisture content decrement of 0.01 kg/kg.

The model predictions for all three configurations are shown in Figure 4-3a. The drying rate flux, N_v, has been normalized on the drying rate from a fully wetted surface at the entering air conditions of 80° C and humidity of 0.0648 kg/kg, N_{ao}, to show relative performance among the different configurations. Note that the drying rate N_{ao} occurs at the entering conditions in the adiabatic concurrent configuration. The dimensionless moisture content against which the drying rates are plotted is given by $(X-X_Z)/(X_O-X_Z)$ where X_O and X_Z are the entering and leaving moisture contents, respectively, such that a moisture content of 1 corresponds to the inlet and 0 to the exit. At the critical moisture content, X_{cr} = 1.2 kg/kg, the dimensionless moisture content is 0.78.

For the adiabatic concurrent configuration, the air and moist material enter at the same end of the dryer. As shown in Figure 4-3a, the drying flux decreases as the air and product progress through the dryer. The decrease in the drying rate is caused by progressive humidification of the air which reduces the humidity potential between the material surface and the air stream. Also, as the material moisture content drops below critical, the drying rate is hindered according to the given characteristic drying curve. The first inflection in the drying rate curve, following from right to left, reflects the influence of hindered drying occurring at the critical moisture content.

Again referring to Figure 4-3a, consider the curve representing the adiabatic countercurrent configuration. Here, the entering moist product contacts the exiting air that has been humidified and cooled as it progressed through the dryer. Accordingly, for moisture contents greater than critical, the drying rate

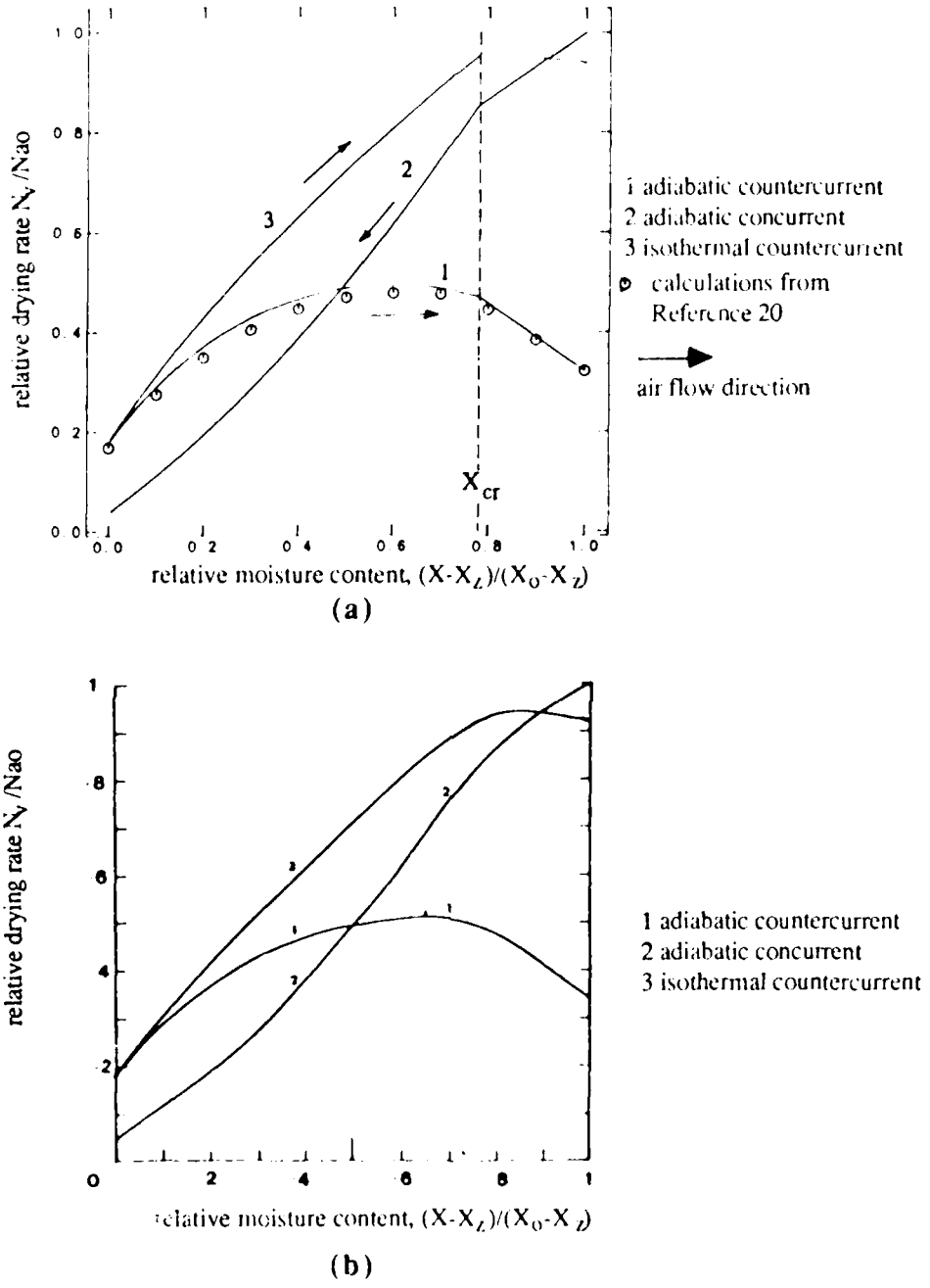

Figure 4-3. Drying rate profiles from a) model predictions, and b) worked example by Keey (25)

increases almost linearly as the material surface encounters hotter and less humid air. When the moisture content reaches the critical point, the drying is then hindered, reflected in the tapering off of the drying rate. As the moisture content drops, the normalized drying rate decreases as the 3/4 power of characteristic moisture content, such that this resistance to internal moisture transport eventually overcomes the effect of decreasing air humidity. Consequently the drying rate continues to fall slowly as the material progresses to the exit.

The last configuration considered is that of isothermal countercurrent air flow. Figure 4-3a shows the inlet drying rate for this case is significantly higher than that for the adiabatic countercurrent case, due to the higher wet bulb temperature for the isothermal case. Recalling the equation for hindered drying, Eq. 3-12, Y_w corresponds to *the saturated humidity at the wet bulb temperature*, which, for a constant air humidity, increases with air temperature. Again, the drying rate increases as the material encounters less humid, although isothermal air. Also, as the moisture content falls below critical, the drying rate turns down and falls to the exiting conditions. Note that the exiting drying rates for both countercurrent cases are equal, corresponding to the equivalence of the air temperatures, humidities and product moisture contents.

Figure 4-3b shows the results for the three configurations as presented in Reference 26. The results are in good agreement, giving credibility to the performance of the model. In a subsequent paper by Keey, tabular data are given corresponding to the adiabatic countercurrent configuration of the example problem (20). The tabulated values for relative drying rate are plotted in Figure 4-3a. The

computer model yields drying rates approximately 4 percent greater than the tabulated values for the adiabatic countercurrent case. The problem, as worked in the reference, uses a simple linear humidity potential for computing the drying flux. The humidity potential coefficient, ϕ, as given in Eq. 2-5, describes the deviation of the approximate linear potential from the more accurate logarithmic potential, which is used in the model. For this case, ϕ increases through the dryer, accounting for most of the observed difference in drying flux. A minor difference in drying flux is attributed to the use of a constant mass transfer coefficient in the reference, while the coefficient used in the model varies with changes in the air properties. The ratio of convective heat to mass transfer coefficients, as given in Eq. 3-21, is proportional to the 2/3 power of the Lewis number. For the adiabatic countercurrent case, the Lewis number decreases through the dryer as air properties change due to the increasing temperature and decreasing humidity. This gives a greater drying rate than obtained by assuming constant mass transfer coefficient.

Predicted surface temperatures are given as a function of moisture content are also available in Reference 20. The surface temperature was evaluated from the equation

$$f = \frac{T_S - T_a}{T_w - T_a} \tag{4-16}$$

which may be derived from considering a surface energy balance, assuming negligible sensible heating of the material. The surface energy balance yields

$$N_v h_{fg} \quad h(T_a - T_S) \tag{4-17}$$

and upon replacing the drying rate flux, N_v, with the definition of the relative drying rate, f, Eq. 4-17 becomes

$$f\, N_{vo}\, h_{fg} = h(T_a - T_s) \tag{4-18}$$

The surface energy balance for a fully wetted surface at the wet bulb temperature, as developed in Chapter 2 yields,

$$N_{vo}\, h_{fg} = h(T_a - T_w) \tag{4-19}$$

Combining Eqs. 4-18 and 4-19 yields the relationship between relative drying rate and the surface temperature as given in Eq. 4-16.

The surface humidity, Y_s, may be approximated through similar derivation as

$$f = \frac{Y_s - Y_a}{Y_w - Y_a} \tag{4-20}$$

The surface temperature values tabulated in the paper are shown with the surface temperature from the model in Figure 4-4, indicating good agreement.

4.2.4 Prediction of experimental drying runs

A major objective of this work includes the coupling of the dryer model with experimentally derived product models. The following case study uses the computational model with a product model for polyurethane foam derived from experimental data. Obviously, the drying time computed by the model must [illegible] with the experimentally measured drying time for the case used as the [illegible]

AD-A187 377 PROCESS DESIGN MODEL FOR A SINGLE-ZONE TUNNEL DRYER(U) 2/2
AIR FORCE INST OF TECH WRIGHT-PATTERSON AFB OH
B A FLAKE DEC 87 AFIT/CI/NR-87-79T

UNCLASSIFIED F/G 13/1 NL

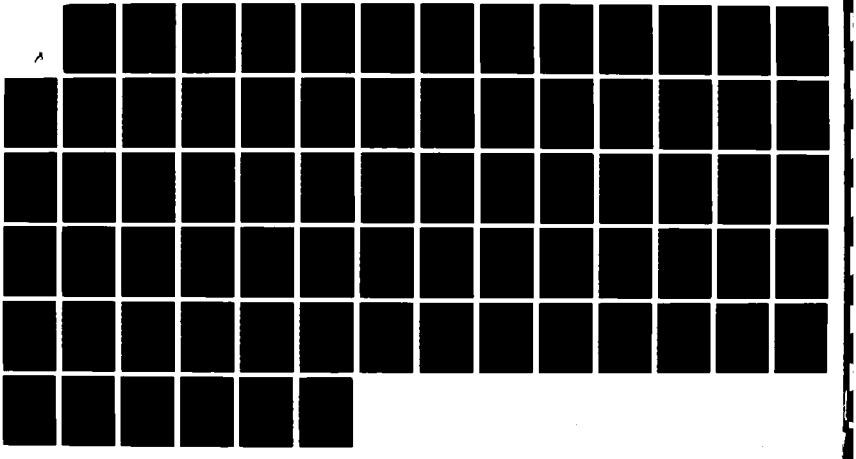

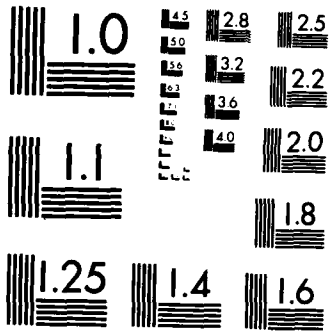

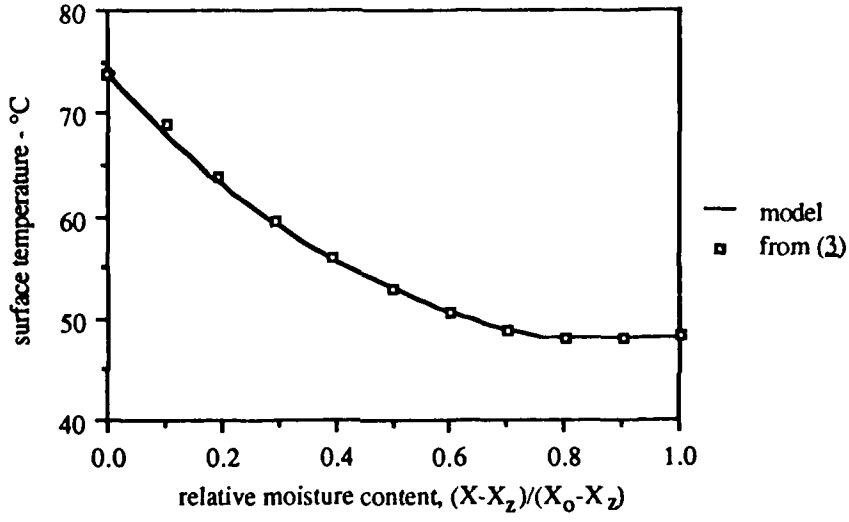

Figure 4-4. Surface temperature profiles, adiabatic countercurrent case

characteristic drying curve. Additionally, using the experimentally derived product model, predictions for the drying time of the same material dried under different air conditions are made and compared with experimental results. This comparison tests the usefulness of the model as a predictive tool.

The experimental data were taken from drying a polyurethane foam sample, which is considered to be nonhygroscopic. The test data included measurements of sample mass and temperature taken at regular time intervals. The drying rate curve and subsequent characteristic drying curve were developed from drying data taken under a constant air temperature of 72° C. A limited drying rate curve between given moisture contents was developed by first plotting the sample mass measurements versus time and making an exponential least squares fit. An expression for the drying rate flux was developed by taking the derivative of the exponential equation, changing its sign, and dividing by the exposed surface area of the sample. The drying rate was evaluated at each time increment and plotted against the corresponding moisture content of the sample. Figure 4-5a shows the sample mass versus time curve and Figure 4-5b shows the resulting drying rate curve of drying rate flux versus moisture content. It is noted here that this analysis was made using a single curve fit over a limited range of moisture content and is intended for illustrative purposes only. More appropriate analytic methods of arriving at drying rate curves from experimental data may be found in the literature and are the topic of a concurrent investigation.

To develop the characteristic drying curve, the normalization parameters N_{vo} (the drying rate from a fully wetted surface) and X_{cr} (the critical

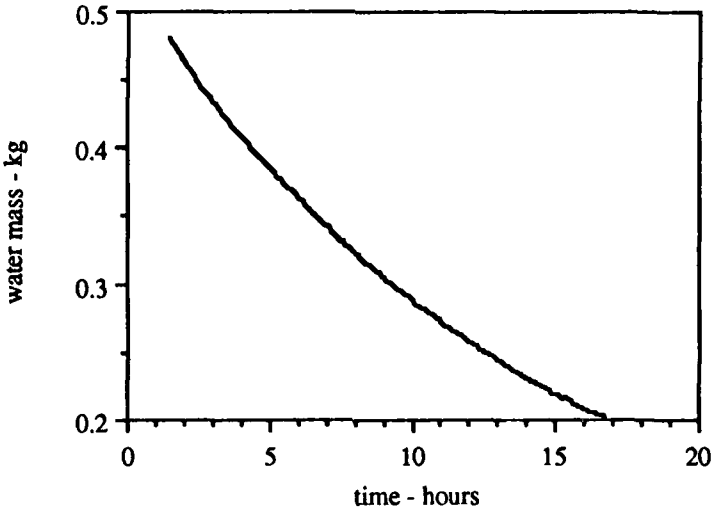

(a)

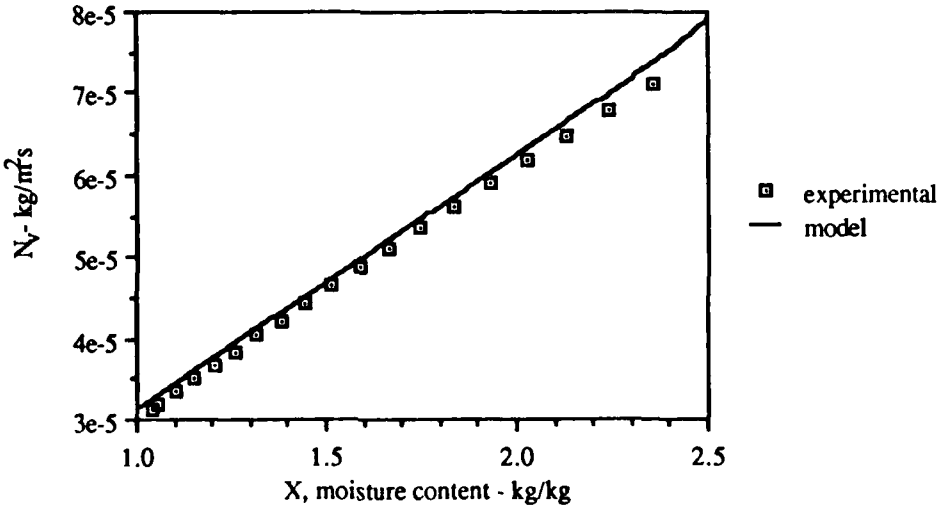

(b)

Figure 4-5. a) Mass vs. time, experimental data, and b) Drying rate curves, model and experimental data for air temperature of 72°C

moisture content) must be known. However, the drying rate data from which the drying rate curve used here did not encompass a constant rate period of drying from a fully wetted surface. Therefore, in lieu of an actual data measurement, N_{vo} was evaluated from Eq. 2-20b

$$N_{vo} = K_o D \ln\left[\frac{D + Y_w}{D + Y_a}\right] \tag{4-21}$$

Included in the experimental data are measurements of air temperature and relative humidity from which both Y_a and Y_w are calculated. An approximation to the mass transfer coefficient, K_o, was made using Eq. 4-21 and data from a limited duration drying test which used a saturated foam sample (surface fully wetted). Also, a corresponding value for the convective heat transfer coefficient, h, was calculated using the heat and mass transfer analogy given in Chapter 2 as

$$\frac{K_o}{h} = \frac{\beta\, Le^{2/3}}{C_p} \tag{4-22}$$

The correlation coefficients used in the model for finding the convective heat transfer coefficient were estimated from the approximated value of h.

In the absence of complete experimental data, the critical moisture content for the foam may be estimated through analysis; an ad-hoc method was used to determine a value for critical moisture content from limited experimental data. Consider the following definition of the characteristic drying curve,

$$f = \Phi^n \tag{4-23}$$

Expressed in terms of the variables X and N_v,

$$\frac{N_v}{N_{vo}} = \left(\frac{X}{X_{cr}}\right)^n \tag{4-24}$$

Considering the constructed drying rate curve of N_v versus X, an exponential curve fit was made to approximate the exponent, n, in Eq. 4-23. As shown in Figure 4-5b, the drying rate curve is almost linear, with n=.99 according to the fit. With values for N_{vo} and n, Eq. 4-24 may now be solved for X_{cr}, where N_v/X is the slope of a linear approximation. For this data, X_{cr} was calculated to be 10 kg/kg.

Using this procedure, a characteristic drying curve for the foam between two given moisture contents was developed. Also, parameters for the calculation of the rate coefficients were approximated. The computational model was then run with the derived product model between specified moisture contents and the drying time compared with that measured in the experiment.

For this case, drying of the foam from a moisture content of 2.5 kg/kg to 1.0 kg/kg is considered. Again the air mass flow rate to dry product mass flow rate ratio is taken to be very large, such that isothermal and isohumid air conditions prevail. Arbitrarily assigning the product dry mass flow rate, L, to be 0.1 kg/s, and the air mass flow rate, G, to be 5×10^6 kg/s, the humidity change is a negligible 3.0×10^{-8} kg/kg.

The air conditions for the test data were a temperature of 72° C, and humidity of 0.01017 kg/kg. These values were input as the entering air conditions

for the model simulation. The entering product temperature was taken as 30° C, the mean foam temperature according to test data taken at the entering moisture content.

To complete the input specifications for the model, the following thermophysical and geometrical values were specified:

POLYURETHANE FOAM PROPERTIES

specific heat	C_{ps} = 1.596 kJ/kg °C
thermal conductivity	κ_d = .021 x 10^{-3} kW/m°C
material thickness	b = 0.0508 m
density	ρ_s = 38.4 kg/m^3

FLOW CONDITIONS

velocity	V = 5.41 m/s
correlation coefficient	C_2 = 0.0199
Reynolds number exponent	m = 0.8
length of sample	Length = 0.375 m

The experimental drying time between the given moisture contents was 16.11 hours. Selecting 150 as the number of steps, the model simulation yielded a drying time of 15.86 hours, within two percent of the experimental value. In Figure 4-5b, the predicted and experimental drying rate curves are compared.

The concept of the characteristic drying curve implies the validity of the product model under varying air conditions. Although the experimental data used were taken under one constant set of air conditions, the product model derived

should be extendable to prediction of drying times for experimental runs at other constant conditions. The characteristic drying curve derived from the data taken at 72° C was used to predict the drying time of the foam with 90° C air; the predicted results using the characteristic drying curve concept were subsequently compared with measured drying time for 90° C air.

The model simulation was run with the same inputs as given above, except that the entering air conditions were taken as 90° C , 0.01029 kg/kg humidity, and 6.20 m/s velocity. The simulation resulted in a computed drying time of 11.08 hours, compared to the experimental time of 10.76 hours, a three percent difference. The drying rate from the simulation is compared with that derived from the experimental data in Figure 4-6.

An additional experiment utilizing 120.5° C air was simulated. For this case, the air humidity was .01069 kg/kg, and velocity 6.20 m/s. The model predicted a drying time of 8.05 hours, within two percent of the experimental time, 8.14 hours.

This final case study demonstrates the usefulness of the characteristic drying curve as a basis for comparative performance estimation. As demonstrated, the dryer model, along with a characteristic drying curve, can be used to predict the dryer length and drying time, among other parameters, in cases of various drying process conditions. It should be noted, however, that the range of conditions which may be simulated with the model concept may be limited and the range may vary for different materials.

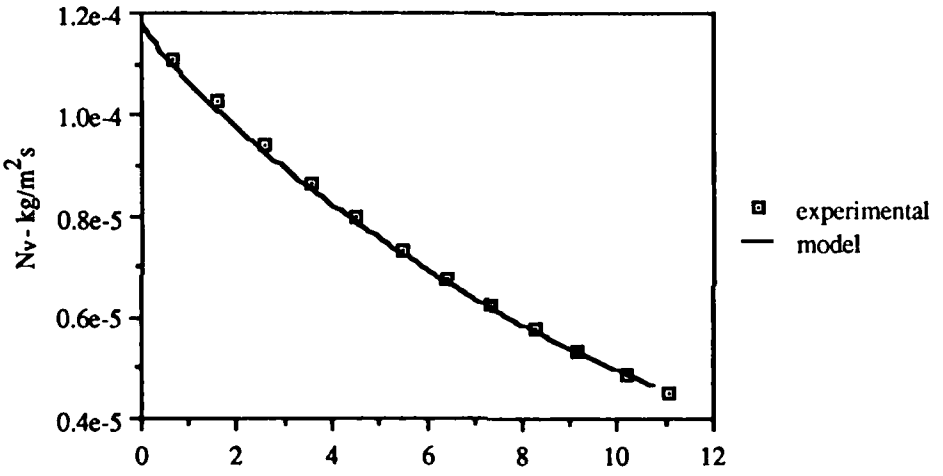

Figure 4-6. Drying rate vs. time, model predictions and experimental data for air temperature of 90°C

CHAPTER 5

CONCLUSIONS AND RECOMMENDATIONS

The work presented here is part of an ongoing investigation of dielectrically assisted drying processes. This section includes conclusions and recommendations for development of the dryer design model, and suggestions on formulation of characteristic drying curves for dielectrically enhanced drying. Some of these recommendations are being incorporated into current investigations directed at providing a well founded and tested model for evaluating performance of dryers with dielectric heating.

5.1 CONCLUSIONS

This section will discuss the current model's performance with respect to the case studies, and the use of the adiabatic saturation temperature in lieu of the wet bulb temperature in drying rate calculations.

5.1.1 Prediction of Wet Bulb Temperature

The characteristic drying curve concept normalizes the drying rate on that for a fully wetted surface at wet bulb conditions, and accuracy in determining the wet bulb temperature directly affects the accuracy of the calculated drying rate.

For the air/water system, the wet bulb temperature is essentially equivalent to the adiabatic saturation temperature throughout most of the air conditions encountered in drying. The largest difference between the two temperatures occurs for hot, dry air conditions. At these conditions, a large potential between the saturated wet bulb and air humidities exists, and a small error in wet bulb temperature results in relatively small error in the calculated drying rate. As humidity increases, the two temperatures approach each other, until at saturation they are equivalent. Error in wet bulb temperature when the humidity potential is small may result in relatively large differences in calculated drying rate, but small potentials between the air and saturated wet bulb humidities occur when air approaches saturation, i.e., when the adiabatic and wet bulb temperatures converge.

Currently the model predicts both adiabatic saturation and wet bulb temperatures. Using the properties of dry air for the heat and mass transfer analogy, the wet bulb temperature predictions are within 0.2° C near saturated conditions, and within 1.3° C for high temperature, low humidity conditions when compared to a psychrometric chart for the air/water system in Reference 3. In comparison, the model predictions for adiabatic saturation temperature are within 0.1° C near saturation and are within 0.7° C at high temperature, low humidity conditions. Since the greatest accuracy in calculating drying rate is required for very humid air conditions, it is recommended that the adiabatic saturation temperature, as calculated in the model, be used for all drying rate calculations.

5.1.3 Case Study Observations

The case studies performed in Section 4 served to verify several aspects of the model. The predictions of psychrometric values were in good agreement with published psychrometric charts. Accuracy of air/water thermodynamic properties is important since the drying rate is directly proportional to the humidity potential between product surface and air stream. The asymptotic approach of temperature shown in the adiabatic saturation and isothermal simulations confirms proper energy balance between the air stream and product. The second study, which effectively numerically integrated a given drying rate curve, established the soundness of the discretization method. Again, this is an important check, since the computed dryer length is the result of the integration.

The model predictions are in good agreement with design problems given in the literature for convective dryers in various configurations. The model developed in this work should be expected, as a minimum, to reproduce results achieved by simple analytical methods. A more important test of the model's value was made in the comparisons with experimental drying rate data.

The prediction of experimental drying time using a product model developed from the same experimental data was a simple check of the model's internal consistency; good results were achieved as expected. The final study displayed the ability of the dryer model, with a product model derived from experimental data, to predict drying times under different conditions. This is an important step toward the development of a capable dryer design tool.

5.2 RECOMMENDATIONS

These recommendations are intended to aid in the further development of dielectrically-enhanced dryer design models. Of significant importance is the development of characteristic drying curves for materials dried with dielectric heating. Also recommended is the extension of the single zone tunnel dryer model to a multizoned dryer model. Future work sh. ·ld include the modeling of different types of industrial dryers, as well as verification of these models and cost estimation of conventional and dielectric drying equipment.

5.2.1 Product Model for Dielectric Drying

The process model developed here incorporates a product model of conventioal convective drying in the form of a characteristic drying curve, used to predict drying rate under varying external air conditions. A drying rate curve for a material dried with combined dielectric and convective heating will differ from that for material dried with convection alone. For the conventional characteristic drying curve, the drying rate is normalized on the drying rate from a fully wetted surface at the wet bulb temperature. If the same normalization parameter were used for different dielectric heating intensities, different characteristic curves will be obtained, limiting predictive capability under varying electric fields. To use the characteristic drying curve in a dielectrically-enhanced drying process, a normalization parameter that accounts for the quantity of dielectric heating is needed.

Although no literature exists that specifically addresses this problem, some direction can be found from the development of the conventional characteristic drying curve, where the normalization factor for drying rate is that from a fully wetted surface. The drying rate from a fully wetted surface, in conventional drying, is simply a function of the air conditions. The air temperature and humidity determine a specific wet bulb temperature while the air velocity relative to the material surface determines the mass transfer coefficient. For dielectric drying, consider a case in which the predominant mode of material heating is dielectric heating. After an initial warm-up to the saturation temperature, there may be a constant rate period where the drying flux is approximately proportional to the rate of dielectric heating

$$N_{vo}\, h_{fg} = P_o\, b \tag{5-1}$$

where N_{vo} is the evaporative mass flux, h_{fg} is the latent heat of vaporization for water, P_o is the dielectric power per unit volume dissipated in the material volume , and b is the material thickness. The dissipated power is a function of the electric field intensity and the material's dielectric properties. For a constant incident electric field, the dielectric power deposition will be constant if the material dielectric properties do not change. Although the effective dielectric loss factor is a function of moisture content, at high moisture contents the loss factor of the wet material may approach that of water. Just as the conventional drying rate from a fully wetted surface is a function of the air conditions and water hygrothermal properties, it is suggested that the corresponding drying rate in the dielectric case is a function of the electric field and water dielectric properties. As shown in Eq. 5-1,

the drying rate in the dielectric case shows a dependence on the material thickness, b. This may constrain a characteristic curve to a given material thickness. However, in Chapter 2, a derivation of the conventional characteristic curve shows it to be dependent on the drying intensity, which is also proportional to material thickness. Continuing the comparison, for conventional drying, as the moisture content falls so does the drying rate due to increased resistance to diffusion in the material. In the dielectric case, as the moisture content falls, the power deposition, and therefore the drying rate should also fall due to the decreasing effective dielectric loss factor as it approaches that of the dry material.

The critical moisture content in the dielectric heating case could be determined in the same manner as conventional drying. That is, the critical moisture content will be the moisture content at which the drying rate ends the constant rate period and enters a falling rate period. The dependence, if any, of the critical moisture content on the magnitude of dielectric heating may be studied coincident with the search for an appropriate drying rate normalization parameter.

Although the suggestions given here are based on a number of simplifying assumptions, they are worthy of investigation. Certainly, if viable normalization parameters which produce a characteristic "dielectric" drying curve can be found through exhaustive analysis of experimental data, they will drastically reduce the amount of experimental data needed to form a basis for design.

Since dielectrically augmented drying is commonly performed with significant convective heating or cooling of the material, a normalization parameter

for the drying rate in the combined case is needed. The "unhindered" drying rate in this case is a function of the net amount of heating from both sources. The convective heating rate is proportional to the difference between the air and surface temperatures. The equilibrium temperature at a fully wetted surface will be somewhere between the wet bulb temperature and the saturation temperature of water. Also, the effective dielectric loss factor, and therefore the electric power deposition, is a function of the material temperature. If a characteristic drying curve for dielectric heating can be found, then perhaps superposing this curve with the conventional characteristic curve will provide a predictive model for the combined case. A means of combining separately produced dielectric and conventional characteristic drying curves for dielectric and convective heating conditions would provide the optimum product model for use in the system model developed in this work.

The development of appropriate normalization parameters for dielectric and combined heating is the subject of current investigations. At the time of this writing, experimental studies are being carried out to provide data necessary for comparing the validity of proposed normalization parameters.

5.2.2 Multizoning

Industrial drying processes are not usually completed in a single-zone tunnel dryer. A product may pass through combinations of isothermal or adiabatic zones of convective heating, and zones of dielectric heating. As the product leaves one zone and moves into another, the air velocity, direction, mass flow rate,

temperature, and humidity may change. As the air becomes saturated in one zone, it may be partially or fully exhausted and drier air entrained before entering the next zone. An obvious extension of this work is to model a multizoned dryer. Simulation of a specific multizoned dryer could be performed using the model developed in this work, run sequentially for each zone of the dryer. An overall model could be constructed where the inlet conditions for each zone are computed and the single zone model called as a subroutine. It is not evident that the single characteristic drying curve used here would be valid for a material subjected to a sudden change in external conditions. The ability to "superpose" drying curves measured under radically different conditions, and the length of the transition zone between curves, will need to be investigated. Certainly, a model which allowed the user to specify the number, type, and configuration of multiple zones would be a valuable tool to the dryer designer.

5.2.3 Other Equipment Models

Although the continuous convective tunnel dryer is a common type, there are many other dryer types used widely in industry that could be augmented with dielectric heating. It is recommended that this work be broadened to develop other equipment models. An equipment model for the through circulation continuous dryer could be readily developed as a minimal extension of the present work. Material dried in a through circulation dryer is conveyed on a perforated belt through which air is blown. Another candidate is a continuous dryer with impingement air flow where air is blown normal to the material surface. The principal difference between these dryers and the one modeled in this work is the

air flow geometry. With suitable correlations for computing heat and mass transfer coefficients, and appropriate control volumes for writing heat and mass balances, equipment models for these dryers can be developed, as was done for the continuous convective tunnel dryer.

Dispersed-type dryers, such as spray or rotary-drum types, present a more formidable modeling problem. Particle transport in the rotary dryer is a function of drum diameter, length, slope, rotational speed, loading, air velocity, flight arrangement and particle characteristics (2). Complex air flow patterns in spray dryers require correspondingly complex particle transport models. Although a more difficult task, equipment models for spray and rotary dryers coupled with product models for dielectrically-heated materials would greatly facilitate investigations of dielectrically-enhanced drying of dispersed materials.

5.2.4 Verification of Dryer Models

Verification of drying equipment models, and models of multizoned dryers must be performed with operational data from full-scale industrial dryers. In addition to comparing predictions of drying rates or drying times, comparisons of parameters calculated through the equipment model such as air temperatures, humidities, velocities, mass flow rates, as well as flow geometries should be made. Cooperation with dryer manufacturers to provide operational data would greatly facilitate verification studies.

5.2.5 Drying Cost Estimation

In most cases, when considering the use of dielectric heating for drying, the bottom line is economic feasibility. Economic decisions based on predictive model studies require knowledge of costs for the amount and type of dielectric heating, as well as costs associated with conventional drying equipment. Careful investigation of the costs of dielectric drying equipment must be made. Overestimation or underestimation of the costs could seriously impede the acceptance of dielectrically-assisted drying.

The recommendations given here are directed toward an end product design tool for dryer design. Such a packaged product would allow the designer to model multiple zones and various configurations and amounts of dielectric and conventional heating, as well as produce figures for economic assessment. The development of such tools is a long-range goal which will require extensive investigation of the modeling of both equipment and dielectrically dried products.

APPENDIX A

Energy and Mass Balances

Energy and Mass Balance Derivations

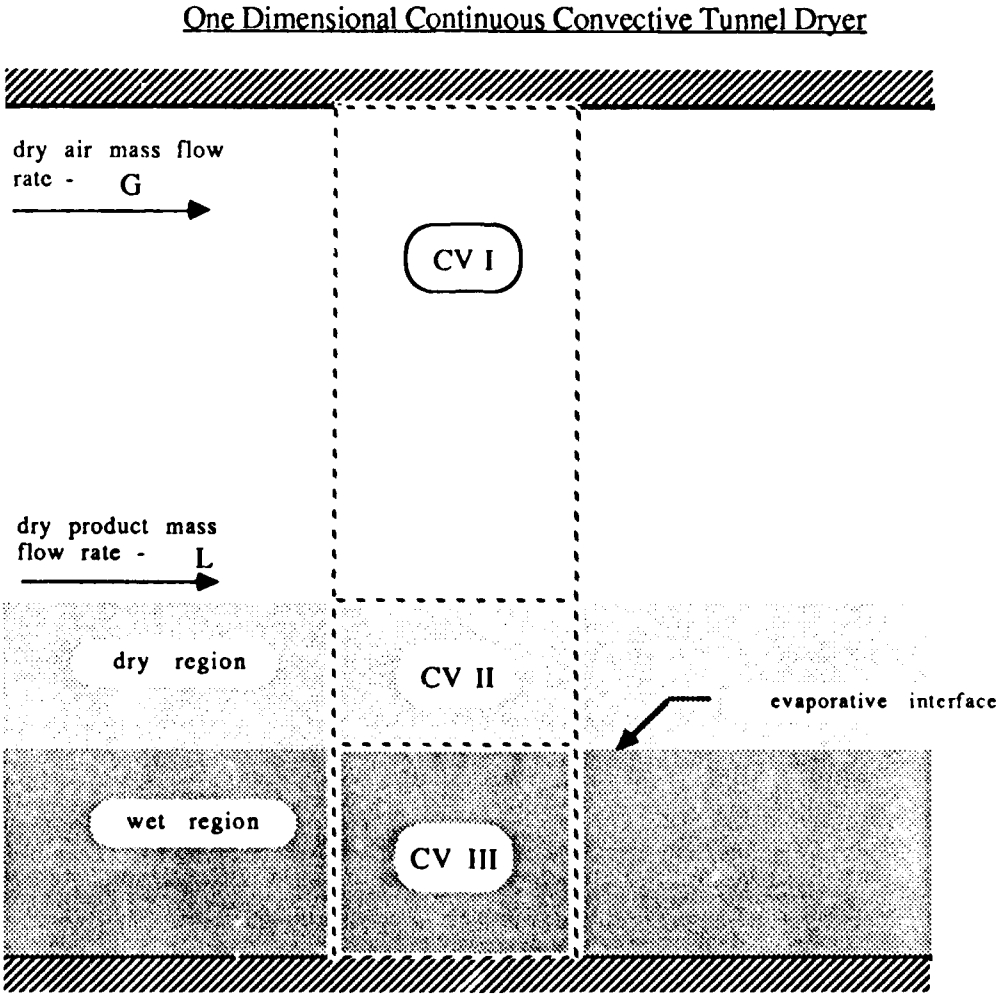

The air, dry and wet product regions correspond to CV I, CV II, and CV III respectively.

Assumptions used for this analysis:

- the top and bottom dryer boundaries are insulated and impermeable
- the process is steady-state with respect to time, $\partial(\ )/\partial t = 0$,and the following conservation laws apply where M and E represent mass and energy respectively

  $$M_{in} + M_{source} = M_{out}$$
  $$E_{in} + E_{source} = E_{out}$$

  however, no mass sources are given in this analysis
- a lumped parameter analysis may be used to represent thermal and mass transport in the y-direction
- thermal and mass diffusion in the z-direction may be neglected

Mass Balances

CV I - air region

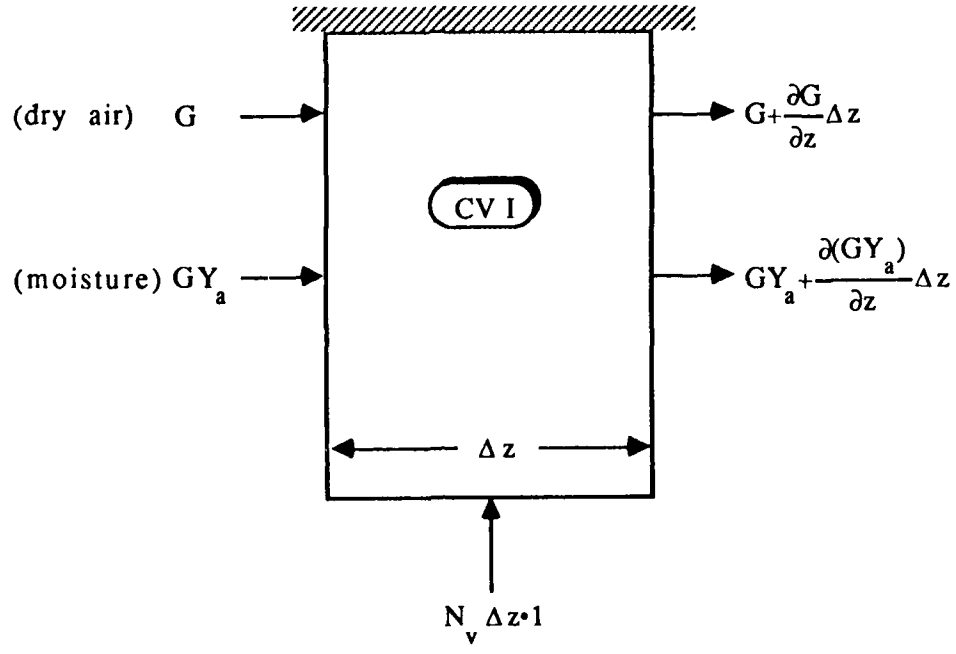

dry air

- neglecting air entering the product

$$G = G + \frac{\partial G}{\partial z}\Delta z \qquad \text{(A-1)}$$

and therefore G is constant throughout the length of the dryer.

moisture in air

- with G taken as constant, and neglecting any condensation of moisture

$$GY_a + N_v\,\Delta z \cdot 1 = GY_a + G\frac{\partial Y_a}{\partial z}\Delta z \qquad \text{(A-2)}$$

$$N_v = G\frac{\partial Y_a}{\partial z}\Delta z \qquad \text{(A-3)}$$

Combined Product Region, CV II and CV III

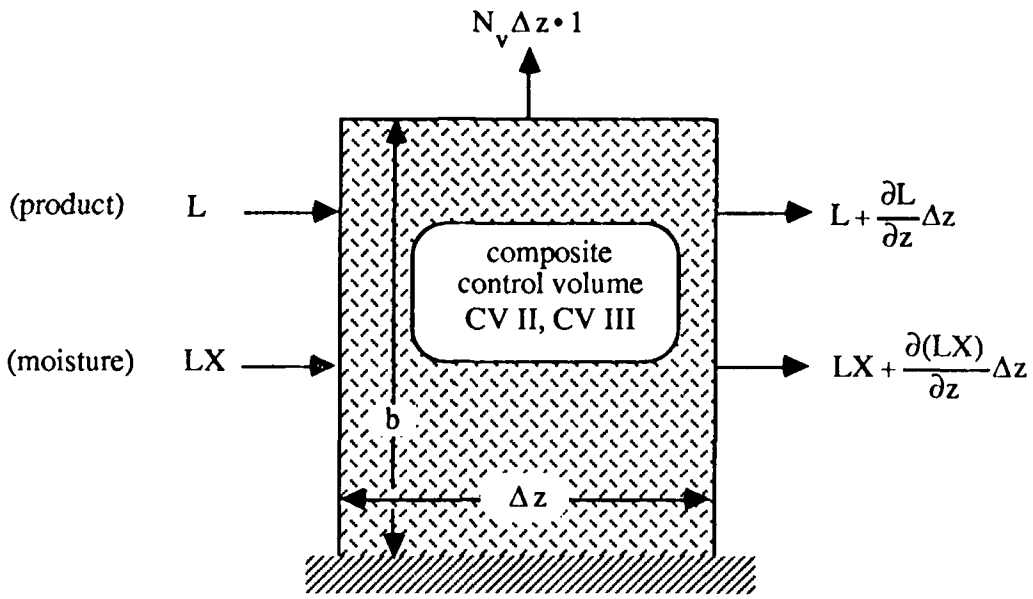

dry product

- assuming no product is entrained in the air stream

$$L = L + \frac{\partial L}{\partial z}\Delta z \qquad \text{(A-4)}$$

thus, L is considered constant throughout the dryer

product moisture

- considering L constant

$$LX = LX + L\frac{\partial X}{\partial z}\Delta z + N_v \Delta z \cdot 1 \qquad \text{(A-5)}$$

$$L\frac{\partial X}{\partial z} = -N_v \qquad \text{(A-6)}$$

Energy Balances

CV I - air region

- considering humid air enthalpy, h_a, to be the total dry air plus vapor enthalpy on a per unit dry air mass basis

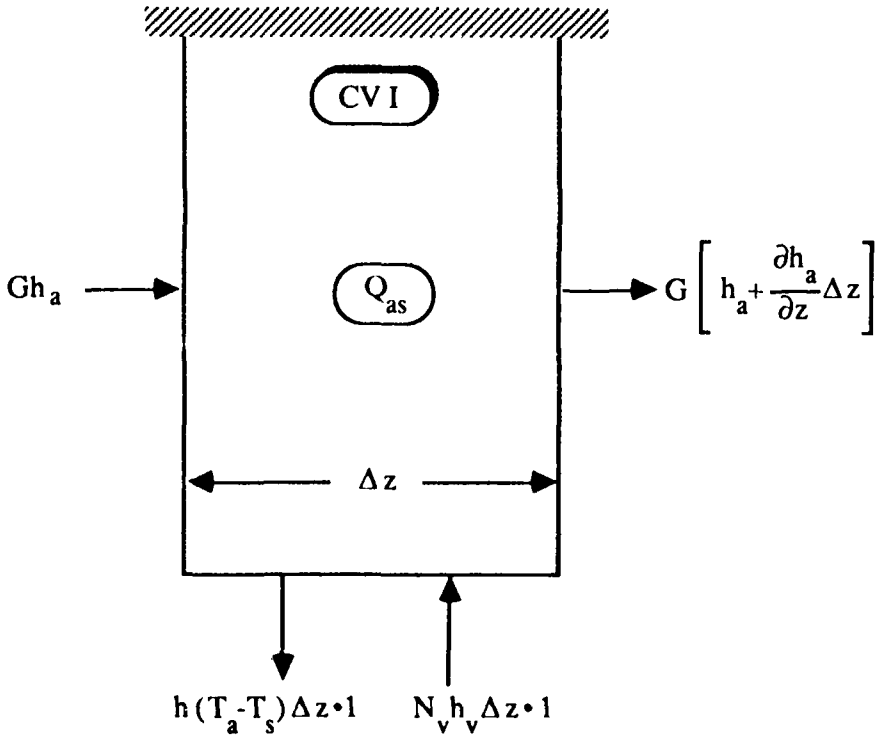

(A-7)

$$Gh_a + N_v h_v\,\Delta z\cdot 1 + Q_{as} = Gh_a + G\frac{\partial h_a}{\partial z}\Delta z + h(T_a-T_s)\,\Delta z\cdot 1$$

Letting $Q'_{as} = \frac{Q_{as}}{\Delta z}$ and simplifying

$$N_v h_v + Q'_{as} = G\frac{\partial h_a}{\partial z} + h(T_a-T_s) \qquad (A\text{-}8)$$

The humid air enthalpy is given by Eq. (3-9)

$$h_a = C_{pa}T_1 + Y_1(C_{pf}T_{dp} + h_{fg} + C_{pv}(T_1-T_{dp})) \qquad (A\text{-}9)$$

CV II - dry product region

- neglecting the enthalpy of wetting
- neglecting vapor enthalpy change due to net convective transport through the dry region
- assuming a linear temperature profile between the surface temperature, T_s, and the evaporative plane temperature, T_e.

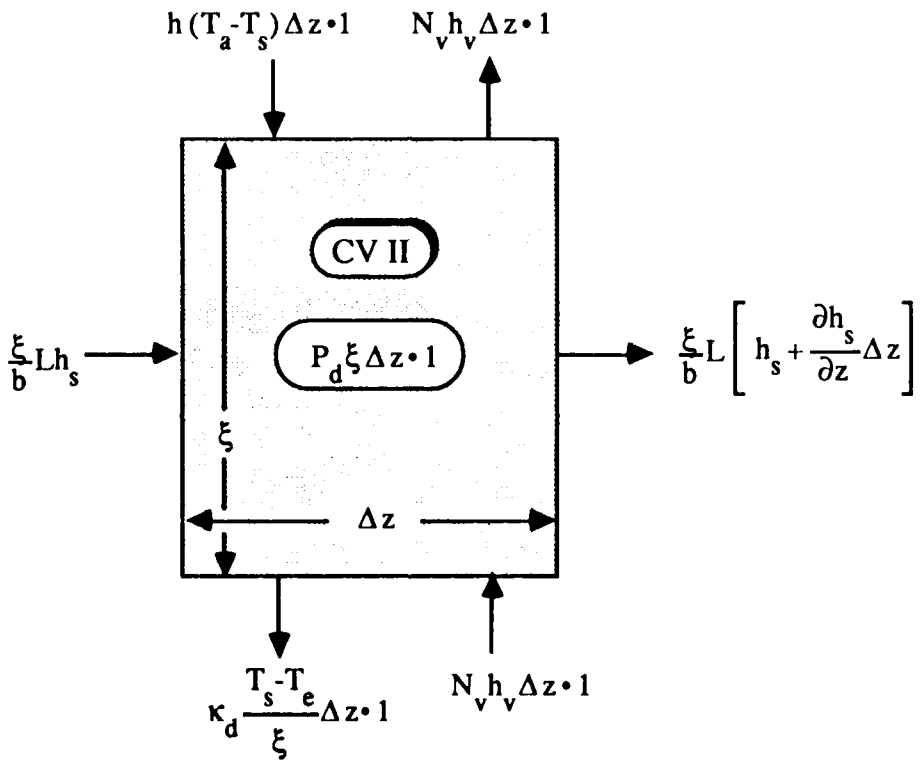

$$\frac{\xi}{b}Lh_s + h(T_a-T_s)\,\Delta z\bullet 1 + N_v h_v\,\Delta z\bullet 1 + P_d\,\xi\,\Delta z\bullet 1 = \frac{\xi}{b}Lh_s + \frac{\xi}{b}L\frac{\partial h_s}{\partial z}\Delta z + \kappa_d\frac{T_s-T_e}{\xi}\Delta z\bullet 1 + N_v h_v\,\Delta z\bullet 1 \qquad \text{(A-10)}$$

$$h(T_a-T_s) + P_d\,\xi = \frac{\xi}{b}L\frac{\partial h_s}{\partial z} + \kappa_d\frac{T_s-T_e}{\xi} \qquad \text{(A-11)}$$

For a linear temperature profile, the mean temperature in the region is:

$$\overline{T_{II}} = \frac{T_s+T_e}{2} \tag{A-12}$$

and for a constant dry product specific heat over the region,

$$\frac{\partial h_s}{\partial z} = C_{ps} \frac{\partial\left[\frac{T_s+T_e}{2}\right]}{\partial z} \tag{A-13}$$

which combined with Eq. A-10 yields

$$h(T_a-T_s) + P_d\xi = \frac{\xi}{b} LC_{ps} \frac{\partial\left[\frac{T_s+T_e}{2}\right]}{\partial z} \tag{A-14}$$

CV III - wet product region

- assuming a uniform temperature profile in the region at the evaporative plane temperature, T_e

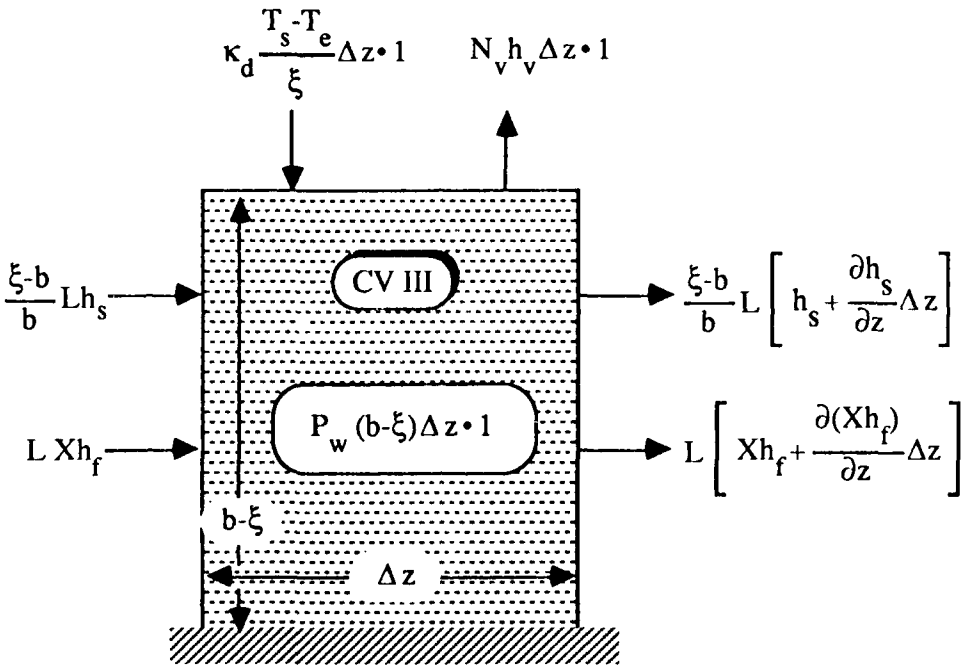

(A-14)

$$\frac{b-\xi}{b} Lh_s + LXh_f + \kappa_d \frac{T_s-T_e}{\xi}\Delta z \cdot 1 + P_w(b-\xi)\,\Delta z \cdot 1 = N_v h_v\,\Delta z \cdot 1$$

$$+ \frac{b-\xi}{b} Lh_s + \frac{b-\xi}{b} L\frac{\partial h_s}{\partial z}\Delta z + LXh_f + L\frac{\partial(Xh_f)}{\partial z}\Delta z$$

Simplifying, applying the chain rule to the last term, and representing the solid and liquid water enthalpy expressions with the product of temperature and specific heat yields

$$k_d \frac{T_s-T_c}{\xi} + P_w(b-\xi) = N_v h_v + \frac{b-\xi}{b} LC_{ps}\frac{\partial T_e}{\partial z} + L\left[X\,C_{pf}\frac{\partial T_e}{\partial z} + h_f\frac{\partial X}{\partial z}\right] \qquad \text{(A-15)}$$

recognizing $L\frac{\partial X}{\partial z}$ is equivalent to $-N_v$ (Eq. A-6), and $h_v - h_f = h_{fg}$

$$k_d \frac{T_s-T_e}{\xi} + P_w(b-\xi) = N_v h_{fg} + L\left[\frac{b-\xi}{b} C_{ps} + XC_{pf}\right]\frac{\partial T_e}{\partial z} \qquad \text{(A-16)}$$

APPENDIX B

Air and Water Thermodynamic and Transport Properties

Air and Water Thermodynamic and Transport Properties

Air Properties

Dry air specific heat

Assuming the following approximate percentage composition of dry air by volume:

78.09	Nitrogen, N_2
20.95	Oxygen, O_2
0.93	Argon, Ar
0.03	Carbon Dioxide, CO_2 and other trace elements

and an ideal solution of gases, neglecting the enthalpy of mixing, the mixture specific heat may be given as

$$C_{pmix} = \frac{1}{n_{mix}} \sum_i y_i \overline{C_{pi}} \qquad \text{(B-1)}$$

where the overbar designates specific heat on a molar basis, and y_i is mole fraction which is equivalent to the volume fraction for ideal gases.

The molecular weight of the air mixture, n_{mix}, is 28.9645 kg/kmole and the temperature dependent specific heats (molar basis) of the air constituents are(4)

$$N_2 \quad \overline{C_p} = 39.060 - 512.79\theta^{-1.5} + 1072.7\theta^{-2} - 820.40\theta^{-3}$$

$$O_2 \quad \overline{C_p} = 37.432 + 0.020102\theta^{1.5} - 178.57\theta^{-1.5} + 236.88\theta^{-2}$$

$$CO_2 \quad \overline{C_p} = -3.7357 + 30.529\theta^{0.5} - 4.1034\theta + 0.024198\theta^2$$

where $\theta = \frac{T(K)}{100}$. The specific heat of the air fraction consisting of CO_2 and other constituents is evaluated with the equation given for CO_2. Lacking an equation for the specific heat of argon, it is assumed constant at 0.5203 kJ/kg K.

Dry air viscosity and thermal conductivity

The following formulas for viscosity and thermal conductivity of air were taken from Reference 32:

$$\mu \times 10^7 = \frac{AT^{3/2}}{T+B} \qquad \text{(B-2)}$$

$A = 145.8$
$B = 10.4$

$$\kappa_a = \frac{a\sqrt{T}}{1 + \frac{b \times 10^{-c/T}}{T}} \qquad \text{(B-3)}$$

$a = 0.6325 \times 10^{-5}$
$b = 245.4$
$c = 12$

where T is temperature (K), μ is viscosity, (poise),and κ_a is thermal conductivity, $\left(\frac{cal}{cm\ s\ K}\right)$.

Air density

Assuming air as an ideal gas, the density (kg/m^3) is given by

$$\rho = \frac{p}{R_a T} \qquad \text{(B-4)}$$

where p is pressure (kPa), T is temperature (K), and R_a is the specific gas constant for air (0.28700 kJ/kg°K).

Water Properties

Water vapor specific heat

The following expression of molal specific heat for water vapor is found in Reference 4. See previous discussion on air specific heat.

$$H_2O \quad \overline{C_p} = 143.05 - 183.54\theta^{0.25} + 82.751\theta^{0.5} - 3.6989\theta \qquad \text{(B-5)}$$

The molecular weight of water is 18.0153 kg/kmole.

Specific heat of liquid water

The equation given for water specific heat, C_{pf} (kJ/kg°C), is derived from a curve fit of saturated-liquid water enthalpy data.

$$C_{pf} = 4.1869 (C_{20} + C_{21} T + C_{22} T^2 + C_{23} T^3 + C_{24} T^4 + C_{25} T^5 + C_{26} T^6) \qquad \text{(B-6)}$$

$C_{20} = 1.02493$
$C_{21} = -8.298 \times 10^{-4}$
$C_{22} = 9.23304 \times 10^{-6}$
$C_{23} = -5.0424 \times 10^{-8}$
$C_{24} = 1.532905 \times 10^{-9}$
$C_{25} = -2.3058 \times 10^{-13}$
$C_{26} = 1.3934 \times 10^{-16}$

Heat of vaporization

The equation for heat of vaporization of water, h_{fg} (kJ/kg), represents a curve fit to tabular enthalpy data where the units of temperature, T, are °C

$$h_{fg} = 2545.5864 \exp(-5.38822711 \times 10^{-4} (\frac{9}{5}T + 32)) \quad \text{(B-7)}$$

Water vapor saturation pressure

The following equation gives the saturation pressure, p_{ws} (Pa), over liquid water as a function of temperature, T (K), for the temperature range of 0 to 200° C (8).

$$p_{ws} = \exp(\frac{C_8}{T} + C_9 + C_{10}T + C_{11}T^2 + C_{12}T^3 + C_{13}\ln(T)) \quad \text{(B-8)}$$

$C_8 = -5800.2206$
$C_9 = 1.3914993$
$C_{10} = -0.04860239$
$C_{11} = 0.41764768 \times 10^{-4}$
$C_{12} = -0.14452093 \times 10^{-7}$
$C_{13} = 6.5459673$

Air/Water System Properties

Relative humidity

The following equation is given for the relative humidity (8)

$$rh = \frac{\omega}{1 - (1 - \omega)(p_{ws}/p)} \quad \text{(B-9)}$$

where $\omega = Y_a/Y_{sat}$, and through Eq. 3-14, $p_{ws}/p = Y_{sat}/(D + Y_{sat})$.

Adiabatic saturation temperature

The expression for the adiabatic saturation temperature is developed from an energy balance about the control volume shown in Figure 2-3. If the entering air conditions of temperature and humidity are T_1 and Y_1, and the adiabatic saturation temperature and saturated humidity are T_{as} and Y_{as} the energy balance results in

$$h_{da\text{-}1} + Y_1 h_{v\text{-}1} + (Y_{as}-Y_1)h_{f\text{-}as} = h_{da\text{-}as} + Y_{as}h_{v\text{-}as} \qquad \text{(B-10)}$$

where h_{da}, h_v, and h_f are the dry air, vapor, and liquid water enthalpies respectively.

Diffusivity of water vapor in air

A relation for diffusivity of water vapor in air, $\mathcal{D}_{ab}$, is given as (33):

$$\mathcal{D}_{ab} = \mathcal{D}_o \left[\frac{T}{T_o}\right]^{1.75} \qquad \text{(B-11)}$$

where $\mathcal{D}_o$ is the value at $T = T_o$ (= 273.15 K), $\mathcal{D}_o = 2.20 \times 10^{-5} \frac{m^2}{s}$

An alternate formula developed from a combination of kinetic theory and the principle of corresponding-states (21):

$$\frac{p\underline{D}_{ab}}{(p_{cA}p_{cB})^{1/3}(T_{cA}T_{cB})^{5/12}\left[\frac{1}{M_A}+\frac{1}{M_B}\right]^{1/2}} = a\left[\frac{T}{\sqrt{T_{cA}T_{cB}}}\right]^b \qquad \text{(B-12)}$$

where, for H_2O with a nonpolar gas, $a = 3.640 \times 10^{-4}$, and $b = 2.334$. For the air water system, the following parameters are used where the subscript, A, designates water and B, air.

critical pressure	$p_{cA} = 218.01$atm $p_{cB} = 37.10$ atm
critical temperature	$T_{cA} = 647.3$ K $T_{cB} = 132.48$ K
molecular weight	$M_A = 18.01534$ kg/kmole $M_B = 28.9645$ kg/kmole

The diffusivity, $\underline{D}_{ab}$ (cm^2/s), is found through Eq. B-12 given a temperature, T (K), and pressure, p (atm).

Coefficient β

The coefficient β used in the heat and mass transfer analogy, Eq 2-14, is found from the following relationship (3)

$$\beta = \frac{\overline{M}_s \ln (\overline{M}_s/\overline{M}_g)}{\frac{(M_w-M_g)D}{D+Y_s} \ln \left[\frac{D+Y_s}{D+Y_g}\right]} \qquad \text{(B-13)}$$

where M_w and M_g are the molecular weights of water and air (gas) respectively (kg/mole), Y_s and Y_g are the surface humidity and air humidity, D is the molecular weight ratio of water to air, and $\overline{M}$ denotes mean molar mass. Mean molar mass is defined in terms of mole fractions y which may be determined from the humidity Y accordingly:

$$y_s = \frac{Y_s}{D+Y_s} \qquad \text{(B-14)}$$

$$y_g = \frac{Y_g}{D+Y_g} \qquad \text{(B-15)}$$

The mean molar mass is defined as

$$\overline{M}_s = M_w y_s + M_g(1 - y_s) \qquad \text{(B-16)}$$

$$\overline{M}_g = M_w y_g + M_g(1 - y_g) \qquad \text{(B-17)}$$

Ackermann correction

The Ackermann correction corrects the convective heat transfer coefficient, h, for significant mass transfer rates (3)

$$h^* = h\left[\frac{E}{\exp(E) - 1}\right] \qquad \text{(B-18)}$$

where for the air/water system, E is defined as

$$E = \frac{N_{vo}C_{pa}}{h} \qquad \text{(B-19)}$$

APPENDIX C

Source Code and Variable Dictionary

with Example Case

CODE LISTING WITH EXAMPLE INPUT AND OUTPUT

Introduction

The Fortran code presented here predicts the process conditions, such as air temperature, humidity, drying rate, and moisture content as a function of position in a continuous convective tunnel dryer. The code is developed from the analysis given in Chapter 3. This section includes a commented source code with example input and output files.

The code was developed on the Control Data Corporation Dual Cyber 170/750 System at the University of Texas at Austin Computation Center. The code is written in Fortran 77 and has been compiled successfully with MNF and FTN5 compilers on the dual Cybers. The code has also been compiled and run on an IBM PC/AT with IBM Professional Fortran Compiler with a few minor changes. For compilation with the Professional Fortran compiler on the PC/AT, the variables should be declared double precision and commands which open and close the input and output files must be included in the code.

Creating an Input File

The input parameters used in the code, which include product and dryer specifications, is read from a specified input file. The parameters are read from the input file in the following order:

```
ISO, XMCL, XMCR, N, IPRINT, TAL, YAL, TPL, G, L
XCR, EXPON, EQUILF, QAS, PWET, PDRY
CPS, KD, RHODS, B, PA
VEL, NUC2, NUEXP1, LENGTH, DELT
```

To illustrate the identification of these parameters for a given case, consider the adiabatic concurrent drying run given in subsection 4.3.2. In an adiabatic or nonisothermal configuration, the flag ISO is set to 2. For this case, the product is to be dried from a initial moisture content of 1.5 kg/kg to a final moisture content of 0.15 kg/kg. Therefore, the product inlet moisture content, XMCL, is 1.5 kg/kg and the exit moisture content, XMCR is 0.15 kg/kg. The characters L and R in these two variable represent left and right ends of the dryer. The product inlet is considered to be at the left end of the dryer, and calculations made in the code start at this end. When in concurrent configuration (a positive value of G) the product and air inlet are at the same end while in countercurrent configuration (a negative value of G) the air exit is at the product inlet.

The number of steps to be made between the inlet and exit moisture contents is set by the variable N. For this case the change in moisture content through the dryer is 1.35 kg/kg and setting N at 135 will yield the step size (Δ X) to be an even .01 kg/kg. The increment at which output variables are to be written to file is given by the variable IPRINT. After each IPRINT number of steps, the

output variables are written. For this case setting IPRINT equal to 5 results in the output variables being written at the first step plus 27 evenly spaced moisture contents.

The air temperature and humidity at the left end of the dryer are entered as TAL and YAL respectively. For the concurrent configuration, these values are the air inlet conditions given as 80° C and 0.0648 kg/kg. The product temperature at the inlet, TPL, is taken at the entering air wet bulb temperature 48.6° C.

The qualitative results of the worked example presented in subsection 4.2.3 are dependent on the ratio of air to product flow rates, G/L, given as 135. For the calculations made in the code, specific values of the flow rates are required. Considering an arbitrary product flow rate, L, of .08 kg/s, the input value for air flow rate, G, is 10.8 kg/s. Note that in the concurrent case the sign of G is positive.

The critical moisture content for the product, XCR is given as 1.2 kg/kg. The function describing the characteristic drying curve is $f = \Phi^n$, where, for this case, $n = 3/4$. The product is hygroscopic where the equilibrium moisture content is determined from $X^* = 0.16\ rh$, where rh is the relative humidity. The input parameter EQUILF, equilibrium moisture content factor, is therefore set to 0.16.

This example is of an adiabatic configured dryer with no dielectric heating. The air heat source, QAS, and power deposition densities in the wet and dry product, PWET and PDRY are therefore entered with values of 0.

For the material properties, the dry material specific heat, CPS, is entered as 1.256 kJ/kg° C, and the thermal conductivity, KD, as .160 x 10-3 kW/m°C. The dry material density, RHODS, is given as 640.0 kg/m^3. The material thickness, B, is taken as .010 m.

Also for this case the drying is considered to be carried out under atmospheric pressure and PA is entered as 1 ATM.

For the purpose of obtaining convective transport coefficients the air velocity with respect to the product is required. The air velocity, VEL, is input as 7.0 m/s. The correlation coefficients NUC2 and NUEXP1 are given as 0.055 and 0.8 respectively. The input parameters NUC2 and NUEXP1 correspond to C_2 and m used in Eq. 3-19. The characteristic length of the product, LENGTH, is taken to be 4.0 m.

The final input parameter, DELT, is used to estimate partial derivatives of equations solved by the subroutine NLSYST. This parameter is described in further detail in Chapter 3. To date, a value of DELT between .005 and .010 has yielded the smallest number of iterations for convergence for most simulations. For this case, DELT is input as .010.

The input file corresponding to the above given values is:

```
2      1.50     0.15     135     5      80.0 0648   47.8    22.5    0.1667
1.20   0.75     0.16     0.0     0.0    0.0
1.256  0.00016  640.0    0.01    1.00
7.00   0.055    0.8      4.0     0.01
```

Description of Output

With the given input file, the code is executed and an output file is created. The output file lists such parameters as moisture content, drying rate, air temperature, air humidity, and dryer position. Output files listing different parameters or multiple output files may be created by editing the source code.

The output file for this case is:

POSITION M	X KG/KG	T-AIR C	Y-AIR KG/KG	TWB C	YS\YW KG/KG	T-SURF C	T-EVAP C	REL RATE	DRYING FLUX KG/S/M^2
.89	1.500	79.98	.06480	48.56	.078365	48.05	48.05	1.0000	.4499E-03
9.91	1.450	79.18	.06517	48.55	.078396	48.05	48.05	1.0000	.4389E-03
19.17	1.400	78.38	.06554	48.55	.078428	48.06	48.06	1.0000	.4279E-03
28.66	1.350	77.58	.06591	48.54	.078460	48.07	48.07	1.0000	.4169E-03
38.41	1.300	76.78	.06628	48.54	.078492	48.07	48.07	1.0000	.4059E-03
48.43	1.250	75.98	.06665	48.54	.078524	48.08	48.08	1.0000	.3949E-03
58.74	1.200	75.19	.06702	48.53	.078561	48.09	48.09	1.0000	.3840E-03
69.55	1.150	74.38	.06739	48.52	.078591	48.58	48.28	.9675	.3607E-03
81.08	1.100	73.57	.06776	48.52	.078617	49.25	48.68	.9344	.3378E-03
93.42	1.050	72.76	.06813	48.51	.078643	50.01	49.18	.9009	.3155E-03
106.65	1.000	71.95	.06850	48.51	.078669	50.79	49.74	.8669	.2937E-03
120.90	.950	71.14	.06887	48.50	.078695	51.55	50.30	.8323	.2725E-03
136.29	.900	70.34	.06924	48.49	.078723	52.27	50.85	.7970	.2519E-03
152.97	.850	69.53	.06961	48.49	.078751	52.95	51.38	.7611	.2319E-03
171.14	.800	68.73	.06999	48.48	.078780	53.58	51.89	.7245	.2126E-03
191.02	.750	67.94	.07036	48.47	.078811	54.16	52.38	.6871	.1939E-03
212.90	.700	67.14	.07073	48.47	.078842	54.68	52.84	.6488	.1758E-03
237.12	.650	66.35	.07110	48.46	.078874	55.16	53.27	.6095	.1583E-03
264.14	.600	65.56	.07147	48.46	.078907	55.59	53.68	.5692	.1415E-03
294.54	.550	64.78	.07184	48.45	.078941	55.97	54.07	.5277	.1253E-03
329.10	.500	64.00	.07221	48.45	.078975	56.30	54.43	.4847	.1097E-03
368.90	.450	63.21	.07258	48.44	.079010	56.59	54.77	.4402	.9474E-04
415.47	.400	62.44	.07295	48.44	.079046	56.82	55.10	.3938	.8039E-04
471.12	.350	61.66	.07332	48.43	.079082	57.02	55.40	.3452	.6664E-04
539.56	.300	60.89	.07369	48.43	.079119	57.17	55.70	.2937	.5345E-04
627.41	.250	60.11	.07406	48.43	.079157	57.28	55.99	.2386	.4078E-04
748.52	.200	59.34	.07443	48.42	.079195	57.37	56.31	.1783	.2850E-04
916.34	.155	58.65	.07476	48.42	.079229	57.43	56.65	.1168	.1750E-04

DRYER LENGTH = 916.34 METERS DRYING TIME = 1221.79 MINUTES
NUMBER OF TRANSFER UNITS, NTU =. 3.27

The first column of the output file indicates dryer position in meters. As the drying rate decreases, the incremental lengths increase such that the change in product moisture content per step is constant. The next column lists the moisture content of the product at each step in kg/kg. For this case, output values are printed at moisture content decrements of .05 kg/kg.

The next three columns indicate the air properties of temperature, humidity and wet bulb temperature respectively. In this example, the dryer is in an adiabatic configuration where the air temperature falls as the air is humidified, and the wet bulb temperature is near constant, changing 0.14° C through the length of the dryer. Just as the moisture content decrement is constant for each step, so is increment in air humidity.

The column labeled YS\YW indicates the saturated humidity at the wet surface temperature for moisture contents greater than critical (f=1) and indicates saturated humidity at the wet bulb temperature for hindered drying (f<1). The drying rate at each step is a function of the potential between the humidity values listed in this column and the air humidity. For f=1, the potential between the saturated humidity at the surface and the air humidity is used according to Eq. 3-11 in determining the drying rate. For f<1, the drying rate is determined by Eq. 3-12 where the saturated humidity at the wet bulb temperature is used.

The product surface and evaporative plane temperatures are listed in the next two columns. According to the evaporative plane model used in the analysis, at moisture contents less than critical the evaporative front recedes below the

surface. Examining the output, at moisture contents greater than critical ($f=1$) the evaporative plane is not receded and the evaporative plane and surface temperatures are equivalent. As the moisture content falls below critical ($f<1$) and the depth of the dry region increases, these temperatures diverge. However, as the product dries to low moisture contents, the amount of evaporative cooling relative to sensible heating is diminished. Thus, with the insulated lower boundary, the temperature gradient in the near dry product approaches zero, and the temperature level approaches the air temperature.

The relative drying rate, f, found through the characteristic drying curve, and drying rate flux, N_v (kg/m^2s), are given in the last two columns. As the product moves through the dryer in this adiabatic concurrent case, the adjacent air stream is progressively humidified and cooled. The result is a decreasing potential for heat and mass transfer and a corresponding decreased drying rate. As the moisture content falls below critical, the drying rate is additionally hindered according to the characteristic drying curve.

The last line of the output file gives the total dryer length, the time required for the product to go from dryer inlet to outlet, and the number of mass transfer units (NTU) for the dryer.

SOURCE CODE

```
      PROGRAM MAIN (INPUT,OUTPUT,TAPE5=INPUT,TAPE7=OUTPUT,TAPE8,
     *  TAPE9,TAPE10)
C
C*****************************************************************
C                                                                *
C                          TUNNEL DRYER                          *
C                                                                *
C        THIS PROGRAM SIMULATES PROCESS CONDITIONS IN A          *
C        CONTINUOUS CONVECTIVE TUNNEL DRYER UNDER ADIABATIC OR   *
C        ISOTHERMAL AIR CONDITIONS.                              *
C                                                                *
C        AT PRESENT, THE CODE SUCCESSFULLY HANDLES PRODUCT       *
C        MODELS OF PURELY CONVECTIVELY DRIED MATERIALS AND IS    *
C        STRUCTURED SUCH THAT FUTURE EDITIONS CAN INCORPORATE    *
C        DRYING KINETICS MODELS OF DIELECTRICALLY HEATED         *
C        MATERIALS.                                              *
C                                                                *
C        THE ACCOMPANYING DESCRIPTION OF INPUT AND OUTPUT FILES  *
C        AND VARIABLE DICTIONARY PROVIDES INFORMATION FOR USE OF *
C        THE CODE.                                               *
C                                                                *
C*****************************************************************
C
C*****************************************************************
C BLOCK A -  DIMENSION VARIABLES, DECLARE COMMON VARIABLES       *
C              READ INPUT PARAMETERS, ETC.                       *
C*****************************************************************
C
      EXTERNAL FCN,TFCN
      DIMENSION F(16),X(16),XT(2),FT(2)
      REAL KD,L,LE,LENGTH,NUC2,NUEXP1,NUL,NTU
C
      COMMON ATM,B,BETA,CPA,CPF,CPFA,CPRAT,CPS,CPV,CPVA,CPY,D,DAB,DELTAX
     *     ,EQUILF,E,EXPON,FRACT,G,HC,HFGA,HFGS,HFGW,ISO,FREL,KD,L,LE,CPAI
     *     ,LENGTH,NUC2,NUEXP1,NUL,PA,PHIH,PR,PRR,PSYRAT,PWS,QAS,QVOL,
     *     QCOND,QCONV,QEVAP,QSENSD,QSENSW,REL,RELHUM,RHOA,RHOMA,RKO,SC,
     *     TAI,VEL,VISC,XCR,XMC,XNORM,YS,YDA,YDS,ZPOS,TMEANO,TEVAPO,ENTHO,
     *     YA,RHODS,FKA,PWET,PDRY
C
C------------------ WRITE HEADERS FOR OUTPUT FILES ------------------
C
      WRITE (7,10)
   10 FORMAT (1X,'DRYER POS',3X,'X',2X,'AIR TEMP',1X,'AIR HUM',3X,'TWB',
     *  4X,'YS\YW ',1X,'T-SURF',1X,'T-EVAP',1X,'REL RATE',1X,
     *  'DRYING FLUX')
      WRITE (7,20)
   20 FORMAT (3X,'METERS',2X,'KG/KG',1X,'DEG C',4X,'KG/KG',3X,'DEG C',3X
     *  ,'KG/KG',3X,'DEG C',2X,'DEG C',12X,'KG/S/M^2')
C
C------------------ SET FLAGS ---------------------------------------
```

```
C
      NEQ = 10
      I = 0
      IFLAGS = 0
C
C ------ SET TOLERANCE PARAMETERS SENT TO NLSYST ------
C
      MAXIT = 120
      DELTA = 0.005
      XTOL = 0.00001
      FTOL = 0.0003
      K = 0
C
C ------ READ INPUT PARAMETERS ------
C
      READ (5,*) ISO,XMCL,XMCR,N,IPRINT,TAL,YAL,TPL,G,L
      READ (5,*) XCR,EXPON,EQUILF,QAS,PWET,PDRY
      READ (5,*) CPS,KD,RHODS,B,PA
      READ (5,*) VEL,NUC2,NUEXPI,LENGTH,DELT
C
C ------ CALCULATE DELTA X AND DELTA Y, PRESSURE IN PASCALS -
C
      IP = IPRINT
      DELTA = DELT
      DELTX = (XMCR-XMCL)/FLOAT(N)
      DELTY = -(L/G)*DELTX
      PA = PA*101325.0
      D = 0.62198
C
C------ SET AIR TEMP, HUMIDITY AND MOISTURE CONTENT TO
C          INLET VALUES
C
      TAI = TAL
      YA = YAL
      XMC = XMCL
C
C------ CALCULATE PRODUCT VELOCITY ------
C
      PVEL = L/(RHODS*B)
C
C------ CALCULATE INITIAL GUESS FOR WET BULB TEMP ------
C
      YWS = YWF(TAL)
      PWA = PA*YAL/(D+YAL)
      TALF = (TAL*9./5.)+32.
      TWMIN = TALF*TALF*(-2.241468E-03)+.8315167*TALF-3.855549
      TGU = TWMIN+(TALF-TWMIN)*PWA/PWS
      TGUC = ((TGU-32.)*5./9.)*1.4
C
C------ SET DEW POINT AND WET BULB TEMPS FOR CALL TO NLSYST --
C
      XT(1) = TGUC
      XT(2) = TGUC
      NTQ = 2
      CALL NLSYST (IECN,NTQ,MAXIT,XT,FT,DELTA,XTOL,FTOL,K)
C
C
```

```
C*********************************************************************
C BLOCK B - INITIALIZE X(I) VARIABLES FOR FIRST CALL TO NLSYST       *
C*********************************************************************
C
C
C--------- SET DEW POINT, WET BULB, AND ADIABATIC SATURATION TEMPS --
C--------- USED IN MAIN CALL TO THE SOLVED VALES
C
      X(7) = XT(2)
      X(8) = XT(1)
      X(9) = XT(2)
C
C-  ------ SET INITIAL POSITION IN DRYER (Z-DIRECTION) AND NTU TO ZERO
C
      ZPOS = 0.0
      NTU = 0.0
C
C---- ----- SET AIR AND PRODUCT TEMPERATURES TO INLET CONDITIONS
C
      X(2) = TAL
      X(3) = TPL
C
C --------- SPECIFIC HEATS AND TRANSPORT COEFFICIENTS ARE FOUND FOR
C             ESTIMATION OF DRYING RATE AND CONTROL VOLUME LENGTH
C
      CPA = CPAF(TAL/2.)
      CPF = CPFF(X(3)/2.)
      HC = HCF(TAL,0.0001,X(3))
      FREL = RMODEL(X)
      CPV = CPVF(X(3)/2.)
      YSAT = YWF(X(7))
      X(10) = YSAT
      RKO = RKOF(TAL,X(10),X(3),FREL,X(8),X(7))
      X(6) = X(3)
      X(1) = FREL*RKO*(YSAT-YA)
      X(4) = (-(L*DELTX)/X(1))
      X(5) = CPAF(TAL/2.)*TAL+YAL*(HFGF(X(8))+CPVF((TAL+X(8))/2.)*(TAL-
     *   X(8))+CPFF(X(8)/2.)*X(8))
C
C---------- C'LD VALUES (I-1) ARE SET TO INLET CONDITIONS ----------
C
      ENTHO = X(5)
      TMEANO = X(3)
      TEVAPO = X(3)
C
C--  ------- IF ISOTHERMAL CONFIGURATION, AIR TEMP AND AIR SPECIFIC
C             HEAT ARE CONSTANT
C
      IF (ISO.EQ.1) THEN
        CPAI = CPAF(TAL/2.)
        X(2) = X(1)*(HFGF(TAL)+CPVF(TAL/2.)*TAL-CPVF(X(3)/2.)*X(3))+HC*
     *     (TAL-X(3))
      ELSE
      ENDIF
C
      K = 0
C
```

```
C     ------ CALL NLSYST TO SOLVE EQUATIONS AT EACH DELTA X DECREMENT
C            HALF STEPS ARE USED AT DRYER INLET AND EXIT
C
      DO 50 I = 1,N+1
        IF (I.EQ.N+1) THEN
          XMC = XMCL+DELTX*FLOAT(I-1)-DELTX/2.
          YA = YAL+DELTY*FLOAT(I-1)-DELTY/2.
          DELTAX = DELTX/2.
        ELSEIF (I.EQ.1) THEN
          XMC = XMCL
          YA = YAL
          DELTAX = DELTX/2.
        ELSE
          XMC = XMCL+DELTX*FLOAT(I-1)
          YA = YAL+DELTY*FLOAT(I-1)
          DELTAX = DELTX
        ENDIF
C
        IF (X(3).GE.1000.0) STOP 'TP EXCEEDS 99 DEGREES'
C
C
        CALL NLSYST (FCN,NEQ,MAXIT,X,F,DELTA,XTOL,FTOL,K)
C
C
C---------- SUM DRYER POSITION (ZPOS) AND NTU ----------
C
        ZPOS = ZPOS+X(4)
        NTU = NTU+(DELTY/(X(1)/RKO))
C
        DRYTIM = ZPOS/PVEL
C
C---------- IF AIR IS SATURATED, SET FLAG ----------
C
        IF (YA.GT.X(10)) IFLAGS = 1
C
C---------- RESET (I-1) VARIABLES TO VALUES AT PREVIOUS STEP
C
        TEVAPO = X(3)
        ENTHO = X(5)
        TMEANO = (X(6)+X(3))/2.
C
        HP = (CPS+XMC*CPF)*X(3)
C
C ---------- IF AT PRINT INCREMENT, WRITE TO OUTPUT FILES ------
C
        IF (IP.EQ.IPRINT.OR.IFLAGS.EQ.1) THEN
C
          IP = 1
C
C ------ SURFACE HUMIDITY, YS, FOR HINDERED DRYING ----------
C            (X<XCR) IS APPROXIMATED BY EQ. 4-20
C
          IF (XMC.LT.XCR) THEN
            YS = (X(10)-YA)*FREL+YA
          ELSE
            YS = X(10)
          ENDIF
```

```
C
          WRITE (7,30) ZPOS,XMC,X(2),YA,X(9),X(10),X(6),X(3),FREL,X(1)
   30      FORMAT  (1X,F8.2,1X,F6.3,1X,F6.2,1X,F8.5,1X,F6.2,1X,F8.6,1X,
     *         F6.2,1X,F6.2,1X,F6.4,1X,E10.4)
          WRITE (8,*) ZPOS,HC,RKO
          WRITE (9,*) ZPOS,PR,SC,LE
          WRITE (10,40) QCOND,QSENSW,QEVAP,QSENSD,QCONV,X(3)
   40      FORMAT (1X,6E13.5)
C
       ELSE
C
          IP = IP+1
       ENDIF
C
C -------- -- IF AIR IS SATURATED, EXIT LOOP ----------
C
       IF (IFLAGS.EQ.1) GO TO 60
C
   50 CONTINUE
   60 CONTINUE
C
C ---- ---- WRITE DRYER LENGTH, DRYING TIME, AND NTU
C
      WRITE (7,70) ZPOS,(DRYTIM/60.),ABS(NTU)
   70 FORMAT (/,1X,'DRYER LENGTH = ',F11.2,'  METERS',4X,
     *   '  DRYING TIME  =',F12.2,'  MINUTES',/,
     *   ' NUMBER OF TRANSFER UNITS, NTU =',F7.2)
C
      IF (IFLAGS.EQ.1) STOP 'CONDENSATION Y-AIR > Y-SURFACE'
      STOP 'END OF PRGM'
      END
C
C**********************************************************************
C      BLOCK C - FCN SUBROUTINE CONTAINING EQNS SOLVED BY NLSYST
C**********************************************************************
C
      SUBROUTINE FCN (X,F)
      DIMENSION X(10),F(10)
      REAL KD,L,LE,LENGTH,NUC2,NUEXP1,NUL
C
      COMMON ATM,B,BETA,CPA,CPF,CPFA,CPRAT,CPS,CPV,CPVA,CPY,D,DAB,DELTAX
     *      ,EQUILF,E,EXPON,FRACT,G,HC,HFGA,HFGS,HFGW,ISO,FREL,KD,L,LE,CPAI
     *      ,LENGTH,NUC2,NUEXP1,NUL,PA,PHIH,PR,PRR,PSYRAT,PWS,QAS,QVOL,
     *      QCOND,QCONV,QEVAP,QSENSD,QSENSW,REL,RELHUM,RHOA,RHOMA,RKO,SC,
     *      TAI,VEL,VISC,XCR,XMC,XNORM,YS,YDA,YDS,ZPOS,TMEANO,TEVAPO,ENTHO,
     *      YA,RHODS,FKA,PWET,PDRY
C
C ---- --- IF ISOTHERMAL CONFIGURATION, USE THIS SET OF EQNS
C
      IF (ISO.EQ.1) THEN
C
C ------- OBTAIN NORMALIZED MOISTURE CONTENT ----------
C
         XNORM = XNORMF(RELHUM,TAI)
C
C ------- CALCULATE DEPTH OF EVAP PLANE   EQ 3.17
C
```

```
      FREL = RMODEL(X)
      FRACT = 1.-SQRT(XNORM/FREL)
C
C ------ SET SPECIFIC HEATS, ENTHALPIES, RATE COEFFICIENTS
C
      CPF = CPFF(X(3)/2.)
      CPV = CPVF(X(3)/2.)
      CPVA = CPVF((TAI+X(8))/2.)
      CPFA = CPFF(X(8)/2.)
      HFGW = HFGF(X(3))
      HFGS = HFGF(X(7))
      HFGA = HFGF(X(8))
      HC = HCF(TAI,X(1),X(6))
      RKO = RKOF(TAI,X(10),X(6),FREL,X(8),X(7))
      YWSAT = YWF(X(7))
C
C ------- IF EVAPORATIVE PLANE IS NOT RECEDED, THEN DRY REGION
C         DOES NOT EXIST, AND THE ENERGY BALANCE ABOUT CV II
C         IS NOT COMPUTED
C
      IF (FRACT.LE.0.) THEN
C
        QCONV = HC*(TAI-X(6))
        QSENSW = L*(CPS+XMC*CPF)*(X(3)-TEVAPO)/X(4)
        QEVAP = X(1)*HFGW
        QVOLW = PWET*B
C
C ------ FOR THIS CASE, F(1) IS AN ENERGY BALANCE ABOUT CVII WITHOUT
C        CONSIDERING CONDUCTION THROUGHT THE DRY REGION
C
        F(1) = QCONV-QSENSW+QVOLW-QEVAP
        F(2) = X(6)-X(3)
C
C ------ IF SURFACE IS FULLY WETTED (X>XCR), THEN SATURATED
C       SURFACE HUMIDITY IS A FUNCTION OF SURFACE TEMP,.
C       ELSE (X<XCR), THE DRYING IS HINDERED AND THE RATE IS
C       COMPUTED FROM EQ 3-12, WHERE THE SATURATED HUMIDITY
C       AT WET BULB, APPROX BY ADIABATIC SAT TEMP (X(10)), IS USE
C
        IF (XMC.LE.XCR) THEN
          F(10) = YWF(X(7))-X(10)
        ELSE
          F(10) = YWF(X(3)) X(10)
C
        ENDIF
C
C ------ IF EVAP. PLANE IS RECEDED, THEN USE THIS SET OF EQS
C        WHICH INCLUDES ENERGY BALACE FOR DRY REGION
C
      ELSE
C
        QCOND = KD*(X(6)-X(3))/(B*FRACT)
        QSENSW = L*((1.-FRACT)*CPS+XMC*CPF)*(X(3) TEVAPO)/X(4)
        QEVAP = X(1)*HFGW
        QSENSD = FRACT*L*CPS*(((X(6)+X(3))/2.)-TMEANO)/X(4)
        QCONV = HC*(TAI X(6))
        QVOLW = PWET*(1. FRACT)*B
```

```
          QVOLD = PDRY*(FRACT)*B
C
C --------- ENERGY BALANCES FOR CV II - F(1), CVIII - F(2)
C           SEE EQS 3-2, 3-3
C
          F(1) = QCOND-QSENSW+QVOLW-QEVAP
          F(2) = QCOND+QSENSD-QCONV-QVOLD
C
          F(10) = YWF(X(7))-X(10)
C
        ENDIF
C
C --------- REMAINING ENERGY BALANCE, MASS BALANCE, RATE
C           EQUATIONS, ETC.
C
C               F(3) - EQ 3-1
C               F(4) - EQ 3-12
C               F(5) - EQ 3-5
C               F(6) - EQ 3-9
C               F(7) - EQ 3-13
C               F(8) - EQ 3-10
C               F(9) - EQ B-10
C
        F(3) = G*(X(5)-ENTHO)/X(4)+HC*(TAI-X(6))-X(2)-X(1)*(CPF*X(3)+
     *    HFGW)
          F(4) = FREL*RKO*D*ALOG((D+X(10))/(D+YA))-X(1)
          F(5) = L*DELTAX+X(1)*X(4)
          F(6) = CPAI*TAI+YA*(CPFA*X(8)+HFGA+CPVA*(TAI-X(8)))-X(5)
          F(7) = RKO*ALOG((D+YWSAT)/(D+YA))*HFGS*D-HC*(TAI-X(7))
          F(8) = YWF(X(8))-YA
          F(9) = YWF(X(9))-(CPAF(X(9)/2.)*X(9)-CPA*TAI-YA*(HFGA+CPVA*TAI-
     *    CPFF(X(9)/2.)*X(9)))/(CPFF(X(9)/2.)*X(9)-HFGF(X(9))-
     *    CPVF(X(9)/2.)*X(9))
C
C --------- IF NOT ISOTHERMAL CONFIG, THEN USE THIS SET OF EQS.
C           THIS SET OF EQUATIONS IS SIMILAR TO THE ABOVE SET,
C           EXCEPT THE VARIABLE X(2) NOW REPRESENTS AIR TEMP
C           RATHER THAN AMOUNT OF AIR SOURCE HEATING.
C
      ELSE
C
          XNORM = XNORMF(RELHUM,X(2))
          FREL = RMODEL(X)
          FRACT = 1.-SQRT(XNORM/FREL)
C
          CPA = CPAF(X(2)/2.)
          CPF = CPFF(X(3)/2.)
          CPV = CPVF(X(3)/2.)
          CPVA = CPVF((X(2)+X(8))/2.)
          CPFA = CPFF(X(8)/2.)
          HFGW = HFGF(X(3))
          HFGS = HFGF(X(7))
          HFGA = HFGF(X(8))
          HC = HCF(X(2),X(1),X(6))
          RKO = RKOF(X(2),X(10),X(6),FREL,X(8),X(7))
          YWSAT = YWF(X(7))
C
```

```
      IF (FRACT.LE.0.) THEN
C
        QCONV = HC*(X(2)-X(6))
        QSENSW = L*(CPS+XMC*CPF)*(X(3)-TEVAPO)/X(4)
        QEVAP = X(1)*HFGW
        QVOLW = PWET*B

C
        F(1) = QCONV-QSENSW+QVOLW-QEVAP
        F(2) = X(6)-X(3)
C
        IF (XMC.LE.XCR) THEN
          F(10) = YWF(X(7)-X(10)
        ELSE
          F(10) = YWF(X(3))-X(10)
        ENDIF
C
      ELSE
C
        QCOND = KD*(X(6)-X(3))/(B*FRACT)
        QSENSW = L*((1.-FRACT)*CPS+XMC*CPF)*(X(3)-TEVAPO)/X(4)
        QEVAP = X(1)*HFGW
        QSENSD = FRACT*L*CPS*(((X(6)+X(3))/2.)-TMEANO)/X(4)
        QCONV = HC*(X(2)-X(6))
        QVOLW = PWET*(1.-FRACT)*B
        QVOLD = PDRY*(FRACT)*B
C
        F(1) = QCOND-QSENSW+QVOLW-QEVAP
        F(2) = QCOND+QSENSD-QCONV-QVOLD
C
        F(10) = YWF(X(7))-X(10)
C
      ENDIF
C
      F(3) = G*(X(5)-ENTHO)/X(4)+HC*(X(2)-X(6))-QAS-X(1)*(CPF*X(3)+
     *     HFGW)
      F(4) = FREL*RKO*D*ALOG((D+X(10))/(D+YA))-X(1)
      F(5) = L*DELTAX+X(1)*X(4)
      F(6) = CPA*X(2)+YA*(CPFA*X(8)+HFGA+CPVA*(X(2)-X(8)))-X(5)
      F(7) = RKO*ALOG((D+YWSAT)/(D+YA))*HFGS*D-HC*(X(2)-X(7))
      F(8) = YWF(X(8))-YA
      F(9) = YWF(X(9))-(CPAF(X(9)/2.)*X(9)-CPA*X(2)-YA*(HFGA+CPVA*
     *   X(2)-CPFF(X(9)/2.)*X(9)))/(CPFF(X(9)/2.)*X(9)-HFGF(X(9))-
     *   CPVF(X(9)/2.)*X(9))
C
    ENDIF
C
    RETURN
    END
C
C*****************************************************************************
C     BLOCK D - SUPPORTING SUBROUTINES
C*****************************************************************************
C
C ------ FUNCTION TO COMPUTE RELATIVE DRYING RATE -----
C          EQ 3-16
C
```

```
      FUNCTION RMODEL (X)
      DIMENSION X(16)
      REAL KD,L,LE,LENGTH,NUC2,NUEXP1,NUL
C
      COMMON ATM,B,BETA,CPA,CPF,CPFA,CPRAT,CPS,CPV,CPVA,CPY,D,DAB,DELTAX
     *     ,EQUILF,E,EXPON,FRACT,G,HC,HFGA,HFGS,HFGW,ISO,FREL,KD,L,LE,CPAI
     *     ,LENGTH,NUC2,NUEXP1,NUL,PA,PHIH,PR,PRR,PSYRAT,PWS,QAS,QVOL,
     *     QCOND,QCONV,QEVAP,QSENSD,QSENSW,REL,RELHUM,RHOA,RHOMA,RKO,SC,
     *     TAI,VEL,VISC,XCR,XMC,XNORM,YS,YDA,YDS,ZPOS,TMEANO,TEVAPO,ENTHO,
     *     YA,RHODS,FKA,PWET,PDRY
C
      NV = X(1)
C
      IF (ISO.EQ.1) THEN
        TA = TAI
      ELSE
        TA = X(2)
      ENDIF
C
      XNORM = XNORMF(RELHUM,TA)
      IF (XNORM.LT.0.) STOP 'XNORM .LT. ZERO'
      IF (XNORM.LT.1.0) THEN
C
C -------- IF CHARACTERISCTIC MOISTURE CONTENT < 0, DRYING IS HINDERED
C          AND THE RELATIVE DRYING RATE, F, IS COMPUTED.  ELSE, THE DR
C          IS FROM A WET SURFACE AND THE RELATIVE DRYING RATE IS 1.
C
        RMODEL = XNORM**EXPON
      ELSE
        RMODEL = 1.0
      ENDIF
C
      RETURN
      END
C
C*********************************************************************
C
C ----- FUNCTION TO COMPUTE CHARACTERISTIC MOISTURE CONTENT ---
C              EQS 2-22, 2-23
C
      FUNCTION XNORMF (RELH,TA)
      REAL KD,L,LE,LENGTH,NUC2,NUEXP1,NUL
C
      COMMON ATM,B,BETA,CPA,CPF,CPFA,CPRAT,CPS,CPV,CPVA,CPY,D,DAB,DELTAX
     *     ,EQUILF,E,EXPON,FRACT,G,HC,HFGA,HFGS,HFGW,ISO,FREL,KD,L,LE,CPAI
     *     ,LENGTH,NUC2,NUEXP1,NUL,PA,PHIH,PR,PRR,PSYRAT,PWS,QAS,QVOL,
     *     QCOND,QCONV,QEVAP,QSENSD,QSENSW,REL,RELHUM,RHOA,RHOMA,RKO,SC,
     *     TAI,VEL,VISC,XCR,XMC,XNORM,YS,YDA,YDS,ZPOS,TMEANO,TEVAPO,ENTHO,
     *     YA,RHODS,FKA,PWET,PDRY
C
C ---- IF EQUILIBRIUM FACTOR IS >0, THEN THE EQUILIBRIUM MOISTURE CONTEN
C       IS COMPUTED FROM THE RELATIVE HUMIDITY
C
      IF (EQUILF.GT.0.0) THEN
C
        RELH = RH(TA,PA,YA)
        RELHUM = RELH
```

```
      XEQ = EQUILF*RELHUM
      IF (XEQ.GT.XMC) STOP 'XEQ > XMC'
C
      ELSE
C
        XEQ = 0.
C
      ENDIF
C
      XNORMF = (XMC-XEQ)/(XCR-XEQ)
C
      RETURN
      END
C
C*********************************************************************
C
C -------- FUNCTION TO COMPUTE SPECIFIC HEAT OF AIR ----------------
C          EQ. B-1
C
      FUNCTION CPAF (TA)
      TK = 273.15+TA
      TK1 = TK/100.
C
      CPN2 = 39.06-512.79/(TK1*SQRT(TK1))+1072.7/TK1**2-820.4/TK1**3
      CPO2 = 37.432+0.020102*TK1*SQRT(TK1)-178.57/(TK1*SQRT(TK1))+236.88
     *  /TK1**2
      CPC02 = -3.7357+30.529*SQRT(TK1)-4.1034*TK1+.024198*TK1**2
      CPAR = 20.7849
      CPAF = (.7809*CPN2+.2095*CPO2+.0093*CPAR+0.0003*CPC02)/28.9645
C
      RETURN
      END
C
C*********************************************************************
C
C ---------- FUNCTION TO COMPUTE SPECIFIC HEAT OF SAT LIQUID WATER
C            EQ. B-6
C
      FUNCTION CPFF (T)
C
      TF = T*9./5.+32.
      C20 = 1.02493
      C21 = -8.298E-04
      C22 = 9.23304E-06
      C23 = -5.0424E-08
      C24 = 1.532905E-10
      C25 = -2.3058E-12
      C26 = 1.3934E-16
C
      CPFF = (C20+C21*TF+C22*TF**2+C23*TF**3+C24*TF**4+C25*TF**5+C26*TF*
     *  *6)*4.1869
C
      RETURN
      END
C
```

```
C**********************************************************************
C
C ---------- FUNCTION TO COMPUTE SPECIFIC HEAT OF WATER VAPOR -
C            EQ. B-5
C
      FUNCTION CPVF (T)
C
      TK = T+273.15
      TK1 = TK/100.
C
      IF (TK.LT.0.0) STOP 'TEMP < 0.0 DEG  CPVF'
C
      CPVF = (143.05-183.54*TK1**0.25+82.751*SQRT(TK1)-3.6989*TK1)/
     *   18.01534
C
      RETURN
      END
C
C**********************************************************************
C
C --- FUNCTION TO COMPUTE SATURATED HUMIDITY --
C     EQ.3-15
C
      FUNCTION YWF (T)
      REAL KD,L,LE,LENGTH,NUC2,NUEXP1,NUL
C
      COMMON ATM,B,BETA,CPA,CPF,CPFA,CPRAT,CPS,CPV,CPVA,CPY,D,DAB,DELTAX
     *      ,EQUILF,E,EXPON,FRACT,G,HC,HFGA,HFGS,HFGW,ISO,FREL,KD,L,LE,CPAI
     *      ,LENGTH,NUC2,NUEXP1,NUL,PA,PHIH,PR,PRR,PSYRAT,PWS,QAS,QVOL,
     *      QCOND,QCONV,QEVAP,QSENSD,QSENSW,REL,RELHUM,RHOA,RHOMA,RKO,SC,
     *      TAI,VEL,VISC,XCR,XMC,XNORM,YS,YDA,YDS,ZPOS,TMEANO,TEVAPO,ENTHO,
     *      YA,RHODS,FKA,PWET,PDRY
C
      TK = 273.15+T
      TK = ABS(TK)
      IF (T.LT.0.0) STOP 'EXPLODING SOLUTION, T < 0 K  YWF'
C
C ------- CALCULATE PARTIAL PRESSURE OF SATURATED VAPOR, EQ B-8
C
      C8 = -5800.2206
      C9 = 1.3914993
      C10 = -0 04860239
      C11 = 0.4176478E-04
      C12 = -0.14452093E-07
      C13 = 6.5459673
C
      PWS = EXP(C8/TK+C9+C10*TK+C11*TK**2+C12*(TK)**3+C13*ALOG(TK))
C
      YWF = .62198*PWS/(PA-PWS)
C
      RETURN
      END
C
C**********************************************************************
C
```

```
C --------- FUNCTION TO CALCULATE LATENT HEAT OF VAPORIZATION
C             EQ. B-7
C
      FUNCTION HFGF (T)
C
      TA = T*9./5.+32.
      IF (TA.LT.0.0) STOP 'EXPLODING SOLN, TA < 0.  HFGF'
C
      HFGF = (1094.40516*EXP(-5.38822711E-04*TA))*2.326
C
      RETURN
      END
C
C*********************************************************************
C
C --------- FUNCTION TO CALCULATE RELATIVE HUMIDITY
C             EQ. B-9
C
      FUNCTION RH (TA,PA,YA)
C
      REAL MU
C
      IF (TA.GT.99.5) THEN
        RH = YA/(YA+1.)
      ELSE
C
        YSAT = YWF(TA)
        MU = YA/YSAT
        PRR = YSAT/(.62198+YSAT)
        RH = MU/(1.-(1.-MU)*PRR)
C
      ENDIF
C
      RETURN
      END
C
C*********************************************************************
C
C ------ FUNCTION TO COMPUTE CONVECTIVE HEAT TRANSFER COEFF. --
C             EQ. 3-19
C
      FUNCTION HCF (TA,NV,TS)
      REAL KD,L,LE,LENGTH,NUC2,NUEXP1,NUL,NV
C
      COMMON ATM,B,BETA,CPA,CPF,CPFA,CPRAT,CPS,CPV,CPVA,CPY,D,DAB,DELTAX
     *      ,EQUILF,E,EXPON,FRACT,G,HC,HFGA,HFGS,HFGW,ISO,FREL,KD,L,LE,CPAI
     *      ,LENGTH,NUC2,NUEXP1,NUL,PA,PHiH,PR,PRR,PSYRAT,PWS,QAS,QVOL,
     *      QCOND,QCONV,QEVAP,QSENSD,QSENSW,REL,RELHUM,RHOA,RHOMA,RKO,SC,
     *      TAI,VEL,VISC,XCR,XMC,XNORM,YS,YDA,YDS,ZPOS,TMEANO,TEVAPO,ENTHO,
     *      YA,RHODS,FKA,PWET,PDRY
C
      TF = (TA+TS)/2.
      VISC = VISCF(TF)
      REL = VEL*LENGTH/VISC
      NUL = NUC2*ABS(REL)**NUEXP1
      HC = NUL*FKAIR(TF)/LENGTH
      E = NV*CPVF((TF)/2.)/HC
```

```
      IF (E.GT.1.E-9) THEN
        PHIH = E/(EXP(E)-1.)
      ELSE
        PHIH = 1.00
      ENDIF
      HCF = HC*PHIH
C
      RETURN
      END
C
C*********************************************************************
C
C ----- FUNCTION TO COMPUTE THERMAL CONDUCTIVITY OF AIR ------
C           EQ B-3
C
      FUNCTION FKAIR (TA)
      REAL K1
C
      TK = TA+273.15
C
      A = 0.6325E-5
      B = 245.4
      C = 27.63102
      K1 = A*SQRT(TK)/(1.+B/(TK*EXP(C/TK)))
      FKAIR = K1*.41873
C
      RETURN
      END
C
C*********************************************************************
C
C ---------- FUNCTION TO COMPUTE AIR VISCOSITY ----------
C             EQ. B-2
C
      FUNCTION VISCF (T)
C
      TK = T+273.15
      A = 145.8
      B = 110.4
      AVISC = ((A*SQRT(TK)*TK)/(TK+B))*1.E-8
      RHOA = 353.13/TK
      VISCF = AVISC/RHOA
C
      RETURN
      END
C
C*********************************************************************
C
C ---------- FUNCTION TO COMPUTE MASS TRANSFER COEFFICIENT ---------
C             EQ. 3-21
C
      FUNCTION RKOF (TA,YW,TS,FC,TDP,TWB)
C
      REAL MW,MA,MBS,MBA
      REAL KD,L,LE,LENGTH,NUC2,NUEXP1,NUL
C
      COMMON ATM,B,BETA,CPA,CPF,CPFA,CPRAT,CPS,CPV,CPVA,CPY,D,DAB,DELTAX
```

```
     *     ,EQUILF,E,EXPON,FRACT,G,HC,HFGA,HFGS,HFGW,ISO,FREL,KD,L,LE,CPAI
     *     ,LENGTH,NUC2,NUEXP1,NUL,PA,PHIH,PR,PRR,PSYRAT,PWS,QAS,QVOL,
     *     QCOND,QCONV,QEVAP,QSENSD,QSENSW,REL,RELHUM,RHOA,RHOMA,RKO,SC,
     *     TAI,VEL,VISC,XCR,XMC,XNORM,YS,YDA,YDS,ZPOS,TMEANO,TEVAPO,ENTHO,
     *     YA,RHODS,FKA,PWET,PDRY
C
      YS = (YW-YA)*FC+YA
C
      TF = (TA+TWB)/2.
      YF = (YA+YW)/2.
C
C --------- COMPUTE COEFFICIENT BETA, EQ. B-13
C
      MW = .01801534
      MA = .0289645
      YDS = YW/(D+YW)
      YDA = YA/(D+YA)
      MBS = MW*YDS+MA*(1.-YDS)
      MBA = MW*YDA+MA*(1.-YDA)
      BETA = MBS*ALOG(MBS/MBA)/((MW-MA)*D*ALOG((D+YW)/(D+YA))/(D+YW))
C
C ---------- CALCULATE DIFFUSIVITY OF WATER VAPOR IN AIR
C            DAB - EQ. B-11, DAB1 - EQ. B-12
C
      TK = 273.15
      DAB = 1.1998806E-09*SQRT(TF+TK)*(TF+TK)*(TF+TK)**(.25)
C
      TCA = 647.3
      TCB = 132.48
      PCA = 218.01
      PCB = 37.10
      RMA = 18.01534
      RMB = 28.9645
      DENOM = (PCA*PCB)**(1./3.)*(TCA*TCB)**(5./12.)*SQRT(1./RMA+1./RMB)
      RAD = SQRT(TCA*TCB)
      C1 = (1./RAD)**2.334
      C = 3.64E-4*C1*DENOM
      DAB1 = C*(TF+TK)**2.334*1.E-4
C
      RHOA = 353.13/(TF+TK)
      FKA = FKAIR(TF)
      VISC = VISCF(TF)
C
C     CPA-SPECIFIC HEAT OF DRY AIR, CPY SPECIFIC HEAT OF HUMID AIR ON
C          A DRY AIR MASS BASIS, CPYT - SPECIFIC HEAT OF HUMID AIR ON
C          TOTAL AIR MASS BASIS.
C
      CPA = CPAF(TF)
      CPY = CPA+YF*CPVF(TF)
      CPYT = CPY/(1.+YF)
C
      PR = CPA*RHOA*VISC/FKA
      SC = VISC/DAB
C
      LE = PR/SC
      RKOF = HC*BETA*LE**(2./3.)/CPA
C
```

```
      RETURN
      END
C
C*********************************************************************
C
C ------- SUBROUTINE CONTAINING EQUATIONS FOR DEW POINT AND WET
C         BULB TEMPERATURES.  THIS SET OF EQS IS USED IN THE INITIAL
C         CALL TO NLSYST.
C
      SUBROUTINE TFCN (X,F)
      DIMENSION F(2),X(2)
      REAL KD,L,LE,LENGTH,NUC2,NUEXP1,NUL
C
      COMMON ATM,B,BETA,CPA,CPF,CPFA,CPRAT,CPS,CPV,CPVA,CPY,D,DAB,DELTAX
     *      ,EQUILF,E,EXPON,FRACT,G,HC,HFGA,HFGS,HFGW,ISO,FREL,KD,L,LE,CPAI
     *      ,LENGTH,NUC2,NUEXP1,NUL,PA,PHIH,PR,PRR,PSYRAT,PWS,QAS,QVOL,
     *      QCOND,QCONV,QEVAP,QSENSD,QSENSW,REL,RELHUM,RHOA,RHOMA,RKO,SC,
     *      TAI,VEL,VISC,XCR,XMC,XNORM,YS,YDA,YDS,ZPOS,TMEANO,TEVAPO,ENTHO,
     *      YA,RHODS,FKA,PWET,PDRY
C
      PWA = PA*YA/(D+YA)
      YWDP = YWF(X(1))
      PWSDP = PWS
      YWSAT = YWF(X(2))
      PWSAT = PWS
C
      HC = HCF(TAI,0.0,X(2))
      RKO = RKOF(TAI,YWSAT,X(2),1.0,X(1),X(2))
      HFGS = HFGF(X(2))
C
      F(1) = PWA-PWSDP
      F(2) = RKO*ALOG((PA-PWA)/(PA-PWSAT))*HFGS*D-HC*(TAI-X(2))
C
      RETURN
      END
C
C*********************************************************************
C*********************************************************************
C*********************************************************************
C
C  THE FOLLOWING SUBROUTINES, NLSYST AND ELIM, ARE TAKEN FROM
C  REFERENCE 24.
C*********************************************************************
C
      SUBROUTINE NLSYST (FCN,N,MAXIT,X,F,DELTA,XTOL,FTOL,I)
C
      DIMENSION X(N),F(N),A(10,11),XSAVE(11),FSAVE(11)
      LOGICAL PRINT
C
      NEQ1 = N
      IF (N.LT.2.OR.N.GT.15) GO TO 180
      PRINT = .TRUE.
      IF (I.NE.0) PRINT = .FALSE.
C
      NP = N+1
      DO 120 IT = 1,MAXIT
        DO 10 IVBL = 1,N
```

```
          XSAVE(IVBL) = X(IVBL)
   10   CONTINUE
        CALL FCN (X,F)
C
        ITEST = 0
        DO 20 IFCN = 1,N
          IF (ABS(F(IFCN)).GT.FTOL) ITEST = ITEST+1
          FSAVE(IFCN) = F(IFCN)
   20   CONTINUE
C
        IF (.NOT.PRINT) GO TO 50
        WRITE (6,30) IT,X
   30   FORMAT (1X,'AFTER ITERATION NUMBER',I3,' X AND F VALUES ARE ',/
     *     ,1X,13F10.4)
        WRITE (6,40) F
   40    FORMAT (1X,13F10.4)
C
   50   IF (ITEST.NE.0) GO TO 60
        I = 2
        RETURN
C
   60    DO 80 JCOL = 1,N
          X(JCOL) = XSAVE(JCOL)+DELTA*XSAVE(JCOL)
          CALL FCN (X,F)
          DO 70 IROW = 1,N
            A(IROW,JCOL) = (F(IROW)-FSAVE(IROW))/(DELTA*XSAVE(JCOL))
   70     CONTINUE
C
          X(JCOL) = XSAVE(JCOL)
   80   CONTINUE
C
        DO 90 IROW = 1,N
          A(IROW,NP) = -FSAVE(IROW)
   90   CONTINUE
        CALL ELIM (A,N,NP,10)
C
        DO 100 IROW = 1,N
          IF (ABS(A(IROW,IROW)).LE.1.E-14) GO TO 160
  100   CONTINUE
C
        ITEST = 0
        DO 110 IVBL = 1,N
          X(IVBL) = XSAVE(IVBL)+A(IVBL,NP)
          IF (ABS(A(IVBL,NP)).GT.XTOL) ITEST = ITEST+1
  110   CONTINUE
C
        IF (ITEST.EQ.0) GO TO 130
  120 CONTINUE
      I = -1
      RETURN
C
  130 I = 1
      IF (.NOT.PRINT) GO TO 150
      WRITE (6,140) IT,X
  140 FORMAT (1X,'AFTER ITERATION NUMBER',I3,
     *  ' X VALUES (MEETING XTOL) ARE ',/,1X,13F10.4)
  150 RETURN
```

```
C
 160 I = -2
     WRITE (6,170)
 170 FORMAT (1X,'CANNOT SOLVE SYSTEM.  MATRIX NEARLY SINGULAR')
     IF (I.EQ.-2) STOP 'NEARLY SINGULAR MATRIX'
     RETURN
C
 180 I = -3
     WRITE (6,190) N
 190 FORMAT (1X,'NUMBER OF EQUATIONS PASSED TO NLSYST IS INVALID.  MUST
    * BE 1 < N < 13. VALUE WAS ',I3)
     RETURN
     END
C
     SUBROUTINE ELIM (AB,N,NP,NDIM)
     DIMENSION AB(NDIM,NP)
C
     NM1 = N-1
     DO 60 I = 1,NM1
C
       IPVT = I
       IP1 = I+1
       DO 10 J = IP1,N
         IF (ABS(AB(IPVT,I)).LT.ABS(AB(J,I))) IPVT = J
  10   CONTINUE
C
       IF (IPVT.EQ.I) GO TO 30
       DO 20 JCOL = I,NP
         SAVE = AB(I,JCOL)
         AB(I,JCOL) = AB(IPVT,JCOL)
         AB(IPVT,JCOL) = SAVE
  20   CONTINUE
C
  30   DO 50 JROW = IP1,N
         IF (AB(JROW,I).EQ.0) GO TO 50
         RATIO = AB(JROW,I)/AB(I,I)
         DO 40 KCOL = IP1,NP
           AB(JROW,KCOL) = AB(JROW,KCOL)-RATIO*AB(I,KCOL)
  40     CONTINUE
  50   CONTINUE
  60 CONTINUE
C
     IF (ABS(AB(N,N)).LT.1.E-14) GO TO 100
C
     NP1 = N+1
     DO 90 KCOL = NP1,NP
       AB(N,KCOL) = AB(N,KCOL)/AB(N,N)
       DO 80 J = 2,N
         NVBL = NP1-J
         L = NVBL+1
         VALUE = AB(NVBL,KCOL)
         DO 70 K = L,N
           VALUE = VALUE-AB(NVBL,K)*AB(K,KCOL)
  70     CONTINUE
         AB(NVBL,KCOL) = VALUE/AB(NVBL,NVBL)
  80   CONTINUE
  90 CONTINUE
```

```
      RETURN
C
 100 WRITE (6,110)
 110 FORMAT (1X,
     * 'SOLUTION NOT FEASIBLE. A NEAR ZERO PIVOT WAS ENCOUNTERED.')
      WRITE (6,*) N,(AB(N,N))
      IF (ABS(AB(N,N)).LT.1.E-14) STOP 'NEAR ZERO PIVOT'
      RETURN
      END
```

VARIABLE DICTIONARY FOR COMPUTER CODE

ATM - Air pressure in dryer, (atmospheres).

B - Product thickness, (meters)

BETA - Coefficient used in heat and mass transfer analogy, (dimensionless), see Eqs. 2-14, 3-21, B-13.

CPA - Dry air specific heat, (kJ/kg°C), see Eq. 3-9.

CPAF - Function subroutine used to calculate dry air specific heat CPA as a function of temperature, see Eq. B-1.

CPAI - Dry air specific heat under isothermal drying conditions. This is separately defined because it remains constant throughout the dryer.

CPF - Specific heat of saturated liquid water, (kJ/kg°C), see Eqs. 3-3, 3-9, B-6.

CPFA - Same as above, *evaluated at* T_{dp} *for use in air enthalpy equation*, Eq.3-9.

CPFF - Function subroutine used to calculate saturated liquid water specific heat, see Eq. B-6.

CPS - Specific heat of the (solid) product, an input variable, (kJ/kg°C).

CPV - Specific heat of water vapor, (kJ/kg K), see Eq. 3-1, 3-9.

CPVA - Same as above, evaluated at T_a for use in air enthalpy equation, Eq. 3-9.

CPVF - Function subroutine used to calculate water vapor specific heat, see Eq. B-5.

D - Ratio of molecular weights of air to water, (dimensionless).

DAB - Diffusivity of water vapor in air, D_{ab}, (m^2/s). See Eq. B-11.

DAB1 - Same as above, except computed according to Eq. B-12.

DELT - Input variable used to calculate perturbation value in nonlinear equation solver subroutine, NLSYST, where for a given unknown variable X(I), the perturbation amount for that variable is DELTA*X(I). See discussion at end of Chapter 3.

DELTAX - Equivalent to DELTX (below), except at end nodes DELTAX = DELTX/2.

DELTX - Decrement value of moisture content, (ΔX), equivalent to X_{in}-X_{out}/N, where N is the number of nodes, (kg/kg). See subsection 3.8.1.

DELTY - Air humidity increment (or decrement in countercurrent case), where DELTY = (L/G) DELTX, (kg/kg). See Eqs. 3-4,3-5.

DRYTIM - Drying time, function of dryer position and product flow rate, (s). See Eqs. 4-13, 4-14.

ENTHO - Humid air enthalpy at i-1 step, set equal to computed air enthalpy X(5) after each step, (kJ/kg).

EQUILF - Equilibrium moisture content factor. Used to determine X^* for hygroscopic materials, where X^* is the product of the equilibrium factor and the air humidity.

EXPON - Exponent n, in the function for the characteristic drying curve, $f = \Phi^n$.

F - Array of equations which, with X(I) unknowns, is solved by NLSYST.

F(1) - Energy balance, wet region, CV III. See Eq. A-16.

F(2) - Energy balance, dry region, CV II. See Eq. A-14.

F(3) - Energy balance, air control volume, CV I. See Eq. A-9.

F(4) - Drying rate equation. See Eq.3-12.

F(5) - Mass balance, composite CV I, CV II. See Eq. A-6.

F(6) - Air enthalpy equation. See Eq. 3-9.

F(7) - Surface energy balance for wet bulb conditions. See Eq. 3-13.

F(8) - Dew point temperature function. See Eq. 3-10

F(9) - Energy balance for adiabatic saturation process. See Eq. B-10

F(10) - Saturated humidity function. See Eq. 3-15.

FCN - Subroutine name containing equations of heat and mass balances, etc, solved at each step by NLSYST.

FKAIR - Function used to compute thermal conductivity of air, κ_a, (kW/m K). See Eq. B-3.

FRACT - Relative depth of evaporative plane (ξ/b). See Eq. 3-17.

FREL - Relative drying rate *f*.

FT - Array of dew point and wet bulb equations solved by initial call to NLSYST.

FTOL - Tolerance parameter used by NLSYST to determine convergence. As a solution converges, the equations being solved F(I) approach zero. Convergence is reached when F(I) < FTOL. See Reference 24.

G - Air mass flow rate, dry air weight basis, ($kg_{dry\ air}$/s). Positive value indicates concurrent air flow, and a negative value, countercurrent.

HC - Convective heat transfer coefficient, h ($kW/m^2°C$)

HCF - Function subroutine used to calculated convective heat transfer coefficient. See Eqs. 2-12, 3-19.

HFGA - Latent heat of vaporization evaluated at T_{dp}, used in air enthalpy equations. See Eq. 3-9.

HFGS - Same as above, evaluated at wet bulb temperature used in wet bulb equation, Eq. 3-13.

HFGW - Same as above, evaluated at adiabatic saturation temperature, T_{as}, used in adiabatic saturation energy balance equation, Eq. B-10.

HFGF - Function used to calculate latent heat of vaporization of water. See Eq. B-7.

I - Counter, steps from 1 to N+1.

IFLAGS - Flag set when air humidity is greater than saturation value. Saturation will occur when air flow rate is not sufficient to entrain

moisture removed from product, when specified entering air humidity is at or greater than saturated humidity or when entering product temperature is less than the dew point temperature (condensation).

IP - Printing counter reset to 1 after each print. See IPRINT below.

IPRINT - Counter used to determine printing increments. For example, if IP is set to 4, variable are printed every fourth step (1,5,9,13, ...,N+1).

ISO - Flag set to 1 if program is to be run in an isothermal configuration, set to 2 if drying configuration is nonisothermal

K - Flag sent to NLSYST. If set to one, values of the solved variables and equations will be printed at each iteration. If solution fails to converge, the equations or variables which did not converge may be found by examining the output. As currently configured, these values are printed only on the first call to NLSYST.

KD - Thermal conductivity of dry product, an input variable, (kW/m°C)

L - Mass flow rate of product, dry mass basis, ($kg_{dry\ product}/s$)

LE - Lewis number. See Eq 2-15.

LENGTH - Characteristic length used in Nusselt number correlation, an input variable. See Eqs 2-12, 3-19.

MAXIT - Maximum number (limit) of iterations to be made in NLSYST.

N - Number of nodes, input variable.

NV - Drying rate flux, N_v, equivalent to X(1), (kg/m^2s).

NEQ - Number of equations to be solved by NLSYST

NLSYST - Subroutine used to solve a system of nonlinear equations. See subsection 3.8.1.

NTQ - Number of equations to be solved by NLSYST in initial call for finding wet bulb and dew point temperatures (NTQ=2).

NTU - Number of transfer units. See Eq. 3-22b.

NUL - Nusselt number. See Eq. 2-12.

NUC2 - Coefficient , C_2,used in Nusselt number correlation. See Eq. 3-19.

NUEXPM - Exponent , m, of Reynolds number used in Nusselt number correlation. See Eq. 3-19.

PA - Air pressure in Pascals.

PDRY - Dielectric power deposition in the dry material, (kW/m^3). See Eq. 3-2.

PHIH - Correction to convective heat transfer coefficients due to high mass transfer rates. See Eqs. B-18,19.

PR - Prandtl number. See Eq. 2-10.

PVEL - Velocity of product through dryer, (m/s). See Eq. 4-14.

PWA - Partial pressure of water vapor in air, (Pascals). See Eq. 3-14.

PWET - Specific dielectric power deposition in wet product, (kW/m^3). See Eq. 3-3

PWS - Saturated partial pressure of water vapor (Pascals). See Eq. B-8.

QAS - Air heating source Q'_{as}, (kW/m), an input variable. See Eq.3-1, A-8. For isothermal configuration, the air heating necessary to provide constant temperature air is calculated and the input value of QAS is not used.

QCOND - The heat conducted through the dry region (kW). See Eq.3-2.

QCONV - The heat convected at the surface (kW). See Eq. 3-2.

QEVAP - The total rate of latent heat of vaporization, $N_v h_{fg}$ (kW). See Eq. 3-3.

QSENSD - Sensible heating in the dry region control volume, (kW). See Eq.3-2.

QSENSW - Sensible heating in the wet region control volume, (kW). See Eq. 3-3.

REL - Reynolds number, Re_L, used in Nusselt number correlation. See Eq. 3-19.

RELHUM - Relative humidity, (dimensionless). See Eq. B-9.

RHOA - Air density, ρ_s, (kg/m^3). See Eq. B-4

RHODS - Density of the dry product (solid), an input variable, (kg/m^3).

RKO - The mass transfer coefficient, K_o , (Kg/m^2s)

RKOF - Function subroutine used to calculate mass transfer coefficient K_o. See Eq. 3-21.

RMODEL - Product model function subroutine used to calculate relative drying rate, f, as a function of normalized moisture content.

SC - Schmidt number. See Eq. 2-11.

TAI - Air temperature in isothermal case, constant throughout the dryer, (°C).

TAL - Air temperature at product inlet (left), an input variable, (°C). This is the entering air temperature in concurrent configuration, exiting air temperature in countercurrent.

TALF - Same as above but in °F. Used in initial calculations of the wet bulb temperature.

TEVAPO - Evaporative plane temperature at previous iteration (old), (°C)

TFCN - Subroutine containing functions for dew point and wet bulb temperature, called by NLSYST.

TGU - Initial guess of wet bulb temperature (°F), before calling NLSYST to solve for wet bulb and dew point temperatures.

TGUC - Same as above, but in °C.

TMEANO - Mean temperature in dry product region $\overline{T_{II}}$ (°C), at previous iteration (old).

TPL - Product temperature at product inlet (left), an input variable (°C).

TWMIN - Minimum wet bulb temperature (°F), used in initial guess calculation for wet bulb temperature.

VEL - Air velocity, an input variable (m/s). Used to compute Reynolds number in heat transfer correlation calculations. See Eq. 3-19.

VISC - Air viscosity, kinematic, ν_a, (m^2/s), found through Eq. B-2 and B-4.

VISCF - Function used to calculated air viscosity, defined above.

X - Variable array, X(I), representing the unknown variables to be solved with equations F(I), given in subroutine FCN.

X(1) - Drying rate flux, N_v, (kg/m^2s)

X(2) - Air temperature, T_a, in nonisothermal configuration (°C), heat added to air necessary to maintain constant air temperature in isothermal configuration, Q_{as}, (kW).

X(3) - Evaporative plane (wet region) temperature, T_e, (°C).

X(4) - Dryer length increment, Δz, (m).

X(5) - Humid air enthalpy, h_a, (kJ/kg).

X(6) - Product surface temperature, T_s, (°C).

X(7) - Wet bulb temperature, T_{wb}, (°C)

X(8) - Dew point temperature, T_{dp}, (°C).

X(9) - Adiabatic saturation temperature, T_{as}, (°C).

X(10) - Saturated air humidity, Y_{sat}, (kg/kg).

XCR - Critical moisture content, X_{cr}, an input variable, (kg/kg).

XMC - Product moisture content at current step, X, (kg/kg).

XMCL - Product moisture content at inlet (left), an input variable (kg/kg).

XMCR - Desired product moisture content at outlet (right), an input variable (kg/kg).

XNORM - Normalized moisture content, Φ.

XNORMF - Function subroutine used to calculate normalized moisture content. See Eqs. 2-22, 2-23.

XT - Variable array where XT(1) is T_{dp}, and XT(2) is T_{wb}. Solved with equation array FT by NLSYST.

XTOL - Tolerance value used by NLSYST to determine convergence. Iteration is stopped at $X(I)-X(I)_{old}<XT$

YA - Current air humidity, Y_a, (kg/kg).

YAL - Air humidity at product inlet (left), an input variable, (kg/kg).

YS - Surface humidity, Y_s, (kg/kg). See Eq. 3-22.

YSAT - Saturated air humidity, Y_{sat}, same as X(10), (kg/kg).

YWF - Function subroutine used to calculated saturated humidity as a function of temperature. See Eqs. 3-14, 3-15, B-8.

YWSAT - Saturated air humidity evaluated at wet bulb temperature, Y_w, (kg/kg). See Eq.3-12.

ZPOS - Current position in dryer, measured from the product inlet, (m). Computed by summation of Δz.

REFERENCES

1. J. van Brakel. "Opinions About Selection and Design of Dryers," Proceedings of The First International Symposium of Drying. Montreal: Science Press, 1978.

2. D. Reay. "Theory in the Design of Dryers," The Chemical Engineer, July, 1979, pp. 501-503,506.

3. R. B. Keey. Introduction to Industrial Drying Operations. New York: Pergamon Press, 1978.

4. G. J. Van Wylen, R. E. Sonntag. Fundamentals of Classical Thermodynamics, SI version, 2nd edition. New York: John Wiley and Sons, 1978.

5. R. B. Keey, M.Kecheng. "On the Humidity-Potential Coefficient," Chemical Engineering Research and Design, vol. 64, 1986, pp. 119-124.

6. E.R.G. Eckert, R. M. Drake. Analysis of Heat and Mass Transfer. New York: McGraw-Hill, 1972.

7. R. E. Treybal. Mass-transfer Operations, 3rd edition. New York: McGraw-Hill, 1980.

8. ASHRAE, ASHRAE Handbook, 1985 Fundamentals, SI version. Atlanta: American Society of Heating, Refrigerating and Air-Conditioning Engineers, Inc., 1985.

9. J. C. Ashworth, R. B. Keey. "The Evaporation of Moisture from Wet Surfaces," Chemical Engineering Science, vol. 27, 1972, pp. 1792-1806.

10. G. Nonhebel, A. A. H. Moss. Drying of Solids in the Chemical Industry. London: Butterworth and Co., 1971.

11. R. B. Keey. Drying: Principles and Practice. New York: Pergamon Press, 1972.

12. A. V. Luikov. Heat and Mass Transfer in Capillary-porous Bodies. London: Pergamon Press Ltd., 1966.

13. H. E. Perry, C. H. Chilton. Chemical Engineers' Handbook, 5th Edition, New York: McGraw Hill, 1973.

14. J. van Brakel. "Mass Transfer in Convective Drying," Advances in Drying, vol. 1. Washington, D.C.: Hemisphere Publishing, 1980, pp.1-22.

15. R. B. Keey, M.Suzuki. "On the Characteristic Drying Curve," International Journal of Heat and Mass Transfer, vol. 17, no. 12, 1974, pp. 1455-1464.

16. M. Suzuki, R. B. Keey, S Maeda. "On the Characteristic Drying Curve," AIChE Symposium Series, vol. 73, no. 163, 1977, pp 47-56.

17. M. Suzuki, S. Maida. "On the Mechanism of Drying of Granular Beds," Journal of Chemical Engineering of Japan, vol. 1, no. 1, 1968, pp. 26-31.

18. A. A. Arzan, R. P. Morgan. "A Transient, Two-Region, Moving Boundary Analysis of the Drying Process," Chemical Engineering Progress Symposium Series, vol. 63, no. 79, 1967, pp. 24-33.

19. M. Kuramae. "Prediction of the drying characteristics of a coarse granular bed using the relationship between the capillary suction pressure and the moisture content," International Chemical Engineering, vol. 24, no. 1, 1984, pp. 112-118.

20. R. B. Keey. "Process Design of Continuous Drying Equipment," AIChE Symposium Series, vol. 73, no. 163, 1977, pp 1-11.

21. R. B. Bird, W. E. Stewart, E. N. Lightfoot. Transport Phenomena. New York: John Wiley, 1960.

22. F. P. Incropera, D. P. DeWitt. Fundamentals of Heat and Mass Transfer, 2nd edition. New York: John Wiley, 1985.

23. S. Sieniutycz. "Lumped parameter modelling and an introduction to optimization of one-dimensional nonadiabatic drying systems," Interanational Journal of Heat and Mass Transfer, vol. 27, no. 11, 1984, pp. 1971-1983.

24. C. F. Gerald. Applied Numerical Analysis, 2nd edition. Reading, Massachusetts: Addison-Wesley, 1980.

25. T. Evans. "Experimental Studies of Microwave/Convective Drying in Nonhygroscopic Porous Beds". Master's of Science in Mechanical Engineering Thesis, University of Texas at Austin, 1986.

26. R. B. Keey. "The process optimisation of a conveyor dryer," New Zealand Engineering, vol. 30, 1975, pp 53-57.

27. R. B. Keey. "Recent Progress in Solids Processing: Some Current Developments in Drying," Chemical Engineering Research and Design, vol. 64, March 1986, pp. 83-88.

28. R. B. Keey. "Theoretical Foundations of Drying Technology," Advances in Drying, vol. 1. Washington, D.C.: Hemisphere Publishing, 1980, pp. 1-22.

29. J. T. Reding, B. P. Shepard, Energy Consuption: Fuel Utilization and Conservation in Industry, EPA 650/2-75-032-d, NTIS PB-246-888, September 1975.

30. A. L. Lydersen. Mass Transfer in Engineering Practice. New York: John Wiley and Sons, 1983.

31. W. M. Kays, M. E. Crawford. Convective Heat and Mass Transfer. New York: McGraw-Hill, 1980.

32. J. Hilsenrath, et al. Tables of Thermodynamic and Transport Properties of Air, Argon, Carbon Dioxide, Carbon Monoxide, Hydrogen, Nitrogen, Oxygen, and Steam. Pergamon Press: New York, 1960.

33. E. W. Washburn. International Critical Tables, Vol. 5. New York: McGraw-Hill, 1926.

END

FILMED

MARCH, 1988

DTIC